

UNIVERSITY OF NATURAL RESOURCES AND LIFE SCIENCES  
VIENNA, AUSTRIA

DIPLOMA THESIS

**Improved acetate co-utilisation by  
*Escherichia coli* W in high  
glucose-acetate fermentation**

Lukas FLÖCKNER , BSc

*submitted in partial fulfillment of the requirements  
for the degree of Dipl.-Ing.*

*in the*  
Department of Biotechnology



*Supervisor:*

Priv.-Doz. FH-Prof. Dr. Michael SAUER

Univ.Ass.Dipl.-Ing.(FH) Dr. Stefan PFLÜGL

– August, 2018 –



# Acknowledgements

I want to thank Prof. Christoph Herwig providing me a great working environment at the Institute for Chemical, Environmental and Bioscience Engineering. I appreciate the stimulating discussions with him and his diverse approaches.

I am very thankful to Dr. Stefan Pflügl for being an encouraging and co-operative supervisor, for his tireless stimulation to implement all this experiments and being always in a good mood giving a pleasant working atmosphere.

A big thank to my research colleagues Anna, Juliane, Katharina, Franzi, Andrea, Tamás, Julian, Charlotte, Philipp and Freddi for their great support and activities throughout and beyond the lab and to the rest of people in the lab for their cheering smile.

I especially want to thank Prof. Michael Sauer supervising me in a professional and straightforward way. He approved this project and provided me with great support during this period.

Above all, I would like to thank my parents, who supported me in every possible way towards the successful completion of my studies.

I would like to dedicate it to you!



# Declaration of Authorship

I declare, that I wrote this thesis and performed the associated research myself, using only literature cited in this volume. If text passages from sources are used literally, they are marked as such.

---

Signature

---

Date



# Abstract

Converting low-cost carbon sources into value-added chemicals is essential for an economically feasible bioprocess. Acetate seems to be a suitable feedstock as it is present in high levels in waste streams, hydrolysates of biomass, and further, can be generated by acetogens via direct fermentation of single-carbon gases. *E. coli* W is known for its high stress tolerance and low acetate secretion and therefore often used as production host for recombinant proteins and several metabolites. However, regulatory mechanisms prevent simultaneous co-utilisation of glucose and other carbon sources such as acetate. Another major challenge is growth inhibition caused by acetate which interferes with the methionine biosynthesis.

The main intention of this work was to allow acetate co-utilisation by *E. coli* W and to strengthen acetate tolerance. Therefore, the acetyl-CoA-synthetase, one of the key enzymes involved in acetate assimilation was successfully modified, assuming to deregulate its activity which is tightly controlled in connection with glucose. Additionally, an aggregation-prone enzyme from the methionine biosynthesis was modified aiming to increase its acetate and heat resistance. A vector library of different gene combinations was created and transformed with host cells to characterise various strains in batch and fed-batch cultivations.

As a result, the best performing strain showed a 2.7-fold increased specific acetate uptake rate in a mixed batch cultivation under high acetate and glucose concentrations ( $10\text{ g l}^{-1}$ ). When acetate was used as the only carbon source, batch duration could significantly be decreased. Promising results were obtained on improved acetate resistance in further strains; however, further analyses are required.





# Zusammenfassung

Die Verwendung von kostengünstigen Kohlenstoffquellen zur Umsetzung hochwertiger Chemikalien ist für wirtschaftlich rentable Bioprozesse unerlässlich. Essigsäure erweist sich dabei als hervorragende Rohstoffquelle, da sie in hohen Anteilen in Abfallströmen und Hydrolysaten von Biomasse vorkommt und zudem von acetogenen Bakterien aus kohlenstoffhaltigen Gasen erzeugt werden kann. *E. coli* W ist für seine hohe Stressresistenz und geringe Essigsäuresekretion bekannt und wird daher oft als Produktionsstamm zur Herstellung rekombinanter Proteine und verschiedenster Metaboliten verwendet. Regulatorische Mechanismen verhindern jedoch die simultane Verwertung von Glucose und anderen Kohlenstoffquellen wie etwa Essigsäure. Eine weitere große Herausforderung ist eine durch Essigsäure verursachte Hemmung der Methionine-Biosynthese.

Das Hauptaugenmerk dieser Arbeit war, in *E. coli* W eine gleichzeitige Essigsäure-Verwertung zu ermöglichen und die Essigsäure Resistenz zu verstärken. Daher wurde die Acetyl-CoA-Synthetase, eines der Schlüsselenzyme, die an der Essigsäure-Assimilation beteiligt sind, erfolgreich modifiziert um deren Aktivität, welche in Verbindung mit Glucose streng kontrolliert wird zu deregulieren. Zusätzlich wurde ein aggregationsanfälliges Enzym aus der Methioninbiosynthese modifiziert, um die Essigsäure- und Hitzebeständigkeit zu erhöhen. Eine Vektorbibliothek verschiedener Genkombinationen wurde erstellt und mit den Wirtszellen transformiert um diese in Batch- und Fed-Batch-Kultivierungen zu charakterisieren.

Als Ergebnis stellte sich ein Stamm heraus, welcher in einer gemischten Batch-Kultivierung bei hohen Essigsäure und Glukose Konzentrationen ( $10 \text{ g l}^{-1}$ ) eine 2.7-fach erhöhte spezifische Essigsäure-Aufnahmerate vorwies. Bei Kultivierungen mit Essigsäure als alleinige Kohlenstoffquelle, konnte zudem die Kultivierungsdauer signifikant verringert werden. Vielversprechend zeigten sich manche Stämme auch im Bezug auf eine verbesserte Essigsäure-Resistenz; jedoch sind dafür noch weitere Analysen erforderlich.



# Contents

<b>Acknowledgements</b>	<b>iii</b>
<b>Declaration of Authorship</b>	<b>v</b>
<b>Abstract</b>	<b>vii</b>
<b>Zusammenfassung</b>	<b>ix</b>
<b>1 Introduction</b>	<b>1</b>
1.1 <i>Escherichia coli</i> as host organism . . . . .	1
1.2 Acetogenesis . . . . .	2
1.3 Relevance of fermentation media . . . . .	4
1.3.1 Acetate as potential carbon source . . . . .	5
1.4 Substrate utilisation . . . . .	7
1.4.1 Carbon catabolite repression . . . . .	7
1.4.2 Acetate utilising pathways . . . . .	8
1.4.3 Glyoxylate shunt and gluconeogenesis . . . . .	9
1.4.4 Acs regulation . . . . .	11
Mutated Acs . . . . .	11
1.5 Acetate tolerance . . . . .	13
1.5.1 Methionine biosynthetic pathway . . . . .	14
Mutated MetE . . . . .	15
1.6 Basics of Golden Gate cloning . . . . .	16
1.6.1 GoldenMOCS . . . . .	16
1.7 Aim of work . . . . .	18
<b>2 Materials and methods</b>	<b>19</b>
2.1 Strains and plasmids . . . . .	19
2.1.1 <i>E. coli</i> strains . . . . .	19
2.1.2 Plasmids . . . . .	19
pIDTSmart vector . . . . .	19

pUC19 vector . . . . .	21
Backbone 1 . . . . .	21
Backbone 2 . . . . .	22
Backbone 3 . . . . .	22
Promoter and terminator . . . . .	22
2.1.3 Primer . . . . .	24
2.2 Media preparation and composition . . . . .	24
Lysogeny broth . . . . .	25
DeLisa medium . . . . .	25
Antibiotics . . . . .	26
2.2.1 Buffer solution . . . . .	27
2.3 Preparation, purification, and analysis of DNA . . . . .	28
2.3.1 DNA amplification (PCR) . . . . .	28
2.3.2 Agarose gel electrophoresis . . . . .	28
2.3.3 Extraction and purification of DNA fragments . . . . .	29
2.3.4 Quantification of DNA/nucleic acids . . . . .	30
2.3.5 Isolation of plasmid DNA (Miniprep) . . . . .	30
2.3.6 Restriction digest of plasmid DNA . . . . .	30
2.3.7 Sequencing . . . . .	31
2.4 Golden Gate assembly . . . . .	31
2.5 Transformation of DNA into <i>E. coli</i> . . . . .	32
2.5.1 Preparation of chemically competent cells . . . . .	32
2.5.2 Chemical transformation . . . . .	33
2.6 Strain conservation . . . . .	33
2.7 Cultivation . . . . .	33
2.7.1 Preculture and inoculum . . . . .	33
2.7.2 Shake flask cultivation . . . . .	34
2.7.3 Elemental analysis . . . . .	34
2.7.4 Bioreactor cultivations . . . . .	36
2.8 Analytical methods . . . . .	37
2.8.1 Cell biomass concentration . . . . .	37
2.8.2 HPLC . . . . .	38
2.8.3 Statistical data evaluation . . . . .	39
<b>3 Results</b>	<b>49</b>
3.1 Genetic constructs . . . . .	49
3.1.1 Characteristics of enzymes and mutations . . . . .	50

3.1.2	Nomenclature . . . . .	53
3.2	Strain characterization in batch cultivations . . . . .	54
3.2.1	Batch cultivations on glucose-acetate . . . . .	54
	ACS and ACS_L641P . . . . .	54
	METE_mut . . . . .	60
	ACS_METE_mut_COBB . . . . .	62
3.2.2	Batch cultivations on glucose . . . . .	65
	ACS_L641P . . . . .	65
3.2.3	Batch cultivations on acetate . . . . .	67
	ACS_L641P . . . . .	67
3.2.4	Fed-batch cultivations on glucose-acetate . . . . .	69
	ACS_L641P . . . . .	69
3.3	Shake flask cultivations . . . . .	74
3.3.1	Improved thermal tolerance by metE_mut . . . . .	74
<b>4</b>	<b>Conclusion and further perspectives</b>	<b>77</b>
	<b>Bibliography</b>	<b>79</b>
<b>5</b>	<b>Appendix</b>	<b>A. I</b>
5.1	Elemental analysis raw data . . . . .	A. I
5.2	Fermentation raw data . . . . .	A. II
5.2.1	Batches . . . . .	A. II
5.2.2	Fed-batches . . . . .	A. XI
5.3	Reprint permissions . . . . .	A. XV



# List of Figures

1	Acetate synthesis and utilisation pathways . . . . .	3
2	The phosphotransferase system (Pts) . . . . .	8
3	Central metabolism pathways . . . . .	10
4	Posttranslational control of Acs by the SDPADS . . . . .	12
5	Methionine biosynthetic pathway . . . . .	15
6	GoldenMOCS cloning scheme . . . . .	17
7	Backbone 1 . . . . .	21
8	Backbone 2 . . . . .	22
9	Backbone 3 . . . . .	23
10	Gene constructs . . . . .	49
11	Batches on glucose-acetate – VC . . . . .	55
12	Batches on glucose-acetate – ACS . . . . .	56
13	Batches on glucose-acetate – ACS_L641P . . . . .	57
14	Batches on glucose-acetate – VC vs. ACS_L641P . . . . .	58
15	Batches on glucose-acetate – METE_mut . . . . .	61
16	Batches on glucose-acetate – ACS_METE_mut_COBB . . . . .	63
17	Batches on glucose – VC – ACS_L641P . . . . .	65
18	Batches on acetate – VC . . . . .	68
19	Batches on acetate – ACS_L641P . . . . .	68
20	Fed-batches on glucose-acetate – VC . . . . .	70
21	Fed-batches on glucose-acetate – ACS_L641P . . . . .	71
22	Fed-batches (mean) on glucose-acetate – VC – ACS_L641P . . . . .	72
23	Comparative growth at various temperatures . . . . .	75
24	Comparative glucose uptake at various temperatures . . . . .	76
A.1	Reprint permission of Figure 1 and 3 . . . . .	A. XV
A.2	Reprint permission of Figure 2 . . . . .	A. XVI
A.3	Reprint permission of Figure 4 . . . . .	A. XVII
A.4	Reprint permission of Figure 5 . . . . .	A. XVII

A.5 Reprint permission of Figure 6 . . . . .	A. XVIII
--	----------



# List of Tables

1	Used <i>E. coli</i> strains . . . . .	19
2	List of plasmids . . . . .	20
3	Fusion sites and Linker . . . . .	23
4	Primer list . . . . .	24
5	Lysogeny broth . . . . .	25
6	Composition of DeLisa medium . . . . .	26
7	Trace metal stock solutions DeLisa medium . . . . .	26
8	Used antibiotics . . . . .	27
9	Buffer soulutions . . . . .	27
10	PCR reaction mix for gene amplification . . . . .	28
11	PCR plan for gene amplification . . . . .	28
12	Thermocycler program amplification . . . . .	29
13	Protocol for restriction digestion . . . . .	30
14	Protocol for Golden Gate assembly reaction . . . . .	32
15	Thermocycler program for Golden Gate assemblies . . . . .	32
16	Main components of <i>E. coli</i> W . . . . .	35
17	Minor components of <i>E. coli</i> W . . . . .	36
18	Standard solutions for 5-point calibration . . . . .	39
19	Rates for batches on glucose-acetate – VC – ACS – ACS_L641P . . . . .	54
20	Yields for batches on glucose-acetate – VC – ACS – ACS_L641P . . . . .	55
21	Rates for batches on glucose-acetate – VC – METE_mut . . . . .	60
22	Yields for batches on glucose-acetate – VC – METE_mut . . . . .	61
23	Rates for batches on glucose-acetate – ACS – ACS_L641P – METE_mut_COBB . . . . .	62
24	Yields for batches on glucose-acetate – ACS – ACS_L641P– METE_mut_COBB . . . . .	63
25	Rates for batches on glucose – VC – ACS_L641P . . . . .	66
26	Yields for batches on glucose – VC – ACS_L641P . . . . .	66
27	Rates for batches on acetate – VC – ACS_L641P . . . . .	67

28	Yields for batches on acetate – VC – ACS_L641P . . . . .	67
29	Rates for fed-batches on glucose-acetate – VC – ACS_L641P . . . . .	71
30	Yields for fed-batches on glucose-acetate – VC – ACS_L641P . . . . .	73
31	MSU-phase in fed-batch . . . . .	73
A.1	Raw data: Main components of <i>E. coli</i> W . . . . .	A. I
A.2	Raw data: Minor components of <i>E. coli</i> W . . . . .	A. I
A.3	F02 B <i>E. coli</i> W metE_mut glc-ace # 1 . . . . .	A. II
A.4	F02 D <i>E. coli</i> W acs_metE_mut_cobB glc-ace # 1 . . . . .	A. II
A.5	F05 A <i>E. coli</i> W vector control glc-ace # 1 . . . . .	A. III
A.6	F05 C <i>E. coli</i> W acs_L641P glc-ace # 2 . . . . .	A. III
A.7	F05 D <i>E. coli</i> W acs glc-ace # 1 . . . . .	A. III
A.8	F06 A <i>E. coli</i> W acs_L641P glc-ace # 3 . . . . .	A. IV
A.9	F06 B <i>E. coli</i> W metE_mut glc-ace # 2 . . . . .	A. IV
A.10	F06 C <i>E. coli</i> W metE_mut glc-ace # 3 . . . . .	A. IV
A.11	F07 A <i>E. coli</i> W acs glc-ace # 2 . . . . .	A. V
A.12	F07 B <i>E. coli</i> W acs glc-ace # 3 . . . . .	A. V
A.13	F07 D <i>E. coli</i> W vector control glc-ace # 2 . . . . .	A. VI
A.14	F08 C <i>E. coli</i> W acs_L641P glc-ace # 1 . . . . .	A. VI
A.15	F08 D <i>E. coli</i> W vector control glc-ace # 3 . . . . .	A. VII
A.16	F09 A <i>E. coli</i> W acs_L641P ace # 1 . . . . .	A. VII
A.17	F09 B <i>E. coli</i> W acs_L641P ace # 2 . . . . .	A. VIII
A.18	F09 C <i>E. coli</i> W vector control ace # 1 . . . . .	A. VIII
A.19	F09 D <i>E. coli</i> W vector control ace # 2 . . . . .	A. IX
A.20	F10 A <i>E. coli</i> W acs_L641P glc # 1 . . . . .	A. IX
A.21	F10 B <i>E. coli</i> W acs_L641P glc # 2 . . . . .	A. IX
A.22	F10 C <i>E. coli</i> W vector control glc # 1 . . . . .	A. X
A.23	F10 D <i>E. coli</i> W vector control glc # 2 . . . . .	A. X
A.24	F11 A <i>E. coli</i> W vector control glc-ACE # 1 . . . . .	A. XI
A.25	F11 B <i>E. coli</i> W vector control glc-ace # 2 . . . . .	A. XII
A.26	F11 C <i>E. coli</i> W acs_L641P glc-ace # 1 . . . . .	A. XIII
A.27	F11 D <i>E. coli</i> W acs_L641P glc-ace # 2 . . . . .	A. XIV

# List of Abbreviations

<b>aa</b>	<b>amino acid</b>
<b>Ac-CoA</b>	<b>acetyl-coenzyme A</b>
<b>Ac</b>	<b>adenylate cyclase</b>
<b>ac</b>	<b>autoclaved</b>
<b>ACE</b>	<b>acetate</b>
<b>AckA</b>	<b>acetate kinase A</b>
<b>Acn</b>	<b>aconitase</b>
<b>Acs</b>	<b>acetyl-coenzyme A synthetase (EC 6.2.1.1)</b>
<b>AMP</b>	<b>adenosine monophosphate</b>
<b>Amp</b>	<b>ampicillin</b>
<b>ATP</b>	<b>adenosine triphosphate</b>
<b>C-recovery</b>	<b>carbon recovery</b>
<b>C-balance</b>	<b>carbon balance</b>
<b>cAMP</b>	<b>cyclic adenosine monophosphate</b>
<b>CCR</b>	<b>carbon catabolite repression</b>
<b>CH<sub>2</sub>=THF</b>	<b>5,10-methylenetetrahydrofolate</b>
<b>CH<sub>3</sub>-THF</b>	<b>5-methyltetrahydrofolate</b>
<b>Cmol</b>	<b>mole carbon</b>
<b>CoASH</b>	<b>coenzyme A</b>
<b>CobB</b>	<b>acetyl-CoA synthetase deacetylase</b>
<b>Crp</b>	<b>cyclic adenosine monophosphate receptor protein</b>
<b>Cs</b>	<b>citrate synthase</b>
<b>dH<sub>2</sub>O</b>	<b>distilled water (in this work deionised with reverse osmosis)</b>
<b>DNA</b>	<b>deoxyribonucleic acid</b>
<b>EDTA</b>	<b>ethylenediaminetetraacetic acid</b>
<b>FAD</b>	<b>flavinadenine dinucleotide</b>
<b>Frd</b>	<b>fumarate reductase</b>
<b>FS</b>	<b>fusion site</b>
<b>Fuma</b>	<b>fumarase</b>
<b>Gapdh</b>	<b>glyceraldehyde-3-phosphate dehydrogenase</b>

<b>gDNA</b>	<b>g</b> enomic <b>d</b> eoxyribonucleic <b>a</b> cid
<b>GG</b>	<b>G</b> olden <b>G</b> ate
<b>GLC</b>	<b>g</b> lucose
<b>GOI</b>	<b>g</b> ene <b>o</b> f interest
<b>GS</b>	<b>g</b> lyoxylate <b>s</b> hunt
<b>HCDC</b>	<b>h</b> igh <b>c</b> ell <b>d</b> ensity <b>c</b> ultivation
<b>HPr</b>	<b>h</b> eat-stable <b>p</b> rotein or <b>h</b> istidine <b>p</b> rotein
<b>Icl</b>	isocitrate <b>l</b> yase
<b>IclR</b>	isocitrate <b>l</b> yase <b>r</b> egulator
<b>Idh</b>	isocitrate <b>d</b> ehydrogenase
<b>in</b>	<b>i</b> nlet
<b>IPTG</b>	isopropyl $\beta$ -D-1-thiogalactopyranoside
<b>Kan</b>	<b>k</b> anamycin
<b>2-KG</b>	<b>2-k</b> etoglutarate or alpha- <b>k</b> etoglutarate
<b>Kgdh</b>	2- <b>k</b> etoglutarate <b>d</b> ehydrogenase
<b>LB</b>	lysogeny <b>b</b> roth
<b>MaeB</b>	<b>m</b> alate <b>e</b> nzyme <b>B</b> (malate dehydrogenase)
<b>Mas</b>	<b>m</b> alate <b>s</b> ynthase
<b>IDHK/P</b>	isocitrate <b>d</b> ehydrogenase <b>k</b> inase/ <b>p</b> hosphatase
<b>MCS</b>	<b>m</b> ultiple <b>c</b> loning <b>s</b> ite
<b>Mdh</b>	<b>m</b> alate <b>d</b> ehydrogenase
<b>MetE</b>	cobalamin-independent <b>m</b> ethionine synthase (EC 2.1.1.14)
<b>MethH</b>	cobalamin-dependent <b>m</b> ethionine synthase (EC 2.1.1.13)
<b>MOCS</b>	<b>m</b> ultiple <b>o</b> rganism <b>c</b> loning <b>s</b> ystem
<b>MOPS</b>	3-( <i>N</i> - <b>m</b> orpholinopropanesulfonic)
<b>MSU-phase</b>	<b>m</b> ain <b>s</b> ubstrate <b>u</b> ptake- <b>p</b> hase
<b>OAA</b>	<b>o</b> xaloacetate
<b>OD<sub>600</sub></b>	optical <b>d</b> ensity at a wavelength of <b>600</b> nm
<b>Omol</b>	<b>m</b> ole <b>o</b> xygen
<b>out</b>	<b>o</b> utlet
<b>Pat</b>	<b>p</b> rotein <b>a</b> cetyltransferase
<b>PckA</b>	<b>p</b> yruvate <b>c</b> arboxy <b>k</b> inase <b>A</b>
<b>PCR</b>	<b>p</b> olymerase <b>c</b> hain <b>r</b> eaction
<b>PdhC</b>	<b>p</b> yruvate <b>d</b> ehydrogenase <b>c</b> omplex
<b>Pep</b>	2- <b>p</b> hoshoenol <b>p</b> yruvate
<b>Pfk</b>	<b>p</b> hosphofructokinase
<b>Pfl</b>	<b>p</b> yruvate <b>f</b> ormate <b>l</b> yase

<b>pH</b>	potential of <b>h</b> ydrogen
<b>PoxB</b>	pyruvate <b>o</b> xidase <b>B</b>
<b>ppGpp</b>	guanosine <b>t</b> etraposphate
<b>Ppsa</b>	2- <b>p</b> hosphoenolpyruvate <b>s</b> ynthase
<b>Pta</b>	<b>p</b> ospho <b>t</b> ransacetylase
<b>Pts</b>	2- <b>p</b> hosphoenolpyruvate-carbohydrate phosphotransferase <b>s</b> ystem
<b>rpm</b>	revolutions <b>p</b> er <b>m</b> inute
<b>SAM</b>	<b>S</b> -adenosyl <b>m</b> ethionine
<b>Scsc</b>	succinyl- <b>C</b> oA <b>s</b> ynthetase <b>c</b> omplex
<b>Sdh</b>	succinate <b>d</b> ehydrogenase
<b>SDPADS</b>	sirtuin- <b>d</b> eendent <b>p</b> rotein <b>a</b> cetylation/ <b>d</b> eacetylation <b>s</b> ystem
<b>sf</b>	sterile <b>f</b> iltrated
<b>SfcA</b>	malat enzyme (malate dehydrogenase)
<b>Sir2</b>	silent information regulator <b>2</b>
<b>T<sub>a</sub></b>	annealing <b>t</b> emperature
<b>T<sub>m</sub></b>	<b>m</b> elting <b>t</b> emperature
<b>TAE</b>	Tris/ <b>a</b> cetate/ <b>E</b> DTA
<b>TBE</b>	Tris/ <b>B</b> orate/ <b>E</b> DTA
<b>TFB</b>	<b>t</b> ransformation <b>b</b> uffer
<b>THF</b>	tetra <b>h</b> ydrofolate
<b>Tpia</b>	triose <b>p</b> hosphate isomerase
<b>TRIS</b>	<b>t</b> ris (hydroxymethyl)aminomethane
<b>vc</b>	vector <b>c</b> ontrol
<b>vvm</b>	volume of air per <b>v</b> olume of medium per <b>m</b> inute
<b>v/v</b>	volume per <b>v</b> olume
<b>v/w</b>	volume per <b>w</b> eight
<b>w/w</b>	<b>w</b> eight per <b>w</b> eight



# List of Symbols

Symbol	Designation	Unit
f	femto	$10^{-15}$
Pa	Pascal	$\text{kg m}^{-1} \text{s}^{-2}$
pn	pinch	0.25 to 0.5 g
rpm	revolution per minute	$\text{min}^{-1}$
sl	standard liter	sl
U	Units	$\mu\text{mol min}^{-1}$
V	Volt	$\text{kg m}^{-2} \text{s}^{-3} \text{A}^{-1}$
$c_i$	molar concentration of component $i$	$\text{mol l}^{-1}$
$ex_{H_2O}$	water content in off-gas	%
$\dot{V}$	volumetric gas flow rate	$\text{l h}^{-1}$
$m_i$	mass amount of component $i$	g
$M_i$	molar mass of comonent $i$	$\text{g mol}^{-1}$
$n_i$	molar amount or component $i$	mol
$\sum n_{CO_2}$	accumulated total amount of carbon dioxide	mol or Cmol
$\sum n_O$	accumulated total amount of oxygen	Omol
$b_{NH_3}$	specific titration rate of base $NH_3$	$\text{mmol g}^{-1} \text{h}^{-1}$
$q_i$	specific uptake/production rate of component $i$	$\text{mmol g}^{-1} \text{h}^{-1}$
$r_i$	volumetric uptake rate of component $i$	$\text{mmol l}^{-1} \text{h}^{-1}$
$Ra_{inert}$	inert gas ratio	—
$s_{xh}$	substrate conc. in the fermenter $x$ hours after inoculation	$\text{mmol l}^{-1}$
$S, \sum n_{c,i_{reactor}}$	total amount of substrate in the fermentation broth	Cmol
$t$	time	h
$v_i$	coefficient of component $i$	—
$x_{xh}, \rho_{cdw_{xh}}$	biomass conc. in the fermenter $x$ hours after inoculation	$\text{g l}^{-1}$
$X, n_{c,cdw_{reactor}}$	total amount of biomass in the fermentation broth	Cmol
$y_{i,in/out}$	content of component $i$ in gas flow inlet/outlet	%
$y_{wet}$	oxygen content in off-gas diluted by water content	%

$Y_{i/j}$	yield of component $i$ to $j$	$\text{mol mol}^{-1}$
$\rho_i$	concentration of component $i$	$\text{g l}^{-1}$
$\mu$	specific growth rate	$\text{h}^{-1}$



# 1 Introduction

## 1.1 *Escherichia coli* as host organism

The prokaryotic model host *Escherichia coli* is an important pathogen and commensal and a key organism for biotechnological applications (Archer et al., 2011). It has been engineered for the synthesis of a wide variety of metabolites which explains the extensive physiological knowledge, well-known features of its central carbon mechanism and the availability of genome sequence information (Archer et al., 2011; Pourmir and Johannes, 2012). *E. coli* was one of the earliest and most commonly used organisms for the production of heterologous proteins and was manipulated for the first useful application of recombinant DNA technology producing human insulin in 1982 (Terpe, 2006; Williams et al., 1982). Moreover, for the applied production of commodity chemicals such as succinic acid, lactic acid, ethanol, pyruvate and 1,3-propanediol, *E. coli* was successfully manipulated by altering fermentative pathway by blocking or introducing crucial branch-point enzymes (Chotani et al., 2000).

The advantages of the *E. coli* system include genetic simplicity, rapid growth, rapid expression of heterologous genes, high product yields, well-understood genetics and its ease and cost-effective culture. Its genome can be precisely and quickly modified with the availability of improved genetic tools, promoter control is not difficult, and plasmid copy number can be readily altered. Apart from that, the *E. coli* system also has some drawbacks, like producing unglycosylated proteins and proteins with endotoxins or the refolding difficulty of proteins with many disulfide bonds and proteins produced as inclusion bodies (Lee, 1996; Cornelis, 2000). Another disadvantage occurs in particular during high cell density cultivations (HCDC) (e.g., greater than 50 g l<sup>-1</sup> dry cell weight) in toxicity due to acetate formation, which is discussed in detail in 1.3.1 (Kleman and W. Strohl, 1994).

The most commonly used *E. coli* laboratory strains are derivatives of only five strains, K-12, B, C, W and Crooks. They are all termed as Risk Group I organisms in biological

safety guidelines as they are unable to colonise the human gut (A. P. Bauer, Ludwig, and Schleifer, 2008; Archer et al., 2011).

Particular outstanding is the *E. coli* W (ATCC 9637), due to its improved properties for industrial applications. The initial W derives from Selman A. Waksman, who first isolated this strain in 1943 (Archer et al., 2011). Besides its good tolerance for environmental stresses such as high ethanol concentrations, acidic conditions, high temperatures and osmotic stress it also produces low amounts of acetate even without tight sugar control. The *E. coli* W is a very fast growing strain and can be grown with ease to HCDC during fed-batch (Shiloach and S. Bauer, 1975; Nagata, 2001).

## 1.2 Acetogenesis

Apart from low acetate secretion of *E. coli* W, for most *E. coli* strains the formation of by-products such as acetate appears as a main hindrance in the production of specific metabolites. The reason of *E. coli* excreting acetate into the environment can either be oxygen starved conditions or due to carbon flux overflow. In the former anaerobic case, the tricarboxylic acid cycle (TCA) does not function in the usual manner, which results in a branched pathway and the excretion of mixed acid fermentation products (ethanol, acetate, formate, lactate, succinate), among which acetate is the most abundant (O'Beirne and Hamer, 2000).

In the second case, carbon flux exceeds the metabolic capacity of the central pathway, the system becomes unbalanced resulting in the excretion of acetate (E. El-Mansi and Holms, 1989). This aerobic acetogenesis has been explained as the "overflow metabolism" (Shin, Chang, and J. G. Pan, 2009) and there have been many theories proposed about different possible limitations in metabolism like limitations in the TCA cycle (Majewski and Domach, 1990), respiratory chain (Han, H. C. Lim, and Hong, 1992), or glyoxylate shunt (GS) activity (Shin, Chang, and J. G. Pan, 2009; Waegeman et al., 2011) and competition for membrane space (Zhuang, Vemuri, and Mahadevan, 2011).

However, the pivotal cause for *E. coli* aerobic and anaerobic acetogenesis is due to the need to regenerate the  $\text{NAD}^+$  consumed by the glycolysis and to recycle the coenzyme A (CoASH) required to convert pyruvate to acetyl-CoA. In oxidative acetogenesis, pyruvate gets first irreversibly decarboxylated into acetyl-CoA under consumption of CoASH and  $\text{NAD}^+$  by the pyruvate dehydrogenase complex (PdhC) (Figure 1). In return, it releases two NADH per glucose which can inhibit in high concentrations the PdhC. Therefore

this reaction does not operate in conditions that do not favour the reduction of  $\text{NAD}^+$  to NADH. The built-up acetyl-CoA is subsequently catalysed by the Pta-AckA pathway. This pathway stands for two reversible reactions:

- phosphate acetyltransferase (Pta), converting acetyl-CoA and inorganic phosphate to acetyl~P and a regenerating CoASH and
- acetate kinase (AckA), generating acetate and ATP.

Through a second pyruvate-decarboxylating enzyme, pyruvate oxidase (PoxB), which is non essential for *E. coli*, pyruvate can be directly converted to acetate by reducing flavin adenine dinucleotide (FAD) (Wolfe, 2005).

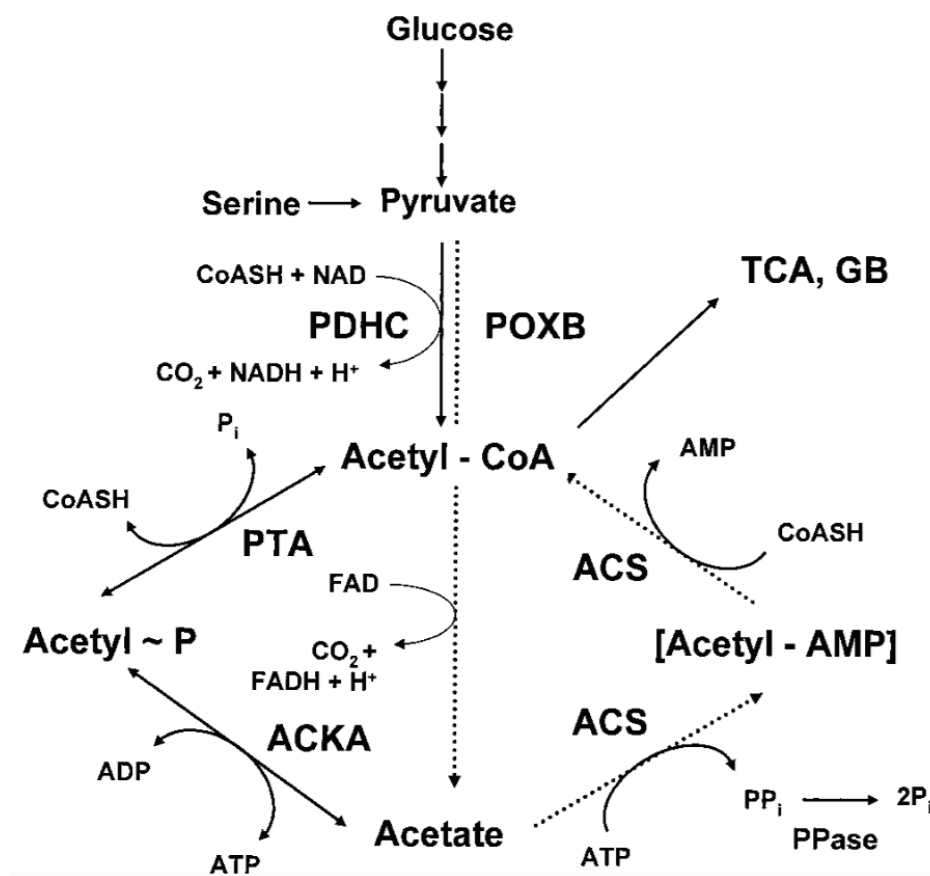


FIGURE 1: Aerobic acetate synthesis and utilisation pathways . pyruvate dehydrogenase complex (PdhC), pyruvate oxidase (PoxB), phosphotransacetylase (Pta), acetate kinase (AckA), AMP-forming acetyl-CoA synthetase (Acs), pyrophosphatase (PPase), tricarboxylic acid cycle (TCA), glyoxylate bypass/shunt (GB). The dotted arrows denote the proposed PdhC bypass formed by PoxB and Acs. Reprinted from Wolfe, 2005, Copyright ©2005, American Society for Microbiology

During anaerobic and microaerophilic conditions, *E. coli* cells catalyse a non oxidative reaction via pyruvate formate-lyase (PFL) which converts pyruvate to acetyl-CoA and

formate (not shown). The acetyl-CoA is thereupon conducted to acetate mainly via the Pta-AckA pathway (Zelcbuch et al., 2016).

### 1.3 Relevance of fermentation media

Nutrients, including carbon and nitrogen sources can have an inhibitory effect on *E. coli* cell growth when they are present in certain concentrations: glucose 50 g l<sup>-1</sup>, ammonia 3 g l<sup>-1</sup>, iron 1.15 g l<sup>-1</sup>, magnesium 8.7 g l<sup>-1</sup>, phosphorous 10 g l<sup>-1</sup>, zinc 0.038 g l<sup>-1</sup> (Riesenberger, 1991).

In a defined medium which is mainly used for HCDC, starting concentrations are below the inhibitory threshold to maintain a high specific growth rate. Semi-defined or complex media with nutrients such as peptone and yeast extract however vary in composition and quality and make fermentations less reproducible. For designing a balanced nutrient medium, all the necessary components for supporting cell growth must be considered while inhibitory concentrations should be avoided.

Glucose is preferably implemented in *E. coli*-based industrial-scale fermentation processes as the primary feedstock due to its high uptake rates and the high specific growth rates associated with glucose. However, an arising imbalance between glucose uptake and the demands for both, biosynthesis and energy production leads to an increase of aerobic acetate production especially at higher growth rates. The critical specific growth rate that leads to acetate formation varies among the strains and the medium used (Lee, 1996).

Usual strategies to prevent acetate accumulation include decreasing the sugar uptake rate ( $q_s$ ) on a molecular level (Lara et al., 2008) for the batch cultivation or confining the feed of sugar on a process level (Kleman and W. Strohl, 1994), which is generally applied for fed-batch and continuous cultivations. On the molecular level, it is feasible to engineer the transport system in *E. coli*. In a previous study, the natural system for glucose transport, the phosphotransferase system (PTS) (see more in 1.4.1) has been deleted and glucose was alternatively internalized through the galactose permease. This transporter is slower and does not directly produce pyruvate, the main precursor of acetyl-CoA. Consequently the acetate accumulation could be reduced while the specific growth rate remained the same and the product production rate increased (De Anda et al., 2006).

Another attempt for reducing the acetate excretion would be to replace glucose. Using glycerol as carbon source for HCDC can be achieved relatively easily. Because of

the lower uptake rate, compared to glucose, glycerol leads to a reduced flux of carbon through glycolysis and hence to a reduced acetate formation. However it should be considered that cell growth on glycerol is more reduced compared to glucose (Korz et al., 1995; Lee, 1996). An additional cheap feedstock is sucrose. *E. coli* W is the only known *E. coli* strain to date which can utilise sucrose as fast as glucose (Archer et al., 2011). In a study with *E. coli* W, lower acetate accumulation was observed in sucrose compared to glucose cultures, which makes this combination valuable for industrial applications (Arifin et al., 2014).

#### 1.3.1 Acetate as potential carbon source

Acetate is the primary by-product produced by *E. coli* during aerobic fermentations with concentrations ranging between 1 and 30 g l<sup>-1</sup> (Aristidou, San, and Bennett, 1994). Growth inhibitory concentrations of acetate vary between 5 and 10 g l<sup>-1</sup> depending on the *E. coli* strain and the media (Gschaedler, Le, and Boudrant, 1994).

Like other weak acids, acetate exists at neutral pH in both dissociated (CH<sub>3</sub>COO<sup>-</sup>) and protonated (CH<sub>3</sub>COOH) states. The more lipophilic protonated form can easily pass through the lipid membrane of the cell, where it dissociates at the higher internal pH (ca.7.5) to CH<sub>3</sub>COO and H<sup>+</sup>. The proton acidifies the cytoplasm and the anion increases the internal osmotic pressure. Additional protonated acid is formed in the medium by the equilibrium, causing a electroneutral hydrogen ion influx. The external pH rarely changes due to the large volume of buffered medium. The decrease in intracellular pH however causes an uncoupling effect. The homeostatic mechanisms of *E. coli* requires energy to adjust to this decrease in intracellular pH (Repaske and Adler, 1981; Smirnova and Oktyabrskii, 1988).

These two main impacts (unbalanced anion concentration and a weakened proton motive force) and further factors mentioned in 1.5.1, are responsible for growth inhibition triggered by acetate (Roe, McLaggan, et al., 1998).

However, *E. coli* can reassimilate excreted acetate which is only partly oxidised, and serves as carbon and energy source once acetogenic carbon sources, such as glucose are depleted. This transition from acetate production (dissimilation) to acetate utilisation (assimilation) (detailed description in 1.4.2) is termed "acetate switch" (Luli and W. R. Strohl, 1990; Wolfe, 2005).

Apart from excretion by *E. coli*, acetate is a promising carbon source as it is a cheap industrial waste product contained in a broad variety of materials (H. G. Lim et al., 2018). For example, acetate is produced as intermediate by stepwise degradation of waste activated sludge under anaerobic conditions (Mao et al., 2015). Various microorganisms recycle the organic waste into several metabolites, whereas currently acetate is utilised as a carbon source for methanogens to produce methane (Adekunle and Okolie, 2015).

During lignocellulose pretreatment for biochemical conversion, acetate is formed as by-product by deacetylation of hemicellulose (Jönsson and Martin, 2016). The hydrolysates often vary in their acetate concentration which is more than  $10\text{ g l}^{-1}$ , however its not properly utilised as acetate inhibits microbial cell growth (Mills, Sandoval, and Gill, 2009).

Acetate can be as well produced by acetogens via direct fermentation of industrial syn-gas including CO, CO<sub>2</sub>, and H<sub>2</sub>. Several microbes such as *Acetobacterium* and *Clostridium* use the Wood-Ljungdahl pathway which converts CO<sub>2</sub> in two different branches into CO and formate which are condensed to acetyl-CoA (Straub et al., 2014; Schuchmann and Müller, 2014).

Furthermore, current studies demonstrated CO<sub>2</sub> fixation aided by electricity. In this process called microbial electrosynthesis, unique microorganisms (e.g., *Sporomusa ovata*) accept electrons directly from a graphite electrode through a biofilm to produce acetate, from CO<sub>2</sub> and electricity. Acetate concentrations of  $10.5\text{ g l}^{-1}$  over 20 days have been reached so far with this process (Marshall et al., 2012).

Processes like this, have a huge potential in the reduction of greenhouse gases and provide acetate as an attractive feedstock for the conversion into more value-added chemicals. Biochemical production with acetate as the sole carbon source have already been reported for organic acids for *E. coli* W (Li et al., 2016; Noh et al., 2018). Fatty acid production was as well tested in *E. coli* and even the production of a single chain monellin protein was demonstrated in a *E. coli* BL21 strain (Xiao et al., 2013; Leone et al., 2015). Whereas, acetate as a co-substrate is highly promising to increase the carbon yield for the production of biochemicals whose main precursor is acetyl-CoA. The conversion of pyruvate to acetyl-CoA involves an inevitable carbon loss in form of carbon dioxide, while produced from acetate there is no carbon loss (Figure 3).

However, there are still some drawbacks like insufficient acetate tolerance and hampered acetate utilisation in mixed fermentations which need to be improved.

## 1.4 Substrate utilisation

### 1.4.1 Carbon catabolite repression

In mixed substrate fermentations of *E. coli*, preferentially carbon sources are used which are most easily accessible and allow fastest growth. Consequently, sugars such as glucose are utilised first instead of co-metabolising secondary carbon sources like acetate. This regulatory phenomenon has been called glucose repression or more generally, carbon catabolite repression (CCR). Another term which is often used in this context is diauxie. Diauxic growth is defined as the sequential use of carbon sources in a mixture of different substrates. The preferred sugar is consumed first, followed by a lag phase before the use of the less preferred substrate (Görke and Stülke, 2008).

The main CCR mechanisms of *E. coli* are mediated via a multiprotein phosphorylase system called Pts (phosphoenolpyruvate-carbohydrate phosphotransferase system). The Pts is the main glucose transport system in *E. coli* transporting carbohydrates across the cytoplasmic membrane via simultaneous phosphorylation. The phosphorylation of the carbohydrate should therefore prevent the transporter from recognizing the substrate again and enables a one-way gradient for primary carbon sources like glucose (Figure 2). The Pts composes at least three distinct proteins: enzyme I (EI), histidine or heat-stable protein (HPr) and enzyme II (EII).

In the process of sugar transport, 2-phosphoenolpyruvate (Pep) autophosphorylates a histidine residue in the EI which in succession transfers the phosphoryl group to the His15 residue of HPr. The HPr again transmits the phosphoryl group to a histidine residue in the A domains of EII. Further on, the phosphoryl group is transferred to a cysteine residue in the EIIB domain and from there to the carbohydrate during its uptake through the transmembrane domain EIIC. The phosphoryl transfer reactions between Pts proteins are all reversible and are determined by two factors, the Pts transport activity and the Pep to pyruvate ratio, which reflects the flux through glycolysis (Görke and Stülke, 2008).

The glucose specific EIIA<sup>Glc</sup> is the central regulator of carbon metabolism in *E. coli*. At high glucose concentrations and during high fluxes of glycolysis, the A domain of EIIA<sup>Glc</sup> is predominantly dephosphorylated. In this state, it binds and inactivates metabolic enzymes and transporters of secondary carbon sources (not shown).

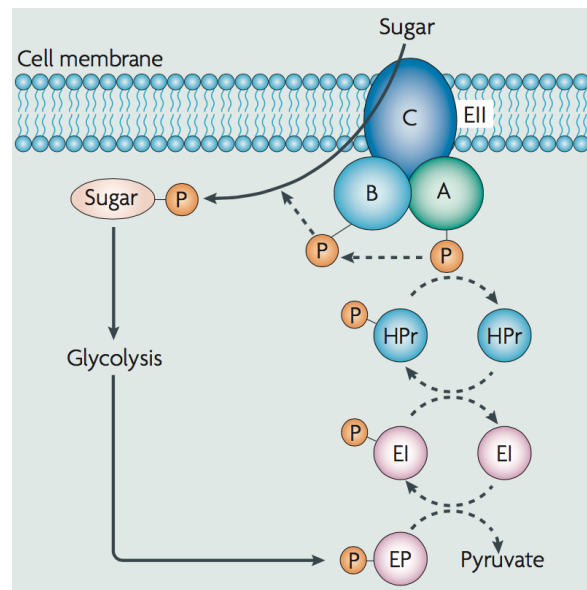


FIGURE 2: The phosphoenolpyruvate–carbohydrate phosphotransferase system (Pts). 2-phosphoenolpyruvate (Pep), enzyme I (EI), histidine protein(HPr), enzyme II (EII). The dashed arrows show phosphate transfer. Reprinted by permission from Springer Customer Service Centre GmbH: on behalf of Cancer Research UK: : Springer Nature, Nature Reviews Microbiology, Görke and Stülke, 2008

Conversely, when the glucose level is low,  $EIIA^{Glc}$  gets phosphorylated and subsequently binds and activates the membrane-bound adenylate cyclase (Ac) (not shown). The activated Ac consequently transforms ATP to cyclic AMP (cAMP) which triggers a complex formation with the transcription activator Crp (cAMP receptor protein). This activated cAMP-Crp complexes bind and activate the promoters of many catabolic genes and operons such as the *acs* gene, encoding acetyl-CoA synthetase (Acs) (EC 6.2.1.1), transforming acetate to acetyl-CoA (Deutscher, 2008; Görke and Stülke, 2008; Kumari, Beatty, et al., 2000; Valgepea et al., 2010; Castaño-Cerezo, Bernal, Blanco-Catalá, et al., 2011).

### 1.4.2 Acetate utilising pathways

There are only two pathways found in *E. coli* that catalyse acetate assimilation. They both consist of two reactions and consume ATP for generating acetyl-CoA for further conversion. The first pathway, which was already described in the reverse direction in 1.2, is the reversible AckA-Pta pathway which proceeds through a high-energy acetyl phosphate intermediate. It is a low-affinity pathway and assimilates acetate in relatively



large concentrations. The enzymes possess  $K_m$  values for acetate in the 7 to 10 mM range (Kumari, Tishel, et al., 1995; Enjalbert et al., 2017).

The second one is the irreversible Acs pathway which also consists of two reactions. In the first reaction, Acs converts acetate and ATP to the (enzyme-bound) intermediate acetyl-AMP while producing pyrophosphate (Figure 1). *In vivo*, an intracellular pyrophosphatase removes this critical pathway intermediate and hence makes the Acs pathway therefore irreversible. In the second reaction, acetyl-AMP is converted together with CoASH to acetyl-CoA, releasing AMP. The Acs pathway is in contrast to the AckA-Pta pathway a high-affinity for its substrate with a  $K_m$  value of 200  $\mu$ M for acetate and uses one ATP more for the conversion to acetyl-CoA (Wolfe, 2005).

Acetyl-CoA is a major branching point in central metabolism and precursor for several pathways, whereas one important role is its oxidation in the TCA cycle to produce energy and reducing cofactors (Wendisch et al., 2000). Provided that acetate is the sole carbon source, the acetyl-CoA from the AckA-Pta or Acs pathway needs to be further transformed into the cellular building blocks with longer carbon chains ( $C_2 \rightarrow C_X$ ), like pyruvate. Some autotrophic bacteria (see 1.3.1) are able to form pyruvate via the condensation of acetyl-CoA and carbon dioxide (Furdui and Ragsdale, 2000). Those microorganisms which are not capable of  $CO_2$  fixation utilise alternative routes like the glyoxylate cycle, which is known as a bypass (glyoxylate shunt) of the TCA cycle (Kornberg and Krebs, 1957; M. El-Mansi et al., 2006).

### 1.4.3 Glyoxylate shunt and gluconeogenesis

The glyoxylate shunt (GS) is a variant of the TCA cycle and shares five of the eight enzymes (Figure 3). It bypasses its carbon dioxide producing steps (Idh and Kgdh) and shortcuts the generation of reduced electron carriers (NADH and  $FADH_2$ , not shown in Figure 3). Consequently, it conserves the carbon atoms for gluconeogenesis while simultaneously diminishing the flux of electrons into respiration (Ahn et al., 2016).

The GS is mediated by two unique enzymes, isocitrate lyase (Icl) (encoded by *aceA*) and malate synthase (Mas) (encoded by *aceB*). Isocitrate is cleaved by Icl to glyoxylate and succinate; glyoxylate is condensed with additional acetyl-CoA to yield malate. Either succinate or malate are converted into oxalacetate, the precursor of another round of the glyoxylate cycle. The remaining molecule (malate or succinate) can be converted to pyruvate for gluconeogenesis by malic enzymes (Ahn et al., 2016).



In presence of sugars, transcription of GS related genes (*aceBAK*) are negatively controlled by isocitrate lyase repressor (*IclR/iclR*) and consequently the GS is inactive. To improve acetate assimilation of *E. coli*, the transcriptional regulator on *aceBAK* can be removed by deletion of *iclR* to activate GS (Liu et al., 2017). This approach leads to a higher growth rate and acetate consumption, for both, glucose cultivations with excreted acetate and cultivations with acetate as the sole carbon source (Wang et al., 2006; Noh et al., 2018). However, co-utilisation of acetate and glucose is already previously regulated, through conversion of acetate to acetyl-CoA by Acs.

#### 1.4.4 Acs regulation

As mentioned above (1.4.1), *acs* is up-regulated at an increasing intracellular cAMP level which is caused by glucose limitation. Generally, *acs* is co-transcribed together with two other genes, putative inner membrane protein *yjcH* and acetate permease *actP*. The *acs-yjcH-actP* transcript is activated by cAMP-CRP. The exact function of *yjcH* is not yet clear, whereas *actP* has previously been described as a cation/acetate symporter responsible for acetate transport. Knock-out strains lacking *actP* activity poorly grow on acetate as the sole source of carbon (Gimenez et al., 2003).

Additional to transcriptional control, via CCR, activity of Acs is also controlled by post-translationally modifications, in detail by acetylation of lysine-609. This acetylation blocks the conversion of acetate to Ac-AMP which is the first of two reactions. The second, the thioester-forming step remains unaffected. For activating and deactivating the Acs enzyme it requires the sirtuin-dependent protein acetylation/deacetylation system (SD-PADS) (Figure 4). Protein acetyltransferase, *patZ/Pat*, uses acetyl-CoA as a substrate to acetylate Acs at K609, inactivating its acetyl-CoA synthase activity ( $Acs^{Ac}$ ). The NAD<sup>+</sup>-dependent Sir2 ortholog protein CobB deacetylates Acs, activating its function and generates 2'-O-acetyl-ADP-ribose and nicotinamide (Starai, Celic, et al., 2002; Starai and Escalante-Semerena, 2004; Wolfe, 2005).

#### Mutated Acs

To improve acetate utilisation, redesigning Acs regulation seems to be a potential approach to avoid its inhibition. In 2005, a specific residue on Acs in *Salmonella enterica* serovar Typhimurium LT2 was identified, which is a critical amino acid (aa) for the acetylation of Acs by Pat. This critical aa, the Leu-641 is located in an  $\alpha$ -helix (residue

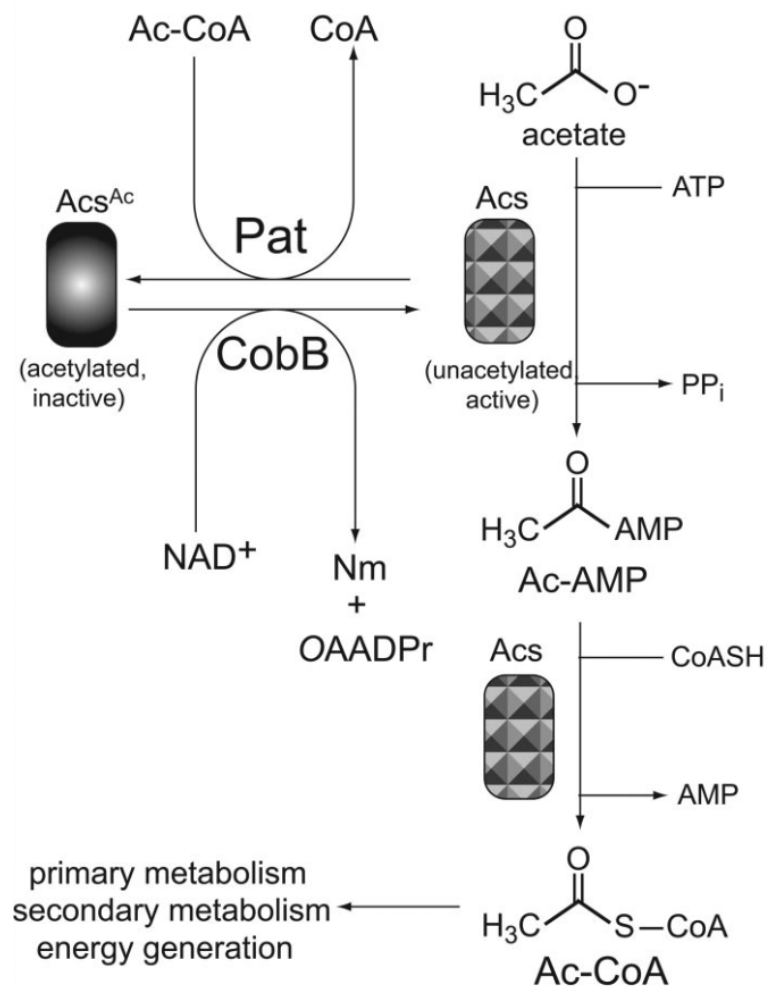


FIGURE 4: Posttranslational control of Acs by the SDPADS: Acs proteins are acetylated along with acetyl-CoA by the protein acetyltransferase (Pat). These acetylated Acs protein is inactive for the adenylation of acetate. CobB deacetylates Acs along with NAD<sup>+</sup>, releasing 2'-O-acetyl-ADP-ribose and nicotianamide. The unacetylated Acs is enabled for converting acetate to acetyl-AMP and acetyl-CoA. Reprinted from Starai, Gardner, and Escalante-Semerena, 2005, Copyright © 2005, American Society for Microbiology

637–645). It is the last  $\alpha$ -helix in the Acs protein and lies close to the site of acetylation of Acs (K609). In an experiment a *S. enterica* strain JE6668 (derivate of serovar Typhimurium LT2) deficient in Acs, Pta and CobB was successfully grown on 10 mM acetate as sole carbon source, carrying plasmids of *acs*, substituted at L641 with either glutamine (Acs<sup>L641Q</sup>), alanine (Acs<sup>L641A</sup>) or proline (Acs<sup>L641P</sup>). That proves that mutation at Leu-641 prevents the acetylation of Acs, and maintains the Acs enzyme in its active state. In this way, it bypasses the need for sirtuin deacetylase activity during growth on acetate (Starai, Gardner, and Escalante-Semerena, 2005). Analysis of *acs* from *E. coli* W revealed same residues at position 609 and 641 as for *Salmonella enterica* serovar Typhimurium LT2, and the two enzymes show an overall amino acid identity of 95%.

That suggests that mutation at position 609 might also make it insensitive to acetylation by Pat.

It was further reported that during exponential growth phase on glucose, *patZ* is up-regulated and that a *patZ*-deficient *E. coli* BL21 strain allowed more efficient growth, both for glucose and for acetate as the sole source of carbon (Castaño-Cerezo, Bernal, Röhrig, et al., 2015). However, more information on acetylation and activity of Acs is scarcely available, especially in the context of co-utilisation of glucose and acetate.

## 1.5 Acetate tolerance

Treatment of *E. coli* cells with weak acids like acetate results in growth inhibition, as described in 1.3.1. There are global effects of altered gene expression observed during weak acid treatment. In case of exposure to acetic acid, it affects the expression of 86 genes in *E. coli* O157:H7 and induces a signal causing the cells to enter stationary phase (Arnold et al., 2001). It has also been shown that weak acids reduce the intracellular concentrations of some aa, including glutamate, aspartate, lysine, arginine, glutamine, and methionine (Roe, O Byrne, et al., 2002).

In order for use of acetate as sole carbon source or co-substrate, the fermenting *E. coli* must be able to tolerate high concentrations of acetate. Therefore, adaptive evolution studies have been conducted at concentrations of 5 g l<sup>-1</sup> acetate to identify beneficial mutations for acetate tolerance and rapid growth. After 450 generations of cultivations the growth rate of the most tolerant strain was 1.24-fold increased, compared to initial strain (Rajaraman et al., 2016). This method appears to be effective, but identification of beneficial mutations are difficult, since the frequency of total mutations within the genome after such a selection is often low. The same applies for transcriptional profiling; phenotypes are caused by physiological alteration which do not involve changes in the expression of relevant genes (Sandoval et al., 2011). Another approach is the use of a plasmid-based genomic library selection for homologous overexpression (Lynch, Warnecke, and Gill, 2007). Cells harbouring the plasmid library were cultivated under selection pressure of 1.75 g l<sup>-1</sup> acetate for enrichment during 72 h. Enriched inserts could offer potential genes which expression leads to acetate tolerance. For instance, genes for cell wall synthesis (*murC* and *murG*), transportation (*yjdL* and *cadA*), amino acid synthesis (*argA*), and acetate assimilation (*acs*) were selected (Sandoval et al., 2011). Notably with the observation of *argA* overexpression is, that simple addition of aa such as methionine or glycine could recover cell growth of acetate affected cells (Han, Hong, and

H. C. Lim, 1993). A major cause is attributed to a malfunction of methionine biosynthesis in non-ideal growth conditions (Hondorp and Matthews, 2004).

### 1.5.1 Methionine biosynthetic pathway

Former studies of the methionine biosynthetic pathway in *E. coli* revealed that environmental stresses like higher temperatures lead to a reduced growth rate, which is caused by partial L-methionine auxotrophy. In that way, the growth of *E. coli* cells in minimal medium at temperatures above 40 °C is inhibited unless the growth medium is supplemented with L-methionine (Ron and Davis, 1971). This observation can be explained by the heat sensitivity of the MetA enzyme. The MetA is the first out of four enzymes converting L-homoserine to L-methionine (Figure 5) and is proposed as a "metabolic fuse". It senses stress conditions that destabilise cellular proteins, and consequently blocks protein synthesis via its inherent instability (Mordukhova and J.-G. Pan, 2013). Mapping mutations conferring defective heat-shock responses received further explanations. As a result, the *glyA* gene was detected which encodes for an enzyme that regenerates essential compounds for the final step of the pathway (Gage and Neidhardt, 1993).

Roe, O Byrne, et al. (2002) investigated the interaction of environmental stress inhibitions correlated to methionine biosynthetic pathway. They found out, that within this pathway, the accumulation of toxic intermediate L-homocysteine is one of the major influencer of acetate inhibition since enzymes below L-homocysteine are directly affected during weak acid stress.

In *E. coli* the substrate for L-homocysteine is the cobalamin-independent methionine synthase (MetE) (EC 2.1.1.14) under aerobic conditions. Under anaerobic conditions, the MetH enzyme, a cobalamin-dependent methionine synthase (EC 2.1.1.13) converts the L-homocysteine. Both enzymes transfer a methyl group to L-homocysteine forming L-methionine. MetH uses 5-methyltetrahydrofolate (CH<sub>3</sub>-THF) as methyl donor while the enzyme MetE uses 5-methyltetrahydropteroyl-tri-L-glutamate. The MetE is approximately 50 times less active than the MetH. As a result MetH is quite abundant in *E. coli*, growing aerobically in glucose minimal medium and taking around 3 to 5 % of the cellular protein content into account (Mordukhova and J.-G. Pan, 2013).

It was also found that MetE is a major aggregation-prone enzyme in *E. coli* at elevated temperatures (45 °C) (Mogk et al., 1999). The MetE protein, therefore, could limit the methionine availability under stress conditions such as heat, acid, and oxidation, which leads to a slow down of cellular biosynthesis.

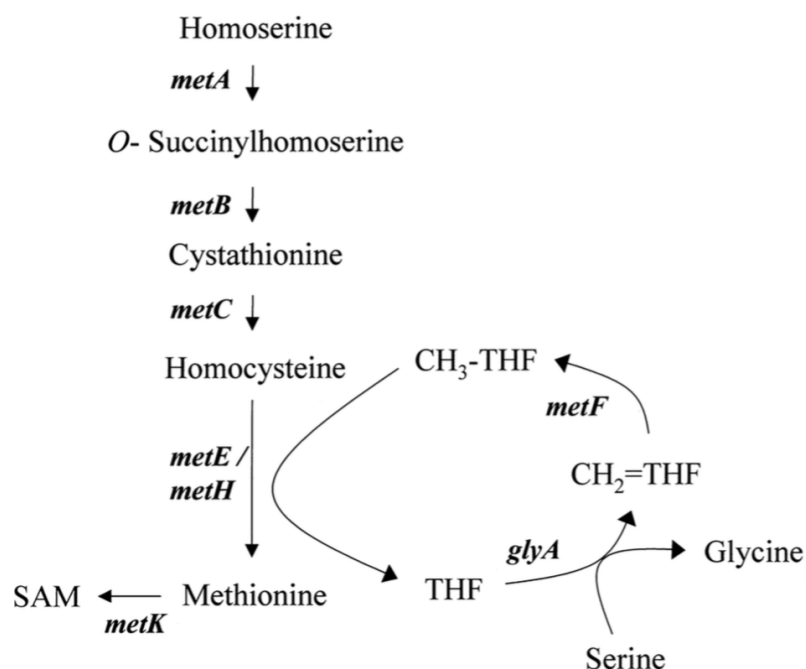


FIGURE 5: Methionine biosynthetic pathway of *E. coli*. Gene names are shown in *italics*. S-adenosylmethionine (SAM), tetrahydrofolate (THF), 5,10-methylenetetrahydrofolate ( $\text{CH}_2=\text{THF}$ ), 5-methyltetrahydrofolate ( $\text{CH}_3\text{-THF}$ ). Reprinted with permission of Microbiology Society, from Roe, O Byrne, et al., 2002; Copyright © 1994; permission conveyed through Copyright Clearance Center, Inc.

### Mutated MetE

In Mordukhova and J.-G. Pan (2013), the MetE enzyme in the *E. coli* K-12 WE strain, was randomly mutated to isolate a mutant enzyme which improves the acetate and temperature resistance of *E. coli*. For creating the mutant library (870 clones), the *metE* gene and its promoter were amplified from genomic DNA of *E. coli* strain W3110 and inserted into the chromosome of *E. coli*  $\text{WE}\Delta\text{metE}::\text{kan}$  strain. Cultivated on acetate-enriched media (8 mM acetate) and elevated temperatures (44 and 45 °C) revealed, that the mutant MetE-214 (V39A, R46C, T106I, and K713E) grew fastest and possesses an enhanced *in vivo* stability.

Additionally, MetE-214 was modified with a substitution of MetE-C645A which was assumed to completely eliminate methionine auxotrophy in oxidatively stressed cells (Hondorp and Matthews, 2009). This mutant showed further improvements for *in vivo* thermal stability with half-lives of 100 min (at 45 °C, pH 7.0) compared to MetE-214 (73 min) and was labelled as MetE-214A. Further, MetE-214A performed best growth in M9 glucose medium at pH 6 and 20 mM sodium acetate ( $\mu = +6\%$  to  $+20\%$  among the *metE* mutants

and wild type, respectively). It was suggested that mutated MetE proteins changed their conformation to an extent which prevents them from unfolding and being inactive in an oxidizing environment (Mordukhova and J.-G. Pan, 2013). However, test on overexpression of *metE* in *E. coli* Frag 1 gained no further improvement in acetate resistance (Roe, O Byrne, et al., 2002).

For all those priorly cited studies, plasmid-based overexpression of genes was the principal strategy of engineering *E. coli* for an improved acetate tolerance and acetate (co-)assimilation. In order to test the modified genes individually or in combination with each other in the preferred host strain *E. coli* W, a method called Golden Gate cloning can be used for rapid plasmid library construction.

## 1.6 Basics of Golden Gate cloning

The Golden Gate (GG) cloning is an efficient cloning approach which was first described by Engler, Kandzia, and Marillonnet (2008) as a "one pot, one step" process referred to the restriction and ligation. This is achieved by the use of type IIS restriction enzymes, cleaving DNA outside their recognition site, resulting in 5' or 3' DNA overhangs (sticky ends) consisting of any nucleotide (depending on the restriction enzyme). The enzyme self-eliminates its recognition sequence whereby the ligated DNA fragments are no longer recognized by the restriction enzyme and the desired product during restriction-ligation cycles increases. Re-ligated DNA reconstitutes restriction sites and gets digested again. Unlike conventional techniques, there are no extra aa in the final protein which are typically expressed from the restriction site sequence. Furthermore, GG cloning allows the simultaneous assembly of multiple DNA inserts into an expression vector. It offers the advantage of a modular design allowing rapid and simultaneous cloning of several genes in combination with variable promoters and terminators for each gene of interest (GOI) (Engler, Kandzia, and Marillonnet, 2008; Weber et al., 2011).

### 1.6.1 GoldenMOCS

An adopted version of the GG cloning system is the GoldenMOCS, standing for golden gate derived multiple organism cloning system (Sarkari et al., 2017). It consists of three main construct levels, so-called backbones (BB), and the type IIS restriction enzymes BsaI and BpiI (BbsI) (Figure 6).



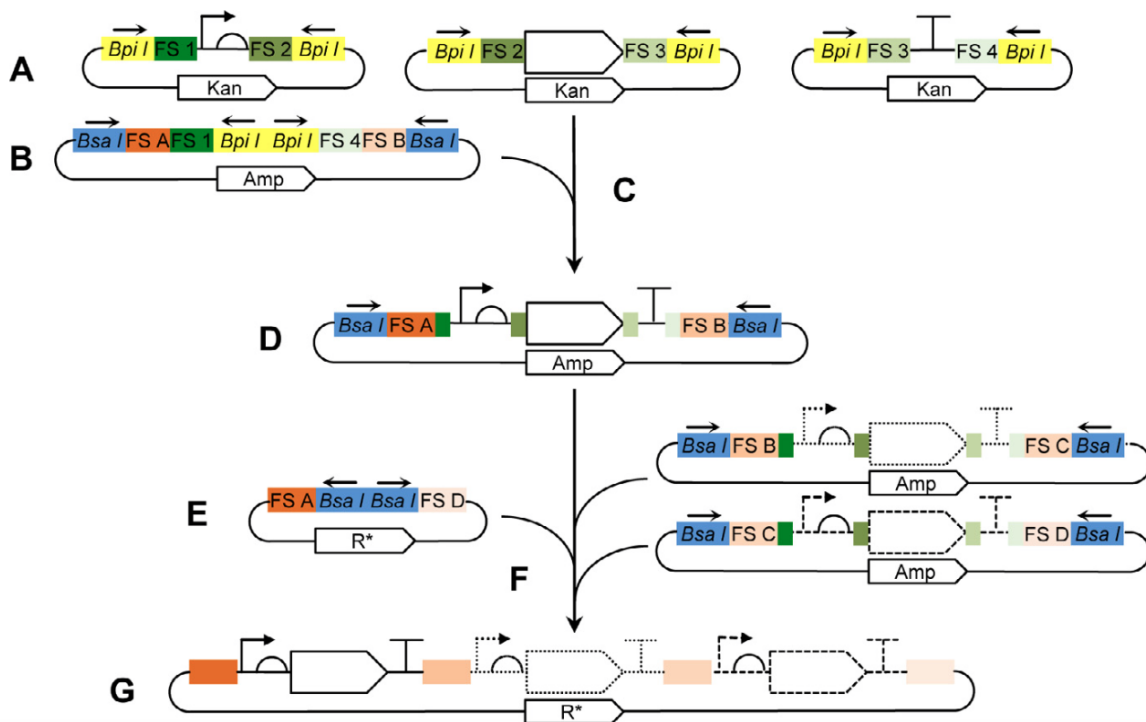


FIGURE 6: Hierarchical scheme for GoldenMOCS cloning strategy. The respective plasmids are referred to as backbones (BB). A) BB1 is a high copy plasmid with fusion sites (FSs) (1-2|2-3|3-4) for the proper direction of functional elements like promoters, gene of interest (GOI), terminator in the BB2. Kan depicts the resistance marker for kanamycin. B) Empty recipient vector for BB2. High copy plasmid with four FSs (A-B|B-C|D-C|C-D) (also called linker) separating the location of each expression cassette in the final vector BB3. Amp depicts the resistance marker for ampicillin. C) Formation of expression vector BB2 by simultaneous restriction-ligation with *BpiI* (*BbsI*) and T4 DNA ligase. D) Completed BB2 including one entire expression cassette. E) Empty recipient vector for BB3. R\* depicts the resistant marker which can be freely chosen, although a different resistant marker than ampicillin is to be preferred to increase cloning efficiency. F) Formation of expression vector BB3 with *BsaI* and T4 DNA ligase. G) Final expression vector BB3 with three individual expression cassetts for further transformation to the target host cell. Cutting directions are implied as black arrows above the restriction sites. Reprinted from Sarkari et al., 2017, Copyright ©2017, Elsevier

In the first cloning level, the individual functional elements, promoter, GOI and terminator are incorporated into BB1 plasmids. The selection of specific fusion sites (FSs) within these backbones are pivotal for the correct position in the expression cassette. Then these desired functional elements are subsequently assembled to a transcription unit in the BB2 plasmid which comprises the distinct linkers. On the third level, multiple expression cassetts can be combined with BB3 containing the complementary linkers. The produced expression vector BB3 has now a defined gene cluster without the original restriction sites and can be transformed into *E. coli* or another suitable organism.

## 1.7 Aim of work

As the literature survey shows, hardly any analysis towards acetate co-utilisation at higher acetate-glucose concentrations ( $>10 \text{ g l}^{-1}$ ) are known so far for *E. coli*. However there are some promising approaches in regulatory engineering which potentially turns out as highly suitable for *E. coli* W as acetate utilising cellular factory.

The first objective of this work was to prove that acetate co-utilization in presence of glucose is possible in an aerobic batch cultivation of glucose-acetate concentrations up to  $10 \text{ g l}^{-1}$ .

The second objective was to prevent extended lag phases and inhibited growth initiated by toxic effects of acetate.

The third and final objective was to achieve a highly effective (continuous) high cell density cultivation provided with a combined glucose-acetate substrate feed where no inhibiting effects of acetate and a constantly high utilisation of acetate is observed.

## 2 Materials and methods

### 2.1 Strains and plasmids

#### 2.1.1 *E. coli* strains

Two *E. coli* strains shown in Table 1 were used for all experiments. *Escherichia coli* BL21 (DE3) was obtained from New England Biolabs (MA, USA) and used as host for plasmid assembly and propagation. *Escherichia coli* W (ATCC 9637) was obtained from DSMZ (Leibnitz Institute DSMZ, Braunschweig, Germany) and used for all cultivations in this study as well as donor organism, providing the gDNA (genomic DNA) for *acs*, *metE*, and *cobB* genes.

TABLE 1: Used *E. coli* strains

Strain	Genotype / Designation	Source
BL21 (DE3)	<i>E. coli</i> B F <sup>-</sup> <i>dcm ompT hsdS</i> (r <sub>B</sub> <sup>-</sup> m <sub>B</sub> <sup>-</sup> ) <i>gal</i> λ(DE3)	NEB
W (ATCC 9637)	<i>E. coli</i> W / DSM 1116 = NCIMB 8666	DSMZ

#### 2.1.2 Plasmids

The empty vectors modified for GG cloning were retrieved from Sarkari et al. (2017). All generated and used plasmids in this work are listed in Table 2.

##### pIDTSmart vector

This vector is denoted as pIDT which stands for plasmid integrated DNA Technologies (IDT) (Coralville/IA, USA) where it originates from. It is a high copy vector which lacks most common restriction sites and promoters found in traditional vectors. Additionally

it possesses a kanamycin resistance gene and it was modified and engaged as BB1 in this work.

TABLE 2: List of all generated plasmids in this work

Designation	Source
BB1_pIDTSmart(Kan <sup>R</sup> )_	
_FS1_114p_FS2	Sarkari et al. (2017)
_FS2_amilCP_FS3	Sarkari et al. (2017)
_FS2_acs_FS3	This work
_FS2_acs_L641P_FS3	This work
_FS2_metE_FS3	This work
_FS2_metE_mut_FS3	Laboratory collection
_FS2_cobB_FS3	This work
BB2_pUC(Amp <sup>R</sup> )_	
_LinkerA_FS1_FS4_LinkerB	Sarkari et al. (2017)
_LinkerB_FS1_FS4_LinkerC	Sarkari et al. (2017)
_LinkerC_FS1_FS4_LinkerD	Sarkari et al. (2017)
_LinkerA_114p_acs_LinkerB	This work
_LinkerA_114p_acs_L641P_LinkerB	This work
_LinkerB_114p_metE_LinkerC	This work
_LinkerB_114p_metE_mut_LinkerC	Laboratory collection
_LinkerC_114p_cobB_LinkerD	This work
BB3_pUC(Kan <sup>R</sup> )_	
_LinkerAB	Sarkari et al. (2017)
_LinkerAC	Sarkari et al. (2017)
_LinkerAD	Sarkari et al. (2017)
_LinkerA_SpacerAB_LinkerB	This work
_LinkerA_114p_	
_acs_BB <sub>a</sub> _B1001_LinkerB	This work
_acs_L641P_BB <sub>a</sub> _B1001_LinkerB	This work
_SpacerAB_metE_BB <sub>a</sub> _B1001_LinkerC	This work
_SpacerAB_metE_mut_BB <sub>a</sub> _B1001_LinkerC	Laboratory collection
_acs_metE_BB <sub>a</sub> _B1001_LinkerC	This work
_acs_metE_mut_BB <sub>a</sub> _B1001_LinkerC	This work
_acs_metE_cobB_BB <sub>a</sub> _B1001_Linkerd	This work
_acs_metE_mut_cobB_BB <sub>a</sub> _B1001_Linkerd	This work

### pUC19 vector

The pUC19 vector is a frequently used model plasmid in research and extensively used as cloning vector. It provides innately many restriction sites for endonucleases in the multiple cloning site (MCS) region such as HindIII, SphI, PstI, SalI, XbaI, BamHI, SmaI, KpnI, SacI and EcoRI which was availed for restriction digest and cloning and construct assembling. With a size of 2686 bp, the circular DNA double stranded vector pUC19 is rather small, but has a high copy number. There is also a N-terminal fragment of  $\beta$ -galactosidase (*lacZ*) gene of *E. coli* and it encodes for an ampicillin resistance gene (Yanisch-Perron, Vieira, and Messing, 1985). In this work BB2 and BB3 derived from the pUC19 vector.

### Backbone 1

This plasmid was derived from the pIDTSmart vector. It provides a kanamycin resistance gene and an *amilCP* gene that expresses a blue chromoprotein (Figure 7). The latter is used as an screening marker to verify the successful insertion of the GOI. By the implementation of the GOI into the vector, the *amilCP* gene is removed, hence all blue clones on the transformation plate can be excluded as they lack of GOI. The fusion sites FS2 and FS3 are generated when BB1 is cut with BsaI.

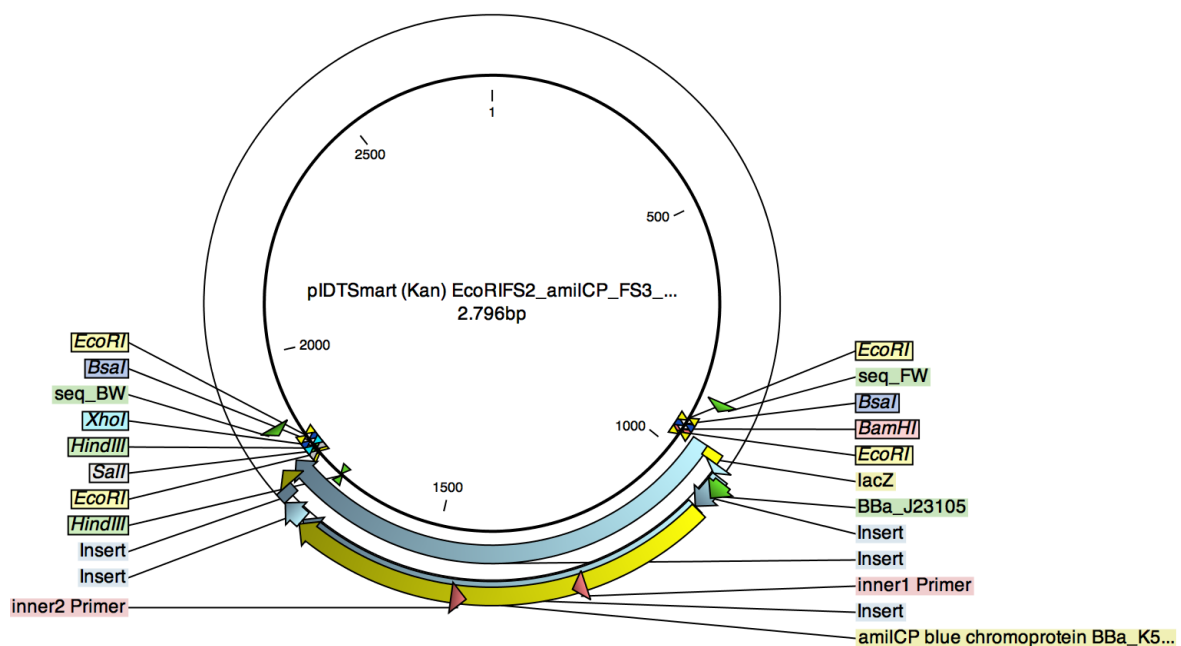


FIGURE 7: Empty BB1 plasmid with selection marker *amilCP*, resistance gene for kanamycin (not shown) and two BsaI restriction sites.

## Backbone 2

This plasmid derived from the pUC19 vector provides an ampicillin resistance gene and a pUC ori. Digestion with Bpil generates the fusion sites FS1, FS2, FS3 or FS4 and adds the specific linkers A, B, C, or D (Table 3) to either side of the gene cassette depending on the BB2 and the defined final gene order in the BB3 vector.

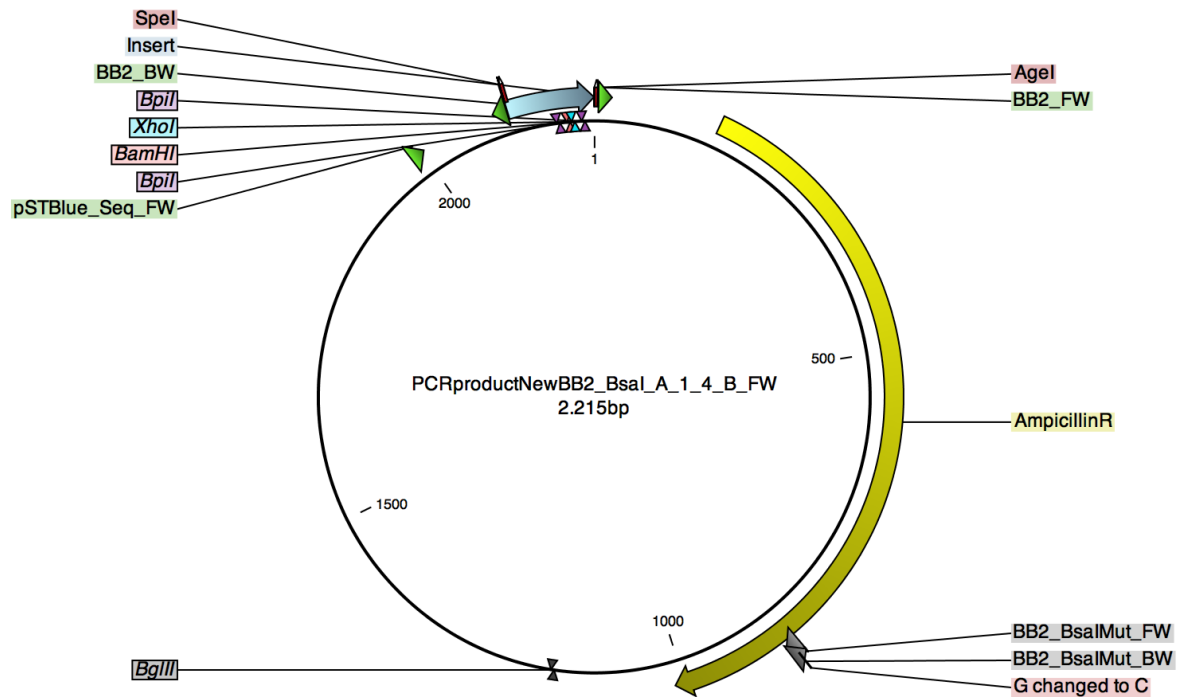


FIGURE 8: Empty BB2 plasmid with resistance gene for ampicillin, two restriction sites for Bpil and linker AB

## Backbone 3

The BB3 plasmid derived as well from pUC19 vector with a kanamycin resistance gene and a pUC ori. The linkers (in Figure 9 A and B) are released after Bsal digestion and assembled with the expression cassette from BB2.

## Promoter and terminator

The promoter and terminator sequences are defined in BB1 on FS1/FS2 and FS3/FS4, respectively and were provided in form of a pIDTSmart and a pSTBLUE vector by Sarkari et al. (2017).

## 2.1. Strains and plasmids

TABLE 3: Fusion sites and linker for GG cloning.

BB1 Fusion sites		Restriction enzyme	Recognitions site
1	5'...GGAG...3'	Bpil (BbsI)	5'...GAA GAC (N) <sub>2</sub> ▼...3' 3'...CTT CTG (N) <sub>6</sub> ▲...5'
2	CATG		
3	GCTT		
4	CGCT		
BB2 Linker		Restriction enzyme	Recognitions site
A	5'...GATC...3'	BsaI-HFv2	5'...GGT CTC (N) <sub>1</sub> ▼...3' 3'...CCA GAG (N) <sub>5</sub> ▲...5'
B	CCGG		
C	AATT		
D	AGCT		
BB3 Fusion sites		Restriction enzyme	Recognitions site
α	5'...GGAG...3'	Bpil (BbsI)	5'...GAA GAC (N) <sub>2</sub> ▼...3' 3'...CTT CTG (N) <sub>6</sub> ▲...5'
β	CATG		
γ	GCTT		
δ	CGCT		

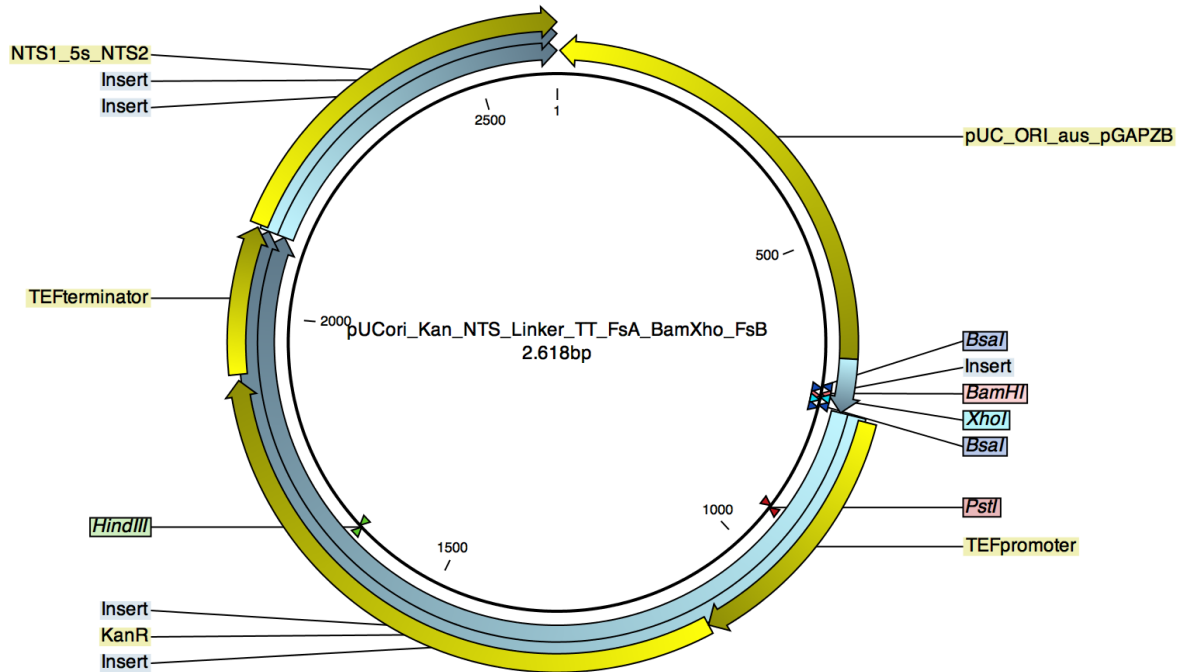


FIGURE 9: Empty BB3 plasmid with resistance gene for kanmycin, two restriction sites for BsaI and linker A and B

The promoter was descended from the Anderson promoter library and is denoted as BBa\_L23114 or p114. As terminator BBa\_B1001 was used.

### 2.1.3 Primer

Sense and antisense primers (Table 4) for the amplification of *acs*, *metE* and *cobB* from *Escherichia coli* W ATCC 9637, were ordered from IDT (Coralville/IA, USA). Modifying primers for creating *acs\_L641P* and for *metE\_mut* were ordered as well by IDT whereby *metE\_mut* as obtained as gBlocks® Gene Fragments.

For the GG assembly reaction the type IIs restriction enzymes BsaI-HFv2 and BpiI (BbsI) (Table 3) were used. Therefore, the amplification primers were designed to produce a BsaI restriction site and FS2 and 3 at the amplified DNA fragments. seq\_FW, seq\_BW and seq\_in primers were used for sequencing the target gene in the recipient plasmids.

TABLE 4: Primer list: fusion sites (**bold**), restriction sites (underlined), inserted mutations ( )

	Nr.	Designation	5'-Nucleotide sequence-3'
sense	1	acs_FW	ATGAGCCAAATTCACAAACAC
	2	FS2_acs_FW	GATCGGTCTC <u>ACAT</u> GAGCCAAATTCACAAACAC
	3	FS2_met_out_FW	GATCGGTCTC <u>ACAT</u> GACAATTCTTAATCACACCC
	4	FS2_cobB_out_FW	GATCGGTCTC <u>ACAT</u> GCTGTGCGGTCG
	5	seq_FW	GCAGTCCAGTTACGCTG
	6	acs_seq_in_FW	GCAGTATTCCGCTGAAG
	7	metE_seq_in_FW	GCCTTCTGACTGGTTGC
antisense	11	FS3_acs_BW	GATCGGTCTCAAAG <b>GCTT</b> ACGATGGCATCGCG
	12	acs_L641P_BW	CTTCAAGC <span style="border: 1px solid black; padding: 0 2px;">G</span> GCTTCTC
	13	FS3_acs_L641P	GATCGGTCTCAAAG <b>GCTT</b> ACGATGGCATCGCGATA
			GCCTGCTTCTCTTCAAGC <span style="border: 1px solid black; padding: 0 2px;">G</span> GCTTCTC
	14	FS3_metE_out_BW	GATCGGTCTCAAAG <b>GCTT</b> ACCCAGACGCAAATTC
	15	FS3_cobB_out_BW	GATCGGTCTCAAAG <b>GCTT</b> ATAATCCCTT
	16	seq_BW	CGTGGACCGATCATACG
	17	acs_seq_in_BW	GGTAGCGCCTTCCAG

## 2.2 Media preparation and composition

Unless stated otherwise all media and solutions were prepared using desalted water and were heat-sterilized by autoclaving at 121 °C and 2 bar for at least 20 min.



### Lysogeny broth

The lysogeny broth (LB) (Table 5) is a complex media and provides rich nutrients for bacterial growth. LB was used for all molecular applications like preparation of plasmid DNA, transformants and streaking them on LB agar plates. For precultures the double amount of soy peptone and yeast extract was used (2 x LB) to provide higher cell density.

TABLE 5: Composition of Lysogeny broth

Component	Concentration
Soy peptone	10 g l <sup>-1</sup>
NaCl	10 g l <sup>-1</sup>
Yeast extract	5 g l <sup>-1</sup>
Agar-Agar <sup>a</sup>	15 g l <sup>-1</sup>

<sup>a</sup> added only for LB agar plates

### DeLisa medium

The defined minimal medium used for all cultivations was prepared according to DeLisa et al. (1999) (Table 6). To prevent precipitation the initial medium was prepared according to a particular protocol.

Acetate and glucose solution (100 g l<sup>-1</sup>) were optionally added for a final batch concentration of 10 g l<sup>-1</sup> each. For preparation, sodium acetate, KH<sub>2</sub>PO<sub>4</sub>, (NH<sub>4</sub>)<sub>2</sub>HPO<sub>4</sub> and citric acid were dissolved in dH<sub>2</sub>O, and the pH was adjusted to pH 7 with solid NaOH. The solution was filled up with dH<sub>2</sub>O to its final volume minus the stock and glucose solution and subsequently autoclaved. The trace metal stock solutions (Table 7) were composed separately and subsequently added via sterile-filtration. The priorly autoclaved glucose solution was added at room temperature.

Preparation of feeding solution was practically the same as described above, excluding KH<sub>2</sub>PO<sub>4</sub>, (NH<sub>4</sub>)<sub>2</sub>HPO<sub>4</sub>, and citric acid. Final concentrations for glucose and acetate in the feeding solutions were 250 and 101.27 g l<sup>-1</sup>, respectively.

TABLE 6: Composition of DeLisa medium

Compound	Batch medium, l <sup>-1</sup>	Feeding solution, l <sup>-1</sup>
Glucose · H <sub>2</sub> O	11 g <sup>a</sup>	275 g
Sodium acetate · 3 H <sub>2</sub> O	13.9 g <sup>a</sup>	140.77 g
KH <sub>2</sub> PO <sub>4</sub>	13.3 g	–
(NH <sub>4</sub> ) <sub>2</sub> HPO <sub>4</sub>	4 g	–
Citric acid	1.7 g	–
MgSO <sub>4</sub> · 7 H <sub>2</sub> O	1.2 g	12.5 g
Fe(III)-citrate	100 mg	25 mg
EDTA	8.4 mg	8.13 mg
Zn(CH <sub>3</sub> COO) <sub>2</sub> · 2 H <sub>2</sub> O	13 mg	10 mg
TE	5 ml	5 ml

<sup>a</sup> optionally added

TABLE 7: Trace metal stock solution of DeLisa medium

Stock solution	Component	Stock concentration	
500 x MgSO <sub>4</sub>	MgSO <sub>4</sub> · 7 H <sub>2</sub> O	300 g l <sup>-1</sup>	ac <sup>a</sup>
100 x Fe(III)-citrate	Fe(III)-citrate · H <sub>2</sub> O	10 g l <sup>-1</sup>	ac
100 x EDTA	EDTA	0.84 g l <sup>-1</sup>	ac
200 x Zn(CH <sub>3</sub> COO) <sub>2</sub>	Zn(CH <sub>3</sub> COO) <sub>2</sub> · 2 H <sub>2</sub> O	2.69 g l <sup>-1</sup>	ac
200 x trace elements	CoCl <sub>2</sub> · 6 H <sub>2</sub> O	0.50 g l <sup>-1</sup>	sf <sup>b</sup>
	MnCl <sub>2</sub> · 4 H <sub>2</sub> O	3.00 g l <sup>-1</sup>	sf
	CuCl <sub>2</sub> · 2 H <sub>2</sub> O	0.24 g l <sup>-1</sup>	sf
	H <sub>3</sub> BO <sub>3</sub>	0.60 g l <sup>-1</sup>	sf
	Na <sub>2</sub> MoO <sub>4</sub> · 2 H <sub>2</sub> O	0.50 g l <sup>-1</sup>	sf

<sup>a</sup> autoclaved<sup>b</sup> sterile filtrated

## Antibiotics

Two antibiotics were used for selection during cloning and cultivation processes. Kanamycin for BB1 and BB3 constructs, and ampicillin for BB2 constructs. The substances (Table 8) were weighed in each on an analytical scale (Mettler Toledo, Columbus/OH, USA) and dissolved in MQ-H<sub>2</sub>O of a 25 ml volumetric flask. The stock solutions were filter sterilized, aliquoted in microfuge tubes and stored at -18 °C.

## 2.2. Media preparation and composition

TABLE 8: Used antibiotics

Antibiotic	Dilution factor	Stock concentration	Working concentration
Ampicillin	1000	100 mg ml <sup>-1</sup>	100 µg ml <sup>-1</sup>
Kanamycin A	1000	50 mg ml <sup>-1</sup>	50 µg ml <sup>-1</sup>

### 2.2.1 Buffer solution

To receive a 100 x TRIS-HCl stock solution (1 M), 121.14 g TRIS was dissolved in 800 ml MQ-H<sub>2</sub>O, and the pH was set to 8.0 with the appropriate volume of concentrated HCl. The solution was autoclaved and stored at room temperature.

TABLE 9: Buffer solutions

Buffer	Component		
TFB1 <sup>a</sup>	30	mM	potassium acetate
	10	mM	CaCl <sub>2</sub>
	50	mM	MnCl <sub>2</sub>
	100	mM	RbCl
	15	%	glycerol pH set to 5.8 with 1 M acetic acid
TFB2 <sup>a</sup>	100	mM	MOPS
	75	mM	CaCl <sub>2</sub>
	10	mM	RbCl
	15	%	glycerol pH set to 6.8 with 1 M KOH
TRIS-HCl buffer	10	mM	(HOCH <sub>2</sub> )CNH <sub>2</sub> (TRIS)
TAE-buffer	242	g	Tris base
	57	ml	glacial acetic acid
	18.5	g	EDTA, disodium salt
HPLC running buffer <sup>b</sup>	4	mM	H <sub>2</sub> SO <sub>4</sub>
	1	pn <sup>c</sup>	NaN <sub>3</sub>

<sup>a</sup> sterile filtrated

<sup>b</sup> dissolved in MQ-H<sub>2</sub>O and degassed for 15 min

<sup>c</sup> pinch (0.25 to 0.5 g)

For the HPLC running buffer a 100 x stock solution (0.4 M) was prepared by adding 7.9 ml of 95 % H<sub>2</sub>SO<sub>4</sub> (1.84 kg l<sup>-1</sup>) to 800 ml MQ-H<sub>2</sub>O and filling up to 1 l. Both buffers were 1 to 10 diluted with MQ-H<sub>2</sub>O to receive the desired concentration (10 x, 1 x).

## 2.3 Preparation, purification, and analysis of DNA

### 2.3.1 DNA amplification (PCR)

For the DNA amplification, the specific primers (Table 4, 11) were mixed with Q5 High-Fidelity DNA Polymerase, Q5 Reaction buffer, dNTPs (all from: New England Biolabs, Ipswich/MA, USA) and gDNA according to the scheme shown in Table 10. The gDNA of *E. coli* W was obtained from DSMZ (Leibnitz Institute DSMZ, Braunschweig, Germany).

TABLE 10: PCR 50  $\mu$ l reaction mix for gene amplification

Component		Volume	Final concentr.
5 x	Q5 Reaction Buffer	10 $\mu$ l	1 x
10 $\mu$ M	dNTPs	1 $\mu$ l	200 $\mu$ M
10 $\mu$ M	Primer sense	2.5 $\mu$ l	0.5 $\mu$ M
10 $\mu$ M	Primer antisense	2.5 $\mu$ l	0.5 $\mu$ M
	Template DNA	variable	10 ng
	Q5 High-Fidelity DNA Polymerase	0.5 $\mu$ l	0.02 U $\mu$ l <sup>-1</sup>
10 $\mu$ M	TRIS-HCl buffer	ad 50 $\mu$ l	

TABLE 11: PCR plan for gene amplification and modification

#	Gene	Primer Nr.		T <sub>a</sub> , °C	Length, bp	Extension time, s	Template
		sense	antisense				
I	FS2_acs_FS3	2	11	61	1930	58	gDNA
II	acs_L641P	1	12	62	1987	60	gDNA
III	FS2_acs_L641P_FS3	2	13	61	849	61	II
IV	FS2_metE_FS3	3	14	61	2289	69	gDNA
V	FS2_cobB_FS3	4	15	61	849	61	gDNA

According to the manufacturer's protocol of the DNA polymerase, the annealing temperature was set between 61 and 62 °C and extension time of 30 s/kb DNA (Table 11, 12).

### 2.3.2 Agarose gel electrophoresis

For efficient separation of linear DNA, 1 % (w/v) agarose gels were used for gel electrophoresis. For one gel 1.5 g of agarose was suspended in 150 ml 1X TAE buffer and carefully brought to boil in the microwave oven. When completely melted, the liquid was

### 2.3. Preparation, purification, and analysis of DNA

TABLE 12: Thermocycler program for DNA amplification. Annealing temperature ( $T_a$ ) and extension times vary on the amplified fragments which are shown in Table 11

Step	Temperature	Time	Cycles
Initial denaturation	98 °C	2:00 min	
Denaturation	98 °C	0:10 min	} 35
Annealing	variable	0:30 min	
Extension	72 °C	variable	
Final extension	72 °C	10:00 min	

swirled under running water cooling down to about 60 °C. The completely clear solution was subsequently displaced with 150  $\mu$ l SYBR<sup>®</sup> Safe (Invitrogen, Carlsbad/CA, USA) and slightly shaken to achieve a homogenous distribution. The liquid gel was poured into a gel tray with an appropriate comb in place, and air bubbles were removed. After solidifying the comb was removed and placed in the electrophoresis chamber with the slots facing the cathode and submerged with 1X TAE buffer.

The sample solution was displaced with the 6X loading buffer (6X MassRuler DNA Loading Dye; Thermo Fisher Scientific, Waltham/MA, USA) and loaded onto the gel. Samples from miniprep digestion generally had a total volume of 20  $\mu$ l, those of PCR runs 50  $\mu$ l. For size determination, 6  $\mu$ l of the ready to use Gene Ruler (1 kb Gene Ladder; Thermo Fisher Scientific, Waltham/MA, USA) was employed. The lid was closed, and a voltage of 120 V was applied for about 1 h (PowerPak<sup>™</sup> Basis Power Supply; Bio-Rad Laboratories, Hercules/CA, USA). As the bromophenol colour front ran past the end of the gel, the electrophoresis was stopped, and the bands were visualized under UV-light with aChemiDoc XRS+ Imaging System (Bio-Rad, Hercules/CA, USA). Desired bands were excised from the gel with a sterile scalpel and purified as described below in 2.3.3.

#### 2.3.3 Extraction and purification of DNA fragments

The DNA was extracted from the agarose gel with the QIAGEN QIAquick Gel Extraction Kit (Thermo Fisher Scientific, Waltham/MA, USA) based on silica membranes in spin columns. The extraction and purification were conducted according to the manufacturer's protocol with a minor deviation. Contrary to the protocol, DNA was eluted in 20  $\mu$ l sterile 10 mM Tris-HCl buffer, instead of elution buffer, provided by the kit.

### 2.3.4 Quantification of DNA/nucleic acids

All DNA measurements were determined with a spectrophotometer (NanoDrop 2000, Thermo Fisher Scientific, Waltham/MA, USA), which allows UV-Vis measurements to be made from 1  $\mu\text{l}$  samples. A sample droplet was merely loaded onto the optical pedestal and drawn by a clamp. The concentration is calculated based on Lambert-Beer's law. The detection range lies between 2  $\text{ng } \mu\text{l}^{-1}$  and 3700  $\text{ng } \mu\text{l}^{-1}$ .

### 2.3.5 Isolation of plasmid DNA (Miniprep)

A single colony was picked from the transformation plate and overnight culture of 2–4 ml LB medium including the appropriate antibiotics were inoculated and incubated at 37 °C and 200 rpm. Simultaneously each picked colony was incubated on an LB master plate including the appropriate antibiotics at 37 °C, over night. Cells were harvested by centrifugation and purification of plasmid DNA was carried out with the Monarch Plasmid Miniprep Kit (NEB) according to the manufacturer's protocol.

### 2.3.6 Restriction digest of plasmid DNA

The purified plasmid DNA was digested with applicable restriction enzyme(s) and appropriate buffer. In case of double digestion, a buffer with the highest activity of both enzymes was used. The right enzyme(s) had to be chosen to ensure a result of at least two bands with differentiating sizes. The digestion mix was pipetted together as specified in Table 13 and was incubated at 37 °C for about 1 h. The fragments were separated and analysed by gel electrophoresis shown in 2.3.2.

TABLE 13: Protocol for 20  $\mu\text{l}$  restriction digestion

Component	Single digest	Double digest
Plasmid DNA ( $\sim 100 \text{ ng } \mu\text{l}^{-1}$ )	2 $\mu\text{l}$	2 $\mu\text{l}$
CutSmart buffer <sup>a</sup>	2 $\mu\text{l}$	2 $\mu\text{l}$
Enzyme 1 <sup>a</sup>	0.5 $\mu\text{l}$	0.25 $\mu\text{l}$
Enzyme 2 <sup>a</sup>	—	0.25 $\mu\text{l}$
Tris-HCl buffer (10 mM)	15.5 $\mu\text{l}$	15.5 $\mu\text{l}$

<sup>a</sup> from NEB

### 2.3.7 Sequencing

To verify the correct amplification, plasmids were externally Sanger sequenced by (Microsynth AG, Switzerland). Therefore, 6 µl plasmid DNA was combined with 3 µl of the sense (seq\_FW) or antisense primer (seq\_BW) (Table 4) and 6 µl 10 mM Tris-HCl buffer each. The prerequisite for effective sequencing is a DNA amount of 480 to 1200 ng in a minimum volume of 12 µl. The sense and antisense primer are binding several base pares up- or downstream of the gene inserts (in this case on BB1) to ensure a complete read through of the sequence. However, sequencing is limited to a length up to 700 bp, thus for longer genes, such as the *acs* or *metE*, additional primers (seq\_in) binding within the gene are needed to receive the full sequence of the gene.

## 2.4 Golden Gate assembly

For GoldenMOCS cloning, FSs had to be added to every gene (Table 11). FSs for the *acs* gene were attached using primers FS2\_acs\_FW and FS3\_acs\_BW. To introduce the L641P mutation into *acs* and to add the FS, two PCR reactions amplified *acs* until position 641 using primers *acs*\_FW and *acs*\_L641P\_BW. In a second PCR reaction, FSs and the rest of the coding sequence were added using primers FS2\_acs\_FW and FS3\_acs\_L641P\_BW. FSs for *metE* and *cobB* were added using primer FS2\_metE\_out\_FW, FS3\_metE\_out\_BW and FS2\_cobB\_out\_FW, FS2\_cobB\_out\_BW, respectively (Table 4).

All inserts and backbones were quantified by NanoDrop 2000 and subsequently diluted to a final concentration of 40 nM with 10 mM Tris-HCl buffer. The reaction mix was set up in a PCR vial as specified in Table 14, whereby 1 µl of the 40 nM stocks equal 40 fmol in total.

The PCR vial was incubated in a thermocycler (Bio-Rad, Hercules/CA, USA) with 45 repetitions of two different temperatures to activate the restriction enzyme and ligase alternately for an effective assembling output (Table 15). A final digestion step at 50 °C cuts plasmids which still contain restriction sites. The last step inactivates both, the restriction enzyme and the ligase. The latter could otherwise religate some of the insert and BB fragments that are still present in the mix since during transformation the mix is kept at room temperature or on ice.

TABLE 14: Protocol for Golden Gate assembly reaction

Component	Concentration	Backbone 1	Backbone 2	Backbone 3
Insert(s)	40 nM	1 $\mu$ l	1 $\mu$ l	1 $\mu$ l
Backbone	40 nM	1 $\mu$ l	1 $\mu$ l	1 $\mu$ l
Promoter	40 nM	—	1 $\mu$ l	—
Terminator	40 nM	—	1 $\mu$ l	—
ATP	40 nM	2 $\mu$ l	2 $\mu$ l	2 $\mu$ l
Bsal <sup>a</sup>	20 U $\mu$ l <sup>-1</sup>	1 $\mu$ l	—	1 $\mu$ l
Bpil <sup>b</sup>	10 U $\mu$ l <sup>-1</sup>	—	2 $\mu$ l	—
T4 DNA Ligase <sup>a</sup>	400 U $\mu$ l <sup>-1</sup>	2.5 $\mu$ l	2.5 $\mu$ l	2.5 $\mu$ l
CutSmart buffer	10 x	2 $\mu$ l	2 $\mu$ l	2 $\mu$ l
Tris-HCl buffer	10 mM	ad 20 $\mu$ l	ad 20 $\mu$ l	ad 20 $\mu$ l

<sup>a</sup> from NEB<sup>b</sup> from Thermo Fisher Scientific, Waltham/MA, USA

TABLE 15: Thermocycler program for Golden Gate assemblies

Step	Temperature	Time	Cycles
Restriction	37 °C	1:00 min	} 45
Ligation	16 °C	2:30 min	
Expanded restriction	37 °C	30:00 min	
Final digestion	50 °C	5:00 min	
Heat inactivation	80 °C	10:00 min	

## 2.5 Transformation of DNA into *E. coli*

### 2.5.1 Preparation of chemically competent cells

The glycerol stocks of *E. coli* BL21 (DE3) and *E. coli* W (ATCC 9637) cells were streaked on LB agar plates and subsequently incubated over night at 37 °C. For the preculture a single colony was picked, inoculated in 10 ml LB medium and incubated over night at 37 °C and 200 rpm.

From this preculture, 2 ml were taken for inoculating the main culture of 200 ml LB medium, which was further incubated (same conditions as preculture) until an OD<sub>600</sub> value of 0.6 was reached. The cell suspension was kept on ice for 10 min and subsequently harvested. The culture was pelleted for 5 min at 4000 g and 4 °C, resuspended in 0.4 volumes of ice-cold TFB1 (Table 9) and once again centrifuged. The cells were now resuspended in 0.04 volumes of ice-cold TFB2 and aliquoted in pre-chilled microfuge



tubes to a volume of 100  $\mu$ l each. Aliquots were flash frozen by dipping the tubes in liquid nitrogen and stored at  $-80^{\circ}\text{C}$ .

### 2.5.2 Chemical transformation

Chemical competent cells were carefully thawed on ice for 5 min and aliquoted to a volume of 250  $\mu$ l. 2.5  $\mu$ l Golden Gate assembly (BB1, BB2 or BB3) was added and kept on ice for further 30 min. Afterwards the cell/DNA mixture was heat shocked for 90 s at  $42^{\circ}\text{C}$  and subsequently chilled on ice for 5 min. For cell recovery, 1 ml LB medium was added and incubated for 45 min (for ampicillin resistance) or 2 h (for kanamycin resistance) at  $37^{\circ}\text{C}$  and 200 rpm. After incubation 20  $\mu$ l and 100  $\mu$ l of the transformed cells were streaked on LB agar plates, with the appropriate antibiotics (either  $50\text{ }\mu\text{g ml}^{-1}$  or  $100\text{ }\mu\text{g ml}^{-1}$ ). The residual transformants were briefly pelleted, resuspended and entirely streaked equally on selective LB agar plates. All streaked transformants were incubated over night at  $37^{\circ}\text{C}$ .

## 2.6 Strain conservation

Bacteria were kept on LB agar plates at  $4^{\circ}\text{C}$  for maximally 2 weeks. For the long-time preservation of strains, cryo-conservation was used. Therefore, the particular cells were inoculated from the LB agar plate in 2–4 ml LB medium including the appropriate antibiotics and incubated over night at  $37^{\circ}\text{C}$  and 200 rpm. Afterwards, the overnight culture was briefly pelleted, resuspended in 1.2 ml and transferred into a sterile cryotube. The suspension was additionally mixed with 0.8 ml of 100 % sterile glycerol to a final glycerol concentration of 40 % (v/v). The cell/glycerol mix was kept at room temperature for 30 min to allow the cells to incorporate glycerol and subsequently stored at  $-80^{\circ}\text{C}$ .

## 2.7 Cultivation

### 2.7.1 Preculture and inoculum

Selected cells from a glycerol stock were streaked out on a selective LB agar plate and incubated over night at  $37^{\circ}\text{C}$ . From this plate a single colony was picked and inoculated

in 250 ml 2 x LB medium of a 1 l shake flask with the appropriate antibiotics and incubated over night at 37 °C and 200 rpm. The overnight culture was allowed to grow for at least 14 h to reach an OD<sub>600</sub> of 4. The cells were harvested by filling the suspension into sterile 300 ml centrifugation beaker and pelleted for 30 min 4800 g at room temperature. The cell pellets were washed twice by resuspension in 80 ml sterile 0.9 % NaCl (v/w) and centrifuged at same conditions as before. After the third centrifugation step, the cells were resuspended in 20 ml sterile dH<sub>2</sub>O, and the OD<sub>600</sub> was measured. Based on the initial OD<sub>600</sub> defined for each cultivation, the volume of each inoculum was calculated.

### 2.7.2 Shake flask cultivation

A volume of 50 ml DeLisa medium complemented with 10 g l<sup>-1</sup> glucose and 50 µg ml<sup>-1</sup> kanamycin was used. 500 ml shake flasks were filled with medium and incubated at three different temperatures (30, 37 and 44 °C) and 200 rpm.

Four inocula of two different constructs in two different strains were prepared and inoculated with an initial OD<sub>600</sub> of 0.5. Samples were taken at least 0, 2, 4, 6 and 27.5 h after inoculation. The OD<sub>600</sub> was immediately measured, and 2 ml of supernatant were stored in microfuge tubes at -18 °C for HPLC analysis. A biomass sample was taken 6 h after inoculation.

### 2.7.3 Elemental analysis

A preculture of *Escherichia coli* W (ATCC 9637) wild type was prepared as described in 2.7.1, with exception of any antibiotics.

For the cultivation six 1 l shake flasks with 200 ml DeLisa medium each supplemented with 10 g l<sup>-1</sup> glucose were incubated at 37 °C and 200 rpm for 7 h until reaching steady state condition. The cells were pelleted at 4 °C and 4800 g for 30 min and washed three times with MQ-H<sub>2</sub>O. The harvested cell pellet was subsequently transferred into a 50 ml falcon tube and stored at -80 °C. Afterwards, the cap of the falcon tube was replaced with a cotton rag and the pellet was lyophilized at -55 °C and 2 Pa (martin christ, alpha 1-4 LD plus, Osterode am Harz, Germany) for 24 h.

The pellet was subsequently milled and the mean elemental composition (carbon, hydrogen, nitrogen, oxygen, phosphorous and sulphur) of *E. coli* W was threefold determined (micro analytical laboratories, University of Vienna, Vienna, Austria) (in the Appendix

## 2.7. Cultivation

Table A.1, A.2). From the results the elemental composition of the biomass was determined to be  $C_{1.000}H_{1.676}N_{0.234}O_{0.438}P_{0.018}S_{0.005}$ , i.e. the carbon content of *E. coli* W dry biomass is 46.1 % (w/w). Particular values are listed in Table 16 and 17.

The average molecular weight of cells ( $\overline{M}_{cell}$ ) is based on the content of main components and is therefore  $24.710 \text{ g mol}^{-1}$ . The average cell dry content of each component was converted with the respective molar mass to obtain the molar amount per 1 g cell dry weight  $n_{i \text{ in } 1 \text{ g CDW}}$ .

$$n_{i \text{ in } 1 \text{ g CDW}} = \frac{\frac{\overline{CDC}_i}{100}}{M_i} \quad \text{mol} \quad (2.1)$$

$\overline{CDC}_i$  is the average cell dry content of component  $i$  in %, while  $M_i$  is the molar mass in  $\text{g mol}^{-1}$ .

To receive the stoichiometric coefficients  $v_i$  for the elemental formula, the amount of each component was related to 1 mol carbon.

$$v_i = \frac{n_{i \text{ in } 1 \text{ g CDW}}}{n_{c \text{ in } 1 \text{ g CDW}}} \quad (2.2)$$

TABLE 16: Main components of *E. coli* W

	Carbon	Hydrogen	Nitrogen	Sulphur	Phosphate	Oxygen	$\Sigma$
<b>Cell dry content, %</b>	46.060 $\pm 0.078$	6.480 $\pm 0.071$	12.570 $\pm 0.064$	0.617 $\pm 0.005$	2.197 $\pm 0.024$	26.920 $\pm 0.057$	94.844 $\pm 0.299$
<b><math>M, \text{ g mol}^{-1}</math></b>	12.011	1.008	14.007	32.065	30.974	15.999	
<b>1 g CDW, mmol</b>	38.344	64.286	8.974	0.192	0.709	16.826	
<b>related to 1 mol C</b>		1.676	0.234	0.005	0.018	0.438	$\overline{M}_{cell}$ 24.710

$$\overline{M}_{cell} = M_c + (M_h \cdot v_h) + (M_n \cdot v_n) + (M_s \cdot v_s) + (M_p \cdot v_p) + (M_o \cdot v_o) \quad \text{g mol}^{-1} \quad (2.3)$$

Indices  $c, h, n, s, p, o$  stand for carbon, hydrogen, nitrogen, sulphur, phosphate and oxygen, respectively.

TABLE 17: Minor components of *E. coli* W

	Potassium	Sodium	Chloride	Ash content	$\Sigma$
<b>Cell dry content, %</b>	1.730 $\pm 0.022$	0.851 $\pm 0.006$	0.904 $\pm 0.107$	9.707 $\pm 0.076$	9.707 $\pm 0.135$
<b><i>M</i>, g mol<sup>-1</sup></b>	39.098	22.990	35.453	–	
<b>1 g CDW, mmol</b>	0.442	0.370	0.255	–	
<b>related to 1 mol C</b>	0.012	0.010	0.007	–	

### 2.7.4 Bioreactor cultivations

For all bioreactor cultivations, DeLisa medium with 50  $\mu\text{g ml}^{-1}$  kanamycin was used at pH 7. The cultures were optionally supplemented with either 10  $\text{g l}^{-1}$  glucose, 10  $\text{g l}^{-1}$  acetate, or both. The solution of autoclavable (ac) components with the exception of glucose (Table 7) were directly autoclaved in the reactor vessel at 121 °C for 20 min and 2 bar. Separately autoclaved glucose solution and sterile filtered kanamycin were mixed and injected through a port on the bioreactor lid, using a sterile syringe.

Per reactor, 500 ml preculture were prepared as described in 2.7.1, and inoculated with an initial  $\text{OD}_{600}$  of 1. The inoculation was carried out via sterile 50 ml syringes and needles that were pierced through fermenter port diaphragm. A system of four parallel DASGIP Benchtop Bioreactors for Microbiology (Eppendorf AG, Hamburg, Germany) were used. The initial batch volume was 1 l, and cultivation temperature was set at 37 °C (TC4, Eppendorf AG, Hamburg, Germany). Reactor aeration was performed with pressurized air at 2 vvm (MX4/4, Eppendorf AG, Hamburg, Germany) and dispersed at constant agitation (three Rushton impeller) at 1400 rpm (SC4, Eppendorf AG, Hamburg, Germany).

A fluorescence dissolved oxygen electrode VisiFerm DO 225 (Hamilton, Reno, NV, USA) was used to monitor and control the dissolved oxygen ( $\text{dO}_2$ ) content. The pH was monitored by a pH electrode (Mettler-Toledo GmbH, Giessen, Germany) and maintained at a value of pH 7 by addition of 12.5 %  $\text{NH}_4\text{OH}$  and 5 M HCl supplied by a peristaltic pump module (MP8, Eppendorf AG, Hamburg, Germany). Off-gas concentrations of oxygen and carbon dioxide were quantified with an off-gas sensor (GA4, Eppendorf AG, Hamburg, Germany).

All technical instruments were attached to the fermenter and calibrated according to the

suppliers' manuals. The pH electrode was calibrated at pH 4.0 and 7.0, and the oxygen electrode was calibrated with nitrogen and pressurized air. Flow rate calibration of the pumping module was applied weighing out the amount dH<sub>2</sub>O conveyed over time.

Biomass samples were taken every 2 h and immediately after depletion of glucose or acetate. For sampling, a pre-sample of 5 ml was drawn and discarded by a syringe, followed by taking a sample of 15 ml cell suspension which was immediately transferred into a pre-chilled falcon tube and kept on ice for further processing. For the fed-batch, additional samples were taken each 0.5 h for measuring residual substrates, metabolites, and OD<sub>600</sub>. Therefore also a pre-sample of 5 ml was drawn and discarded, and subsequent only a sample volume of 2 ml was taken.

When foam formation occurred, sterile antifoam agent Struktol J 673-1 (Schill+Seilacher GmbH, Hamburg, Germany) was added in a 1 to 10 dilution via sterile needles that were pierced through fermenter port diaphragm.

## 2.8 Analytical methods

### 2.8.1 Cell biomass concentration

#### Optical density (OD<sub>600</sub>)

For the analysis, 1 ml of cell suspension was transferred to a single-use plastic cuvette measuring the absorbed and scattered light with a photometer. Values within the linear range (0.2 and 0.8) were measured or otherwise diluted with dH<sub>2</sub>O, which was also used as a blank. For each sample, two measurements were performed.

#### Cell dry weight (CDW)

Glass centrifugation tubes were labeled and dehydrated in an oven at 121 °C for 24 h. Afterwards, they were incubated in a desiccator until reaching room temperature and subsequently tared on an analytical scale (Mettler Toledo, Columbus/OH, USA). A sample volume of 3 times 4 ml cell broth was transferred into 3 weighed centrifugation tubes and subsequently centrifuged at 4 °C and 4800 *g* for 10 min. For HPLC measurements 2 ml of supernatant were stored in a microfuge tube at -18 °C.

The pellets were washed with 4 ml dH<sub>2</sub>O to remove all soluble particles and centrifuged at same conditions as before. The supernatant was discarded, and the tubes were incubated at 121 °C for 72 h. Afterwards, they were again cooled down to room temperature, and the weight-difference was determined which equals the dry biomass included in 4 ml sample. The biomass concentration was calculated by taking the sample-volume into account.

$$\rho_{cdw_{sample}} = \frac{m_{cdw_{sample}} \cdot V_{sample}}{1000} \quad \text{g l}^{-1} \quad (2.4)$$

$m_{cdw_{sample}}$  is the weight-difference of each pre-tared glass tube in g and  $V_{sample}$  is the sample volume in ml. Divided by 1000 results in a cell dry weight concentration in g l<sup>-1</sup>.

## 2.8.2 HPLC

Produced metabolites during cultivation and residual substrates in the fermentation broth were identified and quantified by HPLC in an Agilent system (1100 series, Agilent Technologies, Santa Clara/CA, USA) using an Aminex HPX87H column (300 x, 7.8 mm, Bio-Rad, Hercules/CA, USA) at 60 °C with a flow rate of 0.6 ml min<sup>-1</sup> for 30 min and 4 mM H<sub>2</sub>SO<sub>4</sub> as mobile phase.

450 µl of supernatant residuals from the first centrifugation step (for 10 min 14 000 g, 4 °C) after sampling, was mixed with 50 µl 40 mM H<sub>2</sub>SO<sub>4</sub> to adapt the composition of the mobile phase. To avoid any cell residuals aggregating in the mobile phase clogging the column, samples were once more centrifuged at same conditions as before. The supernatant was transferred to an HPLC vial and placed on a tray in Agilent system autosampler at 4 °C. For analysis a sample volume of 10 µl was injected.

For determining the concentration and retention time measured, stock solutions of glucose, acetate, succinate, lactate, formate, and ethanol were prepared. All substances except ethanol were weighed on an analytical scale (Mettler Toledo, Columbus/OH, USA) and dissolved in MQ-H<sub>2</sub>O of a 25 ml volumetric flask. The amount of 99.9 % (v/v) ethanol for the stock solution was measured volumetrically and dissolved in MQ-H<sub>2</sub>O of a 25 ml volumetric flask. From each stock solution five standard solutions (Table 18) were generated using serial dilution. Afterwards, all standard solutions were treated in the same way as the sample solution, mixing 450 µl solution with 50 µl 40 mM H<sub>2</sub>SO<sub>4</sub> before quantification.

## 2.8. Analytical methods

For detecting the amount of substances eluting from the column, a refractive index detector (Agilent 1100 series G1362A, Agilent Technologies, Santa Clara/CA, USA) and a UV detector (Agilent 1100 series G1315A, Agilent Technologies, Santa Clara/CA, USA) at  $\lambda = 210$  nm, were used.

All operating and detecting instruments were controlled and monitored by ChemStation for LC 3D systems (Agilent Technologies, Santa Clara/CA, USA). For data analysis and for manual peak integration, ChemStation for LC 3D systems was used as well.

TABLE 18: Standard solutions for 5-point calibration

Retention time, min	Substance	Concentration, g l <sup>-1</sup>				
9.328	Glucose	25	12.5	2.5	1.25	0.25
15.467	Acetate					
12.15	Succinate	5	2.5	0.5	0.25	0.05
13.171	Lactate					
14.258	Formate					
21.641	Ethanol					

### 2.8.3 Statistical data evaluation

#### Inert gas ratio

During the bioreactor cultivation, the ration of oxygen gas flow inlet ( $y_{O_2,in}$ ) differs from oxygen gas flow outlet ( $y_{wet}$ ). This occurs since evaporating water from the fermentation broth and produced carbon dioxide dilute, while oxygen consumption deduces the outlet gas flow rate. Therefore both gas flow ratios were measured before inoculation at cultivation conditions (37 °C, 2 vvm, 1400 rpm) to determine the water ratio in the off-gas flow ( $ex_{H_2O,out}$ ). For  $y_{wet}$  and  $y_{O_2}$ , 20.75 and 21.00 % oxygen were measured respectively. That results in an  $ex_{H_2O,out}$  of 1.19 %.

$$ex_{H_2O,out} = 1 - \frac{y_{wet}}{y_{O_2,in}} \quad (2.5)$$

The inert gas ratio  $Ra_{inert}$  relates the molar fraction of inert gas in the inlet gas stream in respect to the molar fraction of the inert gas in the outlet gas stream. In this case, inert gases are gases that do not react with the reactor content (all gases except oxygen, carbon dioxide, and evaporating water). Therefore, the content of inlet gases was divided

by the content of outlet gases (Equation 2.6).  $y_i$  is the content of component  $i$  in percent whereas 1 is indicated as 100 % for all gases.

$$Ra_{inert} = \frac{1 - \left( \frac{y_{O_2,in} + y_{CO_2,in}}{100} \right)}{1 - \left( \frac{y_{O_2,out} + y_{CO_2,out}}{100} \right) - ex_{H_2O,out}} \quad (2.6)$$

$Ra_{inert}$  shifts during cultivation due to  $y_{O_2,out}$  and  $y_{CO_2,out}$ , while  $ex_{H_2O,out}$  is assumed to be constant.

### Off-gas analysis

With the known in-gas flow rate ( $\dot{F}_{in}$ ) and the determined inert gas ratio, the off-gas flow rate ( $\dot{F}_{out}$ ) can be determined at each time point.

$$\dot{F}_{out} = \dot{F}_{in} \cdot Ra_{in} \quad \text{sl h}^{-1} \quad (2.7)$$

The units for  $\dot{F}_{out}$  and  $\dot{F}_{in}$  are standard liter per hour.

For volumetric determination of produced carbon dioxide and consumed oxygen, the net content was converted to decimals, dividing by 100 and multiplied with the off-gas flow rate and period in hours (Equation 2.8, 2.10). This results in the volume of the particular gas indicated as standard liter produced or consumed during a specific period. The molar amount of this volumes were calculated with the standard volume per mol (Equation 2.9, 2.11) to obtain Cmol or Omol (by multiplying  $n_{O_2}$  by 2). The amount of produced carbon dioxide in Cmol and consumed oxygen in Omol were summed up over the period of cultivation (Equation 2.12, 2.13).

$$V_{CO_2} = \frac{(y_{CO_2,out} - y_{CO_2,in}) \cdot \dot{F}_{out}}{100} \cdot dt \quad \text{sl} \quad (2.8)$$

$$n_{CO_2} = \frac{V_{CO_2}}{22.4 \text{ l mol}^{-1}} \quad \text{mol or Cmol} \quad (2.9)$$

$$V_{O_2} = \frac{y_{O_2,in} - (y_{O_2,out} + (y_{O_2,dry} - y_{wet})) \cdot \dot{F}_{out}}{100} \cdot dt \quad \text{sl} \quad (2.10)$$



$$n_O = \frac{V_{O_2}}{22.4 \text{ l mol}^{-1}} \cdot 2 \quad \text{Omol} \quad (2.11)$$

$$\sum n_{CO_2} = \sum_{i=30s}^t n_{CO_2} \quad \text{mol or Cmol} \quad (2.12)$$

$$\sum n_O = \sum_{i=30s}^t n_O \quad \text{Omol} \quad (2.13)$$

In- and off-gas values were recorded every 30 s and  $t$  indicates the actual inoculation time.

### Carbon balance

To validate the correct amount of biomass and metabolites formed in the bioreactor process, the content of recovered carbon to that present at the beginning of the cultivation was determined which is referred as *carbon balance* or *carbon recovery*. If balancing fails, it reveals that something is wrong, either in the process, or the laboratory, or in the calculations. Therefore the carbon content of all components had to be determined. First,  $\rho_i$  was converted into  $c_i$  to obtain all components in  $\text{mol l}^{-1}$ .

$$c_i = \frac{\rho_i}{M_i} \quad \text{mol l}^{-1} \quad (2.14)$$

$\rho_i$  is the concentration of component  $i$  (substrate or metabolite) in  $\text{g l}^{-1}$ , and  $M_i$  is the molar mass of component  $i$  in  $\text{g mol}^{-1}$ .

Furthermore, the molar concentrations were converted into mole carbon. Therefore, the total number of carbon atoms was included in respective of the substance and the reactor volumes.

$$n_{C,i_{\text{reactor}}} = c_i \cdot n_i \cdot V_{\text{reactor}} \quad \text{Cmol} \quad (2.15)$$

$n_i$  is the number of carbon atoms per mol of substance  $i$ , and  $n_{C,i_{\text{reactor}}}$  is the amount of mole carbon in Cmol of substance  $i$  in the reactor.

The carbon content in dry cell biomass was determined by the previously conducted elemental analysis as 46.06 % (w/w) (Table 16).  $M_c$  is the molar mass of carbon for the conversion to mole per liter.

$$n_{c,cdw_{reactor}} = \frac{\rho_{cdw} \cdot 0.4606}{M_c} \cdot V_{reactor} \quad \text{Cmol} \quad (2.16)$$

$\rho_{cdw}$  is the cell dry weight concentration in  $\text{g l}^{-1}$  determined in Equation 2.4.  $n_{c,cdw_{reactor}}$  is the amount of mole carbon (from biomass) in Cmol, that is currently present in the reactor volume  $V_{reactor}$  in liter.

The amount of carbon loss which is caused by sampling was taken into account as well. Therefore, the amount of mole carbon of the respective substances and biomass was determined for each sample.

$$n_{c,i,cdw_{sample}} = \frac{n_{c,i,cdw_{reactor}}}{V_{reactor}} \cdot V_{sample} \quad \text{Cmol} \quad (2.17)$$

The amounts of mole carbon lost during sampling were summed up for each substance and added up with those present in the bioreactor to obtain the actual carbon amount  $n_{c,i,cdw_{actual}}$ .

$$n_{c,i,cdw_{actual}} = n_{c,i,cdw_{reactor}} + \sum n_{c,i,cdw_{sample}} \quad \text{Cmol} \quad (2.18)$$

For carbon balancing, the sum of substrates ( $i$ ), biomass ( $cdw$ ) and accumulated carbon dioxide ( $\text{CO}_2$ ) for each sampling point were compared to the sum at fermentation onset (0 h). Total amounts of carbon were used for all components including carbon loss from sampling.

$$C - recovery_{actual} = \frac{\sum n_{c,i,cdw_{actual}} + \sum n_{\text{CO}_2}}{\sum n_{c,i,cdw_{0h}}} \cdot 100 \quad \% \quad (2.19)$$

### **Uptake rates**

For the sake of comparability, the volumetric and specific substrate uptake rates for glucose and acetate were taken only in the phase of main substrate uptake (MSU-phase) (x h after inoculation until depletion of glucose or acetate if in case acetate was the sole carbon source). The MSU-phase varies regarding the C-sources and construct, and is

highlighted for each cultivation in the results section. For experiments with only acetate as C-source, the MSU-phase ended with the depletion of acetate.

Rates were calculated between each sampling time point (every 2 h) (Equation 2.20) and averaged to a mean volumetric uptake rate. From each respective volumetric uptake rate the specific uptake rate was calculated (Equation 2.21) considering the average biomass concentration present in that time interval.

$$r_{s_{x+2h}} = \frac{s_{xh} - s_{x+2h}}{t_{x+2h} - t_{xh}} = \frac{ds}{dt} \quad \text{mmol l}^{-1} \text{ h}^{-1} \quad (2.20)$$

$$q_{s_{x+2h}} = \frac{r_{s_{x+2h}}}{\frac{x_{xh} + x_{x+2h}}{2}} \quad \text{mmol g}^{-1} \text{ h}^{-1} \quad (2.21)$$

$s_{xh}$  and  $x_{xh} \stackrel{\text{def}}{=} (\rho_{cdw_{xh}})$  are the substrate concentrations in  $\text{mmol l}^{-1}$  and biomass concentrations in  $\text{g l}^{-1}$ , respectively,  $x$  hours after inoculation. Since sampling took place at two-hourly intervals, the volumetric and specific uptake rates are indicated as  $_{x+2h}$ .

The specific uptake rates for each sampling interval were used to calculate the final weighted specific uptake rate for the entire MSU-phase ( $t_{s_{end}} - t_{s_1}$ ).

$$q_{s_{MSU}} = \frac{(q_{s_1} \cdot dt_{s_1}) + (q_{s_2} \cdot dt_{s_2}) + \dots + (q_{s_{end}} \cdot dt_{s_{end}})}{t_{s_{end}} - t_{s_1}} \quad \text{mmol g}^{-1} \text{ h}^{-1} \quad (2.22)$$

$dt$  stands for the exact time interval of each respective rate.  $t_{s_{end}} - t_{s_1}$  is the entire MSU-phase interval which ranges from 2 or 4 hours after inoculation until depletion of glucose or acetate (when acetate is the only C source). Unlike in Equation 2.22, the rates for the feed were taken from the beginning of the feed phase until biomass maximum was reached.

### Carbon dioxide production rate

The specific carbon dioxide production rate  $q_{CO_2_{x+2h}}$  was determined likewise for each sampling time point (each 2 h).

$$q_{CO_2_{x+2h}} = \frac{\frac{\sum n_{CO_2_{xh}} - \sum n_{CO_2_{x+2h/1h}}}{1000}}{\frac{\rho_{cdw_{xh}} + \rho_{cdw_{x+2h}}}{2} \cdot \frac{V_{reactor_{xh}} + V_{reactor_{x+2h}}}{2000}} \cdot dt \quad \text{mmol g}^{-1} \text{ h}^{-1} \quad (2.23)$$

The accumulated amount of carbon dioxide  $\sum n_{CO_2}$  from Equation 2.12 was converted from mol to mmol by dividing by 1000.  $\rho_{cdw}$  is the biomass concentration in  $\text{g l}^{-1}$ , and  $V_{reactor}$  the reactor volume in ml.  $dt$  stands for the exact time interval of each respective rate.

The specific production rates for each sampling interval were used to calculate the final weighted specific production rate for the entire MSU-phase ( $t_{CO_2_{end}} - t_{CO_2_1}$ ).

$$q_{CO_2_{MSU}} = \frac{(q_{CO_2_1} \cdot dt_{CO_2_1}) + (q_{CO_2_2} \cdot dt_{CO_2_2}) + \dots + (q_{CO_2_{end}} \cdot dt_{CO_2_{end}})}{t_{CO_2_{end}} - t_{CO_2_1}} \quad \text{mmol g}^{-1} \text{ h}^{-1} \quad (2.24)$$

As already explained for Equation 2.22, specific rates were taken from the MSU-phase in the batch as well as from a defined phase in the fed (latter not shown).

### Base titration rate

The total volume of 12.5 % (v/v) ammonia for pH regulation was recorded by the pumping system in ml. To yield the total amount of ammonia titrated, the molar concentration was determined first.

$$c_{NH_3(12.5\%)} = \frac{\rho_{NH_3(12.5\%)}}{M_{NH_3}} \cdot 0.125 \quad \text{mol l}^{-1} \text{ or M} \quad (2.25)$$

$\rho_{NH_3(12.5\%)}$  is the density of the particular aqueous ammonia solution with 948 g l<sup>-1</sup> at 20 °C.  $M_{NH_3}$  is the molar mass of NH<sub>3</sub> in g l<sup>-1</sup> and 0.125 stands for 12.5 % (v/v).

Next, the Volume of ammonia solution  $V_{NH_3}$  indicated in ml was taken into account to receive the total amount of ammonia in mmol.

$$n_{NH_3} = V_{NH_3} \cdot c_{NH_3(12.5\%)} \quad \text{mmol} \quad (2.26)$$

The specific titration rate was determined for each sampling interval equally to Equation 2.23.

$$b_{NH_3} = \frac{n_{NH_3_{x+2h}} - n_{NH_3_{xh}}}{\frac{\rho_{cdw_{xh}} + \rho_{cdw_{x+2h}}}{2} \cdot \frac{V_{reactor_{xh}} + V_{reactor_{x+2h}}}{2000} \cdot dt} \quad \text{mmol g}^{-1} \text{ h}^{-1} \quad (2.27)$$

Further, the final weighted specific titration rates were calculated by summing up the single rates multiplied with the particular time interval  $dt$  during the MSU-phase divided by the MSU-phase period ( $t_{end} - t_{NH_3_1}$ ).

$$b_{NH_3_{MSU}} = \frac{(q_{NH_3_1} \cdot dt_{NH_3_1}) + (q_{NH_3_2} \cdot dt_{NH_3_2}) + \dots + (q_{NH_3_{end}} \cdot dt_{end})}{t_{end} - t_{NH_3_1}} \quad \text{mmol g}^{-1} \text{ h}^{-1} \quad (2.28)$$

Calculations for the fed phase were handled the same was as described in Equation 2.22 and 2.24.

### Growth rate

The specific growth rates during the MSU-phases were calculated as well for each sampling interval.

$$\mu_{x+2h} = \frac{\ln(x_{x+2h} - x_{xh})}{t_{x+2h} - t_{xh}} \quad \text{h}^{-1} \quad (2.29)$$

$x_{xh} \stackrel{\text{def}}{=} (\rho_{cdw_{xh}})$  is the biomass concentration in  $\text{g l}^{-1}$ , and  $x+2h$  defines the time interval of sampling.

The final weighted specific growth rate comprises a sum up of all individual rates multiplied with the exact time interval ( $dt$ ), and divided by the whole phase period ( $t_{\text{end}} - t_1$ ).

$$\mu_{\text{MSU}} = \frac{(\mu_1 \cdot dt_1) + (\mu_2 \cdot dt_2) + \dots + (\mu_{\text{end}} \cdot dt_{\text{end}})}{t_{\text{end}} - t_1} \quad \text{h}^{-1} \quad (2.30)$$

### Yields

The specific yields were calculated separately for the whole batch phase and the defined feed phase (from substrate depletion until biomass maximum). In this case only the equations for the batch phases are described since they only differentiate in the indices ( $0h \rightarrow \text{End } S$  and  $\text{End } S \rightarrow \text{End } X_{\text{max}}$ ).

$$Y_{X/S} = \frac{X_{\text{End } S} - X_{0h}}{S_{0h} - S_{\text{End } S}} \quad \text{Cmol Cmol}^{-1} \quad (2.31)$$

$$Y_{\text{CO}_2/S} = \frac{n_{\text{CO}_2 \text{End } S} - n_{\text{CO}_2 0h}}{S_{0h} - S_{\text{End } S}} \quad \text{Cmol Cmol}^{-1} \quad (2.32)$$

$$Y_{\text{O}_2/S} = \frac{n_{\text{O}_2 \text{End } S} - n_{\text{O}_2 0h}}{S_{0h} - S_{\text{End } S}} \quad \text{Omol Cmol}^{-1} \quad (2.33)$$

$$Y_{\text{CO}_2/X} = \frac{n_{\text{CO}_2 \text{End } S} - n_{\text{CO}_2 0h}}{X_{0h} - X_{\text{End } S}} \quad \text{Cmol Cmol}^{-1} \quad (2.34)$$

## 2.8. Analytical methods

---

$X$  is the amount of biomass in Cmol in the reactor and is equal to  $n_{c,cdw_{reactor}}$ .  $S$  is the amount of all substrates (glucose and/or acetate)  $i$  in Cmol in the reactor and is equal to  $\sum n_{c,i_{reactor}}$ .





## 3 Results

### 3.1 Genetic constructs

To reach the first two objectives of co-utilising acetate in presence of glucose and reducing adverse effects of acetate, three different genes were chosen to create a library of various gene combinations (Figure 10). For cloning performance, *E. coli* BL21 turned out as a suitable host for plasmid assembly and propagation, presumably due to its favourable modifications like the *hsdSB* mutation which prevents plasmid loss (Rosano and Ceccarelli, 2014).

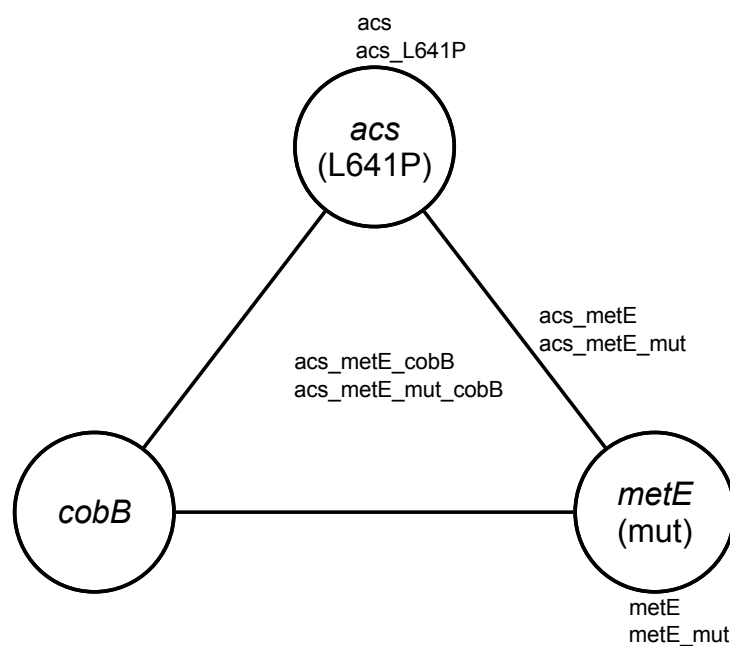


FIGURE 10: Gene constructs generated in this work. Names of constructs are listed corresponding to their genes (spheres) encoding for: acetyl-CoA synthetase (*acs*), cobalamin-independent methionine synthase (*metE*), acetyl-CoA synthetase deacetylase (*cobB*).

### 3.1.1 Characteristics of enzymes and mutations

All genes are under control of the constitutive promoters BBa\_J23114 of the Anderson promoter library.

#### **acs**

Function of overexpression:

- overexpression of *acs* increases level of acetyl-CoA synthetase, responsible for acetate utilisation

Hypothesis:

- increased level of Acs improves acetate utilisation
- increased level of Acs compensates down-regulated Acs activity in presence of glucose
- increased level of Acs enables co-utilisation of acetate in presence of glucose

#### **acs\_L641P**

Function of modification:

- modification in *acs\_L641P* leads to acetylation insensitive acetyl-CoA synthetase

Hypothesis:

- *Acs\_L641P* enables co-utilisation of acetate in presence of glucose by circumventing both transcriptional and posttranslational control of Acs activity by CCR

#### **metE**

Function of overexpression:

- overexpression of *metE* increases level of methionine synthase

Hypothesis:

- increased level of MetE compensates decreasing MetE activity in presence of acetate

#### **metE\_mut**

Function of modifications:

- modifications in *metE\_mut* leads to a stabilization of enzyme methionine synthase in oxidative environments

Hypothesis:

- in presence of acetate, MetE\_mut prevents accumulation of toxic L-homocysteine in methionine biosynthetic pathway
- in presence of acetate, MetE\_mut maintains intracellular level of methionine for cell growth
- MetE\_mut enables growth up to 44 °C

#### **acs\_metE**

Function of overexpression:

- overexpression of *acs* increases level of acetyl-CoA synthetase
- overexpression of *metE* increases level of methionine synthase

Hypothesis:

- increased level of Acs improves acetate utilisation
- increased level of Acs compensates down-regulated Acs activity in presence of glucose
- increased level of Acs enables co-utilisation of acetate in presence of glucose
- increased level of MetE compensates decreasing MetE activity in presence of acetate

#### **acs\_metE\_mut**

Function of overexpression and modifications:

- overexpression of *acs* increases level of acetyl-CoA synthetase
- modifications in *metE\_mut* leads to a stabilization of enzyme methionine synthase in oxidative environments

Hypothesis:

- increased level of Acs improves acetate utilisation
- increased level of Acs compensates down-regulated Acs activity in presence of glucose
- increased level of Acs enables co-utilisation of acetate in presence of glucose
- in presence of acetate, MetE\_mut prevents accumulation of toxic L-homocysteine in methionine biosynthetic pathway
- in presence of acetate, MetE\_mut maintains intracellular level of methionine for cell growth
- MetE\_mut enables growth up to 44 °C

### **acs\_metE\_cobB**

Function of overexpression:

- overexpression of *acs* increases level of acetyl-CoA synthetase
- overexpression of *metE* increases level of methionine synthase
- overexpression of *cobB* increases level of acetyl-CoA synthetase deacetylase

Hypothesis:

- increased level of Acs improves acetate utilisation
- increased level of Acs compensates down-regulated Acs activity in presence of glucose
- increased level of Acs enables co-utilisation of acetate in presence of glucose
- increased level of MetE compensates decreasing MetE activity in presence of acetate
- increased level of CobB overcomes posttranslational regulation by SDPADS

### **acs\_metE\_mut\_cobB**

Function of overexpression and modifications:

- overexpression of *acs* increases level of acetyl-CoA synthetase
- modifications in *metE\_mut* leads to a stabilization of enzyme methionine synthase in oxidative environments
- overexpression of *cobB* increases level of acetyl-CoA synthetase deacetylase

Hypothesis:

- increased level of Acs improves acetate utilisation
- increased level of Acs compensates down-regulated Acs activity in presence of glucose
- increased level of Acs enables co-utilisation of acetate in presence of glucose
- in presence of acetate, MetE\_mut prevents accumulation of toxic L-homocysteine in methionine biosynthetic pathway
- in presence of acetate, MetE\_mut maintains intracellular level of methionine for cell growth
- MetE\_mut enables growth up to 44 °C
- increased level of CobB overcomes posttranslational regulation by SDPADS

#### **vector control**

Function:

- enables growth in presence of kanamycin

Hypothesis:

- grows alike wild type host strain

#### **3.1.2 Nomenclature**

The nomenclature for *E. coli* W strains with the respective constructs were named after their gene, denoted in capital letters. The control strain of *E. coli* W, possessing an empty BB3 plasmid was labelled as VC.

## 3.2 Strain characterization in batch cultivations

### 3.2.1 Batch cultivations on glucose-acetate

#### ACS and ACS\_L641P

Co-utilization of glucose and acetate was tested in three different strains of *E. coli* W: The first strain (ACS\_L641P) had an acetylation insensitive acetyl-CoA synthetase under a constitutive promoter. It was hypothesised that this strain is able to co-utilise glucose and acetate by circumventing both transcriptional and posttranslational control of Acs activity by CCR. In a second strain (ACS), the native *acs* was expressed from a constitutive promoter without the L641P mutation, thus still sensitive to acetylation. VC was used as control strain, carrying an empty vector with the kanamycin resistance gene. All batch cultivations were performed for each strain at least three times on defined media supplemented with 1 % (w/v) glucose and 1 % (w/v) acetate.

All the specific rates (growth:  $\mu$ ; uptake:  $q_{\text{GLC}}$ ,  $q_{\text{ACE}}$ ; production:  $q_{\text{CO}_2}$ ; titration:  $b_{\text{NH}_3}$ ) mentioned in this paragraph and shown in Table 19 are for the main substrate uptake phase (MSU-phase; cultivation time  $\sim 4$  h until depletion of glucose), because it complies best with the phase where glucose and acetate are co-utilised. The yields ( $Y_{\text{X/S}}$ ,  $Y_{\text{CO}_2/\text{S}}$ ,  $Y_{\text{O}_2/\text{S}}$ ,  $Y_{\text{CO}_2/\text{X}}$ ) mentioned and shown in Table 20 are for the whole batch phase. The substrate (S) indicated in carbon mole comprises the sum of glucose and acetate. Table 20 also contains the carbon recovery. It comprises the sum of  $Y_{\text{X/S}}$  and  $Y_{\text{CO}_2/\text{S}}$ , presenting the recovery values at the end of the batch.

TABLE 19: Specific growth, uptake, production and titration rates for batches on 1 % (w/v) glucose-acetate, during MSU-phase.

		VC	ACS	ACS_L641P
$\mu$	$\text{h}^{-1}$	$0.23 \pm 0.05$	$0.20 \pm 0.03$	$0.27 \pm 0.04$
$q_{\text{GLC}}$	$\text{mmol g}^{-1} \text{h}^{-1}$	$2.85 \pm 0.29$	$2.71 \pm 0.81$	$3.20 \pm 0.38$
$q_{\text{ACE}}$	$\text{mmol g}^{-1} \text{h}^{-1}$	$1.76 \pm 0.26$	$1.91 \pm 0.58$	$4.72 \pm 0.26$
$q_{\text{CO}_2}$	$\text{mmol g}^{-1} \text{h}^{-1}$	$8.23 \pm 1.69$	$5.96 \pm 2.26$	$16.33 \pm 0.88$
$b_{\text{NH}_3}$	$\text{mmol g}^{-1} \text{h}^{-1}$	$3.55 \pm 0.58$	$3.29 \pm 0.74$	$1.44 \pm 0.86$

Figures 11, 12 and 13 show the course of substrate and CDW concentrations plus accumulated carbon dioxide over time of each strain (VC, ACS and ACS\_L641P, respectively). The single batches are presented in a, b, and c. The mean values are plotted in d, with

### 3.2. Strain characterization in batch cultivations

TABLE 20: Yields and carbon recoveries for batches on 1 % (w/v) glucose-acetate.

		VC	ACS	ACS_L641P
$Y_{X/S}$	$\text{Cmol Cmol}^{-1}$	$0.37 \pm 0.06$	$0.37 \pm 0.05$	$0.29 \pm 0.03$
$Y_{\text{CO}_2/S}$	$\text{Cmol Cmol}^{-1}$	$0.54 \pm 0.01$	$0.56 \pm 0.02$	$0.65 \pm 0.04$
$Y_{\text{O}_2/S}$	$\text{Omol Cmol}^{-1}$	$0.99 \pm 0.16$	$0.96 \pm 0.27$	$1.26 \pm 0.11$
$Y_{\text{CO}_2/X}$	$\text{Cmol Cmol}^{-1}$	$1.52 \pm 0.14$	$1.52 \pm 0.34$	$1.93 \pm 0.50$
C-recovery	%	91 $\pm$ 7	92 $\pm$ 7	94 $\pm$ 7

error bars illustrating the standard deviation. Raw data of each fermentation are listed separately in the Appendix (5.2).

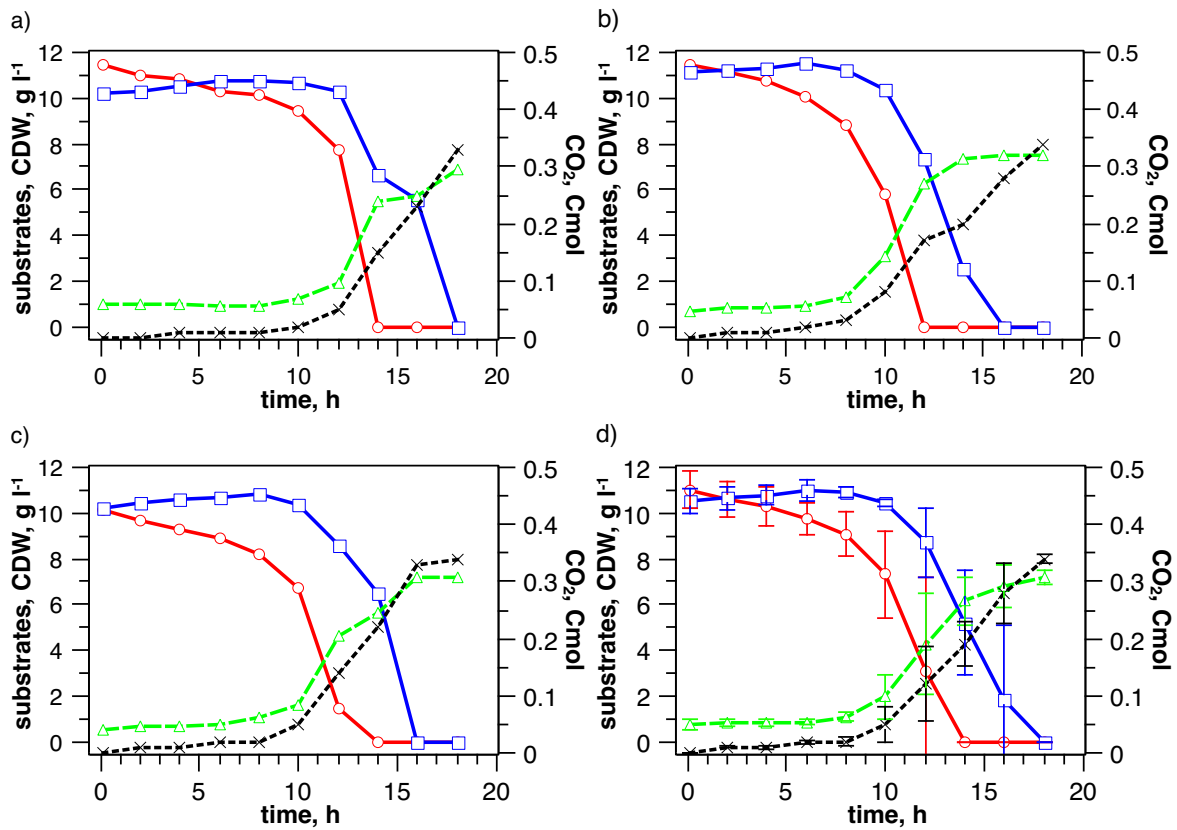


FIGURE 11: Batches on 1 % (w/v) glucose-acetate with vector control in *E. coli* W. Concentration of glucose (○), acetate (□), CDW (△), cumulated CO<sub>2</sub> (×). a) VC (F05 A) b) VC (F07 D) c) VC (F08 D) d) VC (mean)

As it can be seen from Figures 11 - 13, all three strains displayed a lag phase of around 4 h. Upon entering MSU-phase, similar specific growth and glucose uptake rates for all three strains were observed (Table 19). At the time glucose was depleted, a mean biomass concentration of  $6.16 \pm 1.06 \text{ g l}^{-1}$ ,  $5.32 \pm 2.14 \text{ g l}^{-1}$  and  $5.69 \pm 0.41 \text{ g l}^{-1}$  was

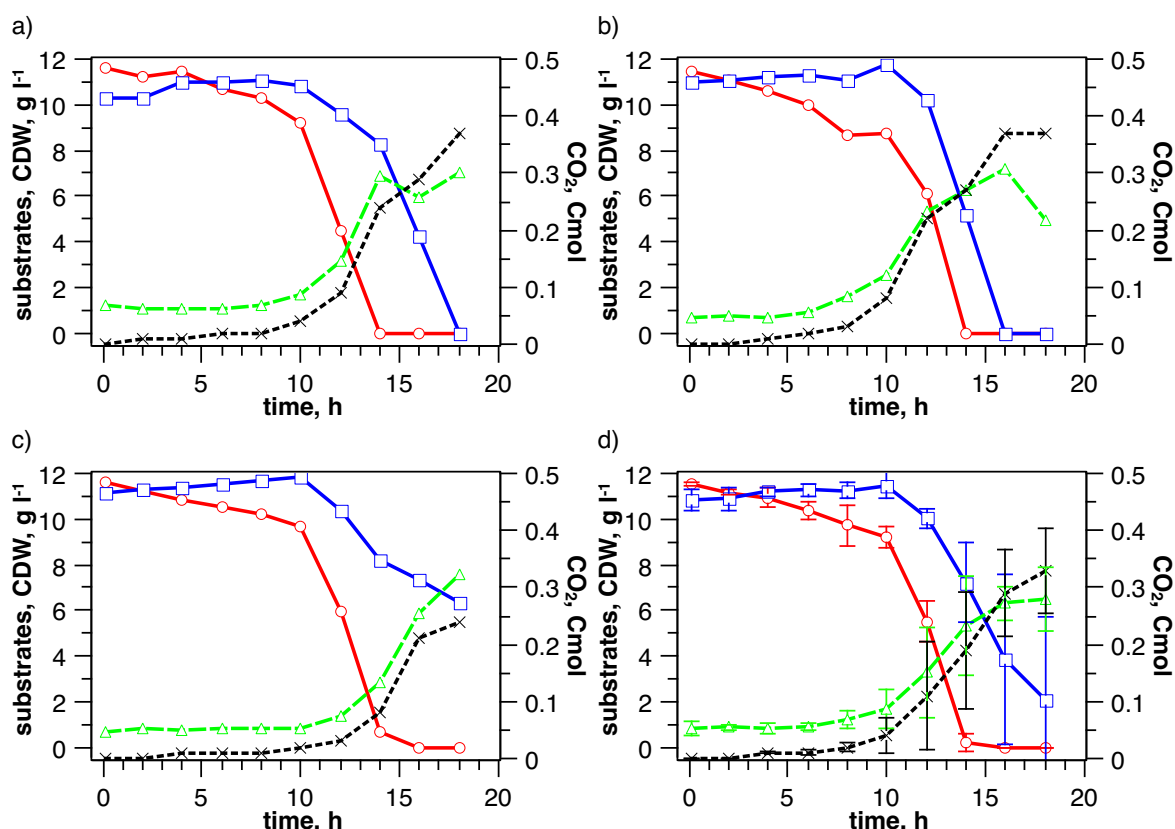


FIGURE 12: Batches on 1 % (w/v) glucose-acetate with overexpressed *acs* in *E. coli* W. Concentration of glucose (○—), acetate (□—), CDW (△—), cumulated CO<sub>2</sub> (×—). a) ACS (F05 D) b) ACS (F07 A) c) ACS (F07 B) d) ACS (mean)

measured. By this point, the residual mean acetate concentration for VC and ACS was significantly higher compared to ACS\_L641P ( $5.20 \pm 2.29 \text{ g l}^{-1}$ ,  $7.21 \pm 1.74 \text{ g l}^{-1}$  and  $3.20 \pm 1.23 \text{ g l}^{-1}$ , respectively).

Since the biomass concentration was alike for all strains, a lower acetate concentration at the stage of glucose depletion, in turn, indicates that ACS\_L641P took up acetate with a higher specific rate. Actually, a 2.7-fold increase was observed for  $q_{\text{ACE}}$  of ACS\_L641P, whereas ACS remained unchanged compared to VC (Table 19). Notable was that a similar 2-fold increase in  $q_{\text{CO}_2}$  of ACS\_L641P was observed, while similar to  $q_{\text{ACE}}$  the specific carbon dioxide production rate of ACS was comparable to that of VC.

Besides a higher specific acetate uptake and carbon dioxide production rate, ACS\_L641P displayed a 2.5-fold lower specific base titration rate ( $b_{\text{NH}_3}$ ). This indicates that due to higher acetate consumption less ammonia was required per biomass to adjust the pH because of glucose catabolism related acidification.



### 3.2. Strain characterization in batch cultivations

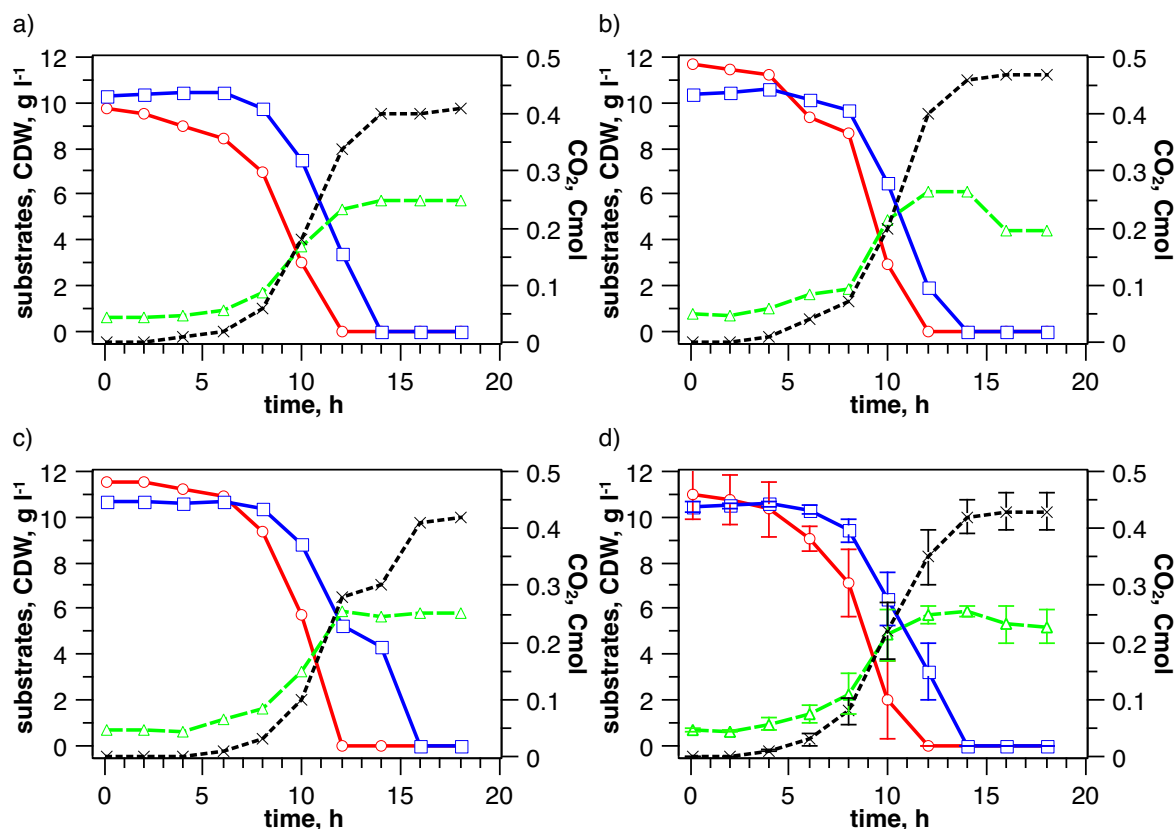


FIGURE 13: Batches on 1 % (w/v) glucose-acetate with *acs\_L641P* in *E. coli* W. Concentration of glucose (○—), acetate (□—), CDW (△—), cumulated CO<sub>2</sub> (×—). a) ACS\_L641P (F08 C) b) ACS\_L641P (F05 C) c) ACS\_L641P (F06 A) d) ACS\_L641P (mean)

The different behaviour of ACS\_L641P concerning carbon uptake and production compared to VC and ACS can also be identified in the yields. In comparison to VC, ACS\_L641P showed a 21% decrease in  $Y_{X/S}$  while  $Y_{CO_2/S}$  was increased by 20%. Accompanied with the high amount of carbon dioxide produced by ACS\_L641P, also the oxygen consumption per substrate ( $Y_{O_2/S}$ ) and the carbon dioxide production per biomass ( $Y_{CO_2/X}$ ) were both increased by 37%, compared to VC.

## Discussion

The most remarkable finding in this experiment was, that ACS\_L641P showed a 2.7-fold increased specific acetate uptake rate, whereas no change in  $q_{ACE}$  was observed for ACS compared to VC. Comparing the residual substrate curves between ACS\_L641P and VC illustrates clear (Figure 14), that ACS\_L641P accumulated almost any further acetate in the first half of cultivation and utilised already two-third of acetate when glucose was depleted, contrary to VC.

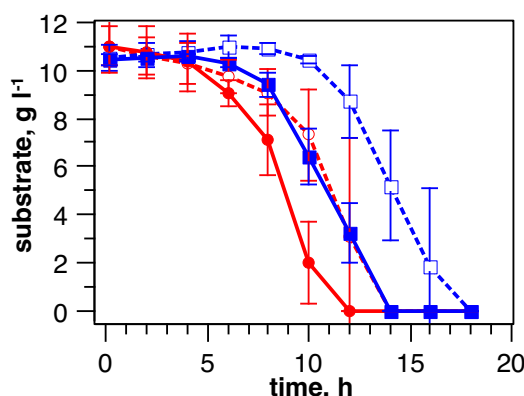


FIGURE 14: Batches on 1 % (w/v) glucose-acetate. Comparison vector control versus *acs\_L641P* in *E. coli* W. Concentration of glucose VC (○---), acetate VC (□---), glucose ACS\_L641P (●—), acetate ACS\_L641P (■—).

It seems to confirm with the hypothesis, that activity of ACS alone during metabolism of high concentrations of glucose are sufficient to enable more efficient co-utilization of acetate. This would prove that, under high glucose and acetate concentrations, where only Pta-AckA but not Acs are active, constitutive expression of *acs*, which is insensitive to post-translational acetylation is sufficient to partially overcome control mechanisms by CCR.

In contrast to the expectations, overexpression of *acs* under a constitutive promoter could not exceed the posttranslational control of the Pat enzyme, acetylating Acs. In a study, Lin et al. (2006) demonstrated the overexpression of *acs* in *E. coli* with an attempt to lower the accumulation of acetate through its enhanced assimilation. Therefore an *E. coli* MG1655 strain was modified with *acs* overexpressed vectors (inducible via IPTG) and cultivated aerobically on minimal medium M9. The media was supplemented with either 5 g l<sup>-1</sup> glucose or 3.87 g l<sup>-1</sup> acetate. The resulting fermentations showed a reduction of acetate during glucose metabolism and faster glucose consumption. The overexpression of *acs* also revealed enhanced assimilation of acetate when it was used as the sole carbon source. However, due to 2 to 3-fold lower glucose and acetate concentrations, separated cultivations (glucose or acetate), and usage of a different strain, these results can not be directly correlated.

Another interesting aspect for ACS\_L641P is an approximately 20 % increase in  $Y_{CO_2/S}$ , and therefore lower  $Y_{X/S}$ , namely more CO<sub>2</sub> and less biomass were produced compared to ACS and VC. A plausible explanation for this shift in  $Y_{X/S}$  and  $Y_{CO_2/S}$  would be the steady energy input required for gene expressing and protein production for Acs and Acs\_L641P (Valgepea et al., 2010), but comparing ACS and ACS\_L641P contradicts

that, since no shift is observed for ACS.

Further explanations, that could be argued that different behaviour of ACS\_L641P would either be higher energy requirements by the constant activity of Acs in ACS\_L641P or a different metabolic flux pattern.

Referring to energy consumption of the Pta-AckA-Acs cycle, following can be stated. Acs catalyses the reaction of acetate to acetyl-CoA, requiring 2 ATP, while Pta-AckA converts acetyl-CoA to acetate via acetyl-P which yields 1 ATP per acetyl-CoA recycled. Hence, the whole cycle results in the consumption of 1 ATP (Valgepea et al., 2010; Enjalbert et al., 2017). An increasing activity of Acs in ACS\_L641P by overexpression would likely result in higher overall activity of the Pta-AckA-Acs cycle. This energy would not be available for biomass formation and thus, lowering  $Y_{X/S}$  and increasing  $Y_{CO_2/S}$ . Acs in ACS would be despite overexpression, still mostly inactive and VC would only transcribe Acs in low quantities, which would not influence energy consumption to an equal extent.

Referring to a different metabolic flux pattern, it can be assumed that the anaplerotic GS is inactive under high glucose concentrations due to negative control by isocitrate lyase regulator (IcIR) (see 1.4.3). Once glucose is depleted, the GS is activated, presumably by the activity of cAMP-Crp (Waegeman et al., 2011). The glyoxylate shunt is therefore likely inactive during co-utilisation. Acetate which is co-utilised by ACS\_L641P in presence of glucose is consequently channelled into the TCA cycle, rather than the GS.

A comparable observation was already described in an previous conducted metabolic flux analysis for *E. coli* MC4100. During glucose consumption, little activity for the GS was observed, while high fluxes via the GS and only low fluxes through the TCA cycle were observed during catabolism of acetate (Oh et al., 2002).

It seems feasible that the activity of Acs in ACS\_L641P under high glucose concentrations would result in catabolism of acetate via the TCA cycle and to a smaller extent via the GS, compared to AC and VC. Since metabolism of carbon via the TCA cycle results in production of 2 mol carbon dioxide per cycle, while in the GS no carbon dioxide is formed, this presumably explains the higher carbon dioxide producing phenotype of ACS\_L641P. Therefore overexpression of GS genes (*acsA*, *acsB*) as well as interfering into its regulation (deletion of *icIR*) could presumably reduce the formation of carbon dioxide.

## METE\_mut

Tests on *E. coli* K-12 WE have shown that mutations in the MetE protein increase acetate tolerance due to conformational changes ( $\mu = +20\%$  in M9 media, pH 6, 20 mM sodium acetate) (Mordukhova and J.-G. Pan, 2013). These changes prevent MetE from unfolding in oxidative environments and keeps it active for converting the toxic L-homocysteine to L-methionine (Mordukhova and J.-G. Pan, 2013).

The main intention of this experiment was to test this MetE-214A (MetE\_mut) construct in the acetate tolerant *E. coli* W to prove that plasmid based overexpression of stabilized MetE could supplement cell's regular acetate-prone MetE during methionine biosynthesis in presence of acetate. By this, a limitation of intracellular methionine which slows down many cellular biosynthetic processes (protein, RNA, and DNA biosynthesis) should be prevented (Katz et al., 2009). As a result, a shortened lag phase and an increased specific growth rate, compared to VC was expected. Furthermore, it would have been interesting if overexpression of *metE\_mut* influences acetate assimilation, as this has not been tested so far.

METE\_mut was cultivated in defined media supplemented with 1 % (w/v) glucose-acetate. Specific rates, yields and the time course of all cultivations are presented in Table 21, 22 and Figure 15, respectively. Strains were cultivated in three independent batches whereby one strain (F02 B) unexpectedly differed significantly from the other two strains (F06 B). Therefore the particular results were presented separately.

TABLE 21: Specific growth, uptake, production and titration rates for batches on 1 % (w/v) glucose-acetate, during MSU-phase.

		METE_mut		
		VC	F02 B	F06 BC
$\mu$	$\text{h}^{-1}$	$0.23 \pm 0.05$	0.38	$0.20 \pm 0.01$
$q_{\text{GLC}}$	$\text{mmol g}^{-1} \text{h}^{-1}$	$2.85 \pm 0.29$	2.96	$2.34 \pm 0.14$
$q_{\text{ACE}}$	$\text{mmol g}^{-1} \text{h}^{-1}$	$1.76 \pm 0.26$	3.87	$1.39 \pm 0.25$
$q_{\text{CO}_2}$	$\text{mmol g}^{-1} \text{h}^{-1}$	$8.23 \pm 1.69$	12.71	$8.16 \pm 1.09$
$b_{\text{NH}_3}$	$\text{mmol g}^{-1} \text{h}^{-1}$	$3.55 \pm 0.58$	4.85	$4.66 \pm 0.01$

The specific growth rate in cultivation F02 B was distinctly higher than all previous strains, tested at equal conditions ( $\mu = +65\%$  towards VC,  $+41\%$  towards ACS\_L641P). Consequently, glucose was already depleted after 10 h whereas the concentration of residual acetate at this stage was still  $6.68 \text{ g l}^{-1}$ . Due to high biomass formation, the specific glucose uptake rate was not particularly higher than those for VC. The specific acetate

### 3.2. Strain characterization in batch cultivations

TABLE 22: Yields and carbon recoveries for batches on 1 % (w/v) glucose-acetate.

		METE_mut		
		VC	F02 B	F06 BC
$Y_{X/S}$	$\text{Cmol Cmol}^{-1}$	$0.37 \pm 0.06$	0.38	$0.36 \pm 0.03$
$Y_{\text{CO}_2/S}$	$\text{Cmol Cmol}^{-1}$	$0.54 \pm 0.01$	0.51	$0.54 \pm 0.02$
$Y_{\text{O}_2/S}$	$\text{Omol Cmol}^{-1}$	$0.99 \pm 0.16$	1.02	$1.04 \pm 0.06$
$Y_{\text{CO}_2/X}$	$\text{Cmol Cmol}^{-1}$	$1.52 \pm 0.14$	1.35	$1.54 \pm 0.22$
C-recovery	%	91 $\pm$ 7	89	90 $\pm$ 5

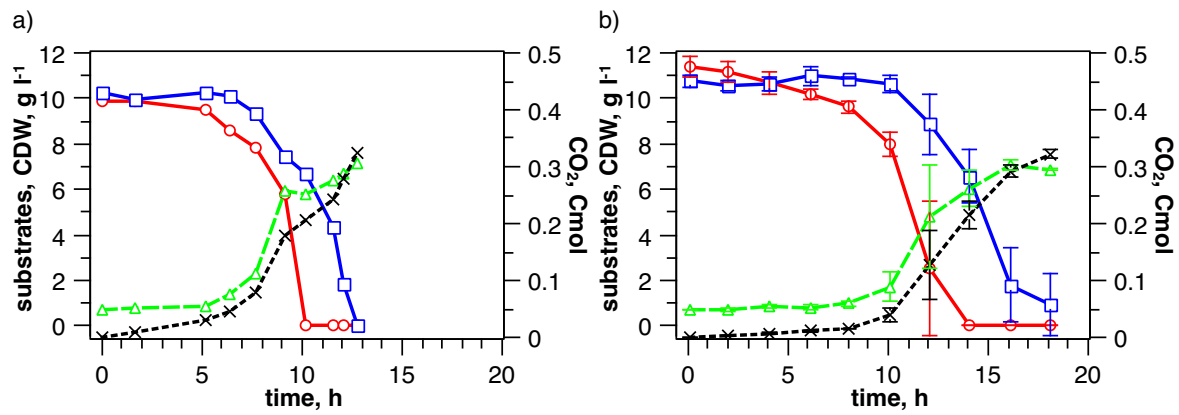


FIGURE 15: Batches on 1 % (w/v) glucose-acetate with metE\_mut in *E. coli* W. Concentration of glucose (○—), acetate (□—), CDW (△—), cumulated CO<sub>2</sub> (×—). a) METE\_mut (F02 B) b) METE\_mut mean (F06 BC)

uptake rate was 2.3-fold increased compared to VC, and specific carbon dioxide production rate was as well heightened (+54 % towards VC). Strains in cultivation F06 B and F06 C showed similar values such as VC. No differences were observed for the yields between all three METE cultivations and VC.

## Discussion

The rather highly differing results of F02 B compared to F06 B and F06 C suggests, that these strains did not represent the same physiological properties as it was expected. Provided that the right cryo-cell-stock was applied, there are still several reasons which could explain the results. One possible explanation would be a random mutation that leads to higher overexpression of target genes. For instance jackpot clones are often used to refer to high-copy-number strains due to increased antibiotic resistance (Vogl et al., 2018). However, in the absence of any sequencing results of the particular strains,

no evaluation can be stated. Another interesting approach to test strain F02 B for its improved acetate tolerance would have been to cultivate it in comparison to F06 BC at same conditions but without added acetate.

### ACS\_METE\_mut\_COBB

Since overexpression of *acs* under a constitutive promoter could not exceed the post-translational control for co-utilisation of glucose and acetate (1 % (w/v)), the genes for deacetylase CobB were expressed under a constitutive promoter in combination with those of Acs and MetE\_mut. It was hypothesised that an increased level of NAD<sup>+</sup>-dependent Sir2 ortholog protein CobB, which deacetylates Acs<sup>Ac</sup>, could overcome posttranslational regulation by the SDPADS. CobB should counteract to protein acetyltransferase Pat, and therefore restrain Acs-acetylation, for maintaining Acs active. Simultaneous overexpression of *acs* purposes an increased intracellular level of Acs despite counteracting CCR. Also, overexpression of *metE\_mut* is believed to improve acetate tolerance and should therefore reduce the lag phase.

Cultivation was performed only once in minimal media supplemented with 1 % (w/v) glucose-acetate. Specific rates (from the MSU-phase) and yields are listed in comparison with previously tested strains in Table 23, 24. The time course is shown in Figure 16.

TABLE 23: Specific growth, uptake, production and titration rates for batches on 1 % (w/v) glucose-acetate, during MSU-phase.

		ACS	ACS_L641P	ACS_METE_mut_COBB
$\mu$	$\text{h}^{-1}$	$0.20 \pm 0.03$	$0.27 \pm 0.04$	0.53
$q_{\text{GLC}}$	$\text{mmol g}^{-1} \text{h}^{-1}$	$2.71 \pm 0.81$	$3.20 \pm 0.38$	4.97
$q_{\text{ACE}}$	$\text{mmol g}^{-1} \text{h}^{-1}$	$1.91 \pm 0.58$	$4.72 \pm 0.26$	3.96
$q_{\text{CO}_2}$	$\text{mmol g}^{-1} \text{h}^{-1}$	$5.96 \pm 2.26$	$16.33 \pm 0.88$	4.39
$b_{\text{NH}_3}$	$\text{mmol g}^{-1} \text{h}^{-1}$	$3.29 \pm 0.74$	$1.44 \pm 0.86$	0.54

A remarkable high specific growth rate of  $0.53 \text{ h}^{-1}$  was observed in the MSU-phase which goes along with an increased specific glucose uptake rate. Upon glucose was depleted (after 8 h) a decelerated biomass formation and acetate utilization was observed (Figure 16). This suggests that cells rearranged their metabolism to altered conditions without glucose. The residual acetate concentration was  $6.81 \text{ g l}^{-1}$  which is still high compared to those of ACS\_L641P double as high ( $3.32 \text{ g l}^{-1}$ ). The biomass concentration at batch

### 3.2. Strain characterization in batch cultivations

TABLE 24: Yields and carbon recoveries for batches on 1 % (w/v) glucose-acetate.

		ACS	ACS_L641P	ACS_ METE_mut_ COBB
$Y_{X/S}$	$\text{Cmol Cmol}^{-1}$	$0.37 \pm 0.05$	$0.29 \pm 0.03$	0.41
$Y_{\text{CO}_2/S}$	$\text{Cmol Cmol}^{-1}$	$0.56 \pm 0.02$	$0.65 \pm 0.04$	0.35
$Y_{\text{O}_2/S}$	$\text{Omol Cmol}^{-1}$	$0.96 \pm 0.27$	$1.26 \pm 0.11$	1.79
$Y_{\text{CO}_2/X}$	$\text{Cmol Cmol}^{-1}$	$1.52 \pm 0.34$	$1.93 \pm 0.50$	0.84
C-recovery	%	92 $\pm$ 7	94 $\pm$ 7	76

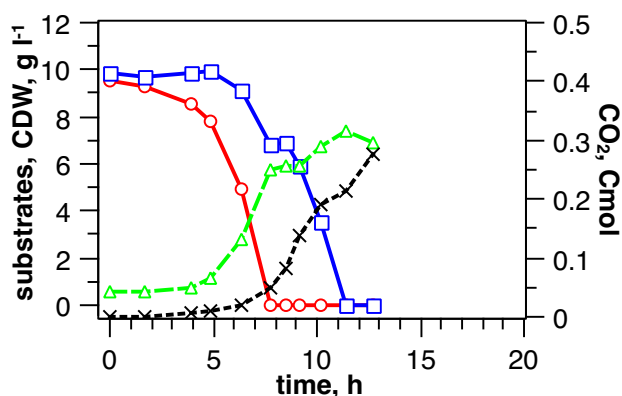


FIGURE 16: Batches on 1 % (w/v) glucose-acetate with *acs\_metE\_mut\_cobB* in *E. coli* W. Concentration of glucose (○—), acetate (□—), CDW (△—), cumulated  $\text{CO}_2$  (×—). (F02 D)

end was with  $7.38 \text{ g l}^{-1}$  alike all previous cultivations ( $7.00$  to  $7.33 \text{ g l}^{-1}$ ) with exception of ACS\_L641P which reached due to high carbon dioxide production only a mean biomass concentration of  $5.91 \text{ g l}^{-1}$  (–18 % compared to VC).

The specific acetate uptake rate was increased as well and reached almost an equivalent high number as in ACS\_L641P (–22 %), but most of the acetate was utilised after glucose was depleted. Unusual was the low specific carbon dioxide production rate which corresponded 53 % of the value measured for VC and 26 % for ACS\_L641P. Reduced values for  $Y_{\text{CO}_2/S}$  and  $Y_{\text{CO}_2/X}$  exhibited that the amount of carbon dioxide over the whole batch was low. In that connection the carbon recovery was as well remarkably low, which indicates a shortage of measured biomass, substrate, carbon dioxide or intermediates/products which were not determined. Also the ammonia titration rate showed an abnormal low value.

## Discussion

The combination of Acs, MetE\_mut, and cobB constitutively expressed in *E. coli* W shows a high potential since it grew rapidly and less inhibited in the presence of high concentrations of acetate. A similar behaviour was already observed for METE\_mut (F02 B) which also appeared to be more acetate resistant. In Figures 15 a) and Figure 16, the similarities are clearly visible. As well remarkable was the lag phase at the time when glucose was depleted, indicated by the acetate and CDW curves. It shows a typical behaviour for diauxic growth (Görke and Stülke, 2008). It is supposed, that enzymes of acetate-utilizing pathways (Acs, AckA-Pta) were still down-regulated to maintain the current growth rate on acetate only. This assumption is controversial and interesting since Acs and CobB were as well transcribed constitutively which should result in an increased level of deacetylated (active) Acs enzymes in the presence of glucose and acetate.

Tests on CobB deficient *S. enterica* strains have shown reduced growth (~50 %) on 10 mM acetate (Starai and Escalante-Semerena, 2004). Investigations on higher acetate concentrations and overexpressed *cobB* in *E. coli* are so far not known.

Within this experiment it is challenging to determine the single influences of *acs*, *metE\_mut* and *cobB* in *E. coli* W. It would be interesting if *E. coli* yields similar results when it constitutively expresses *acs\_L641P* and *metE\_mut* since the mutation in Acs\_L641P should have the similar effects of keeping Acs activated and bypasses the need of the deacetylase protein CobB although it needs to be considered that these enzymes have still further functions.

A potential explanation for the low specific carbon dioxide rate was not found, but considering the carbon recovery it could be assumed that off-gas measuring failed. The fermentation raw data (Table A.4) shows the carbon recovery in detail as well as the oxygen consumption which was compared to all other cultivations around twofold higher. The low specific base titration rate was achieved due to rapid growth and as a result the increased base titration in the first 4 h of cultivation (~3-fold compared to VC), which was not included in the calculation.



### 3.2.2 Batch cultivations on glucose

#### ACS\_L641P

Another attempt was made to further characterize the expression effect of acetylation insensitive acetyl-CoA synthetase (*acs\_L641P*) in *E. coli* on glucose as the sole carbon source. Therefore ACS\_L641P and VC were cultivated twofold in a batch of defined media supplemented with 1 % (w/v) glucose. Time courses over the whole cultivation periods are shown in Figure 17 for VC (a, b) and ACS\_L641P (c, d). All the specific rates are for the MSU-phase (cultivation time ~2 h until depletion of glucose) and shown in Table 25. The yields and carbon recoveries are listed in Table 26.

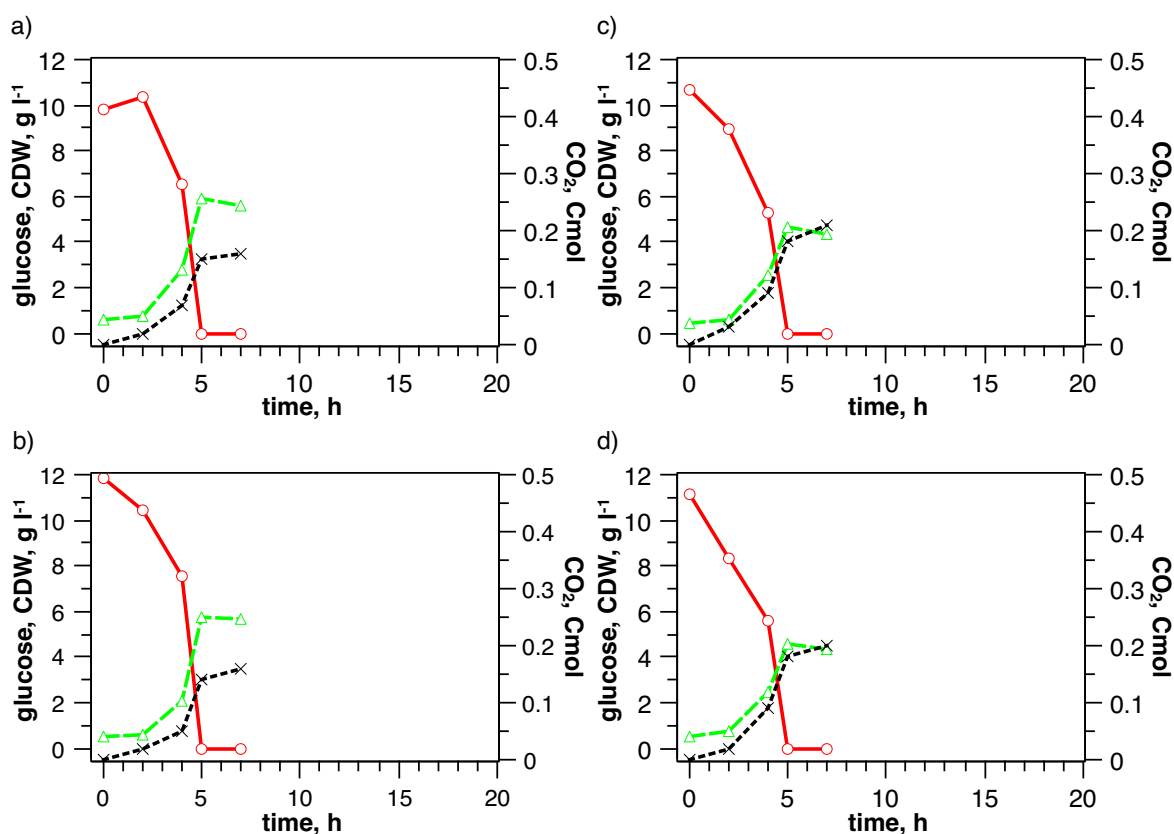


FIGURE 17: Batches on 1 % (w/v) glucose with vector control and *acs\_L641P* in *E. coli* W. Concentration of glucose (○—), CDW (△—), cumulated CO<sub>2</sub> (×—). a) VC (F10 C) b) VC (F10 D) c) ACS\_L641P (F10 A) d) ACS\_L641P (F10 B)

The cultivations showed no significant differences in specific growth and glucose uptake for ACS\_L641P and VC (Table 25). However, compared to VC, ACS\_L641P had a much higher carbon dioxide production rate (+60 %  $q_{CO_2}$ ) which lowered the biomass per substrate yield (-20 %  $Y_{X/S}$ ) and in turn resulted in an increased carbon dioxide per substrate

TABLE 25: Specific growth, uptake, production and titration rates for batches on 1 % (w/v) glucose, during MSU-phase.

		VC	ACS_L641P
$\mu$	$\text{h}^{-1}$	$0.72 \pm 0.01$	$0.68 \pm 0.07$
$q_{\text{GLC}}$	$\text{mmol g}^{-1} \text{h}^{-1}$	$7.24 \pm 0.18$	$6.90 \pm 0.89$
$q_{\text{CO}_2}$	$\text{mmol g}^{-1} \text{h}^{-1}$	$16.16 \pm 0.11$	$23.98 \pm 0.78$
$b_{\text{NH}_3}$	$\text{mmol g}^{-1} \text{h}^{-1}$	$5.35 \pm 0.97$	$6.30 \pm 0.41$

TABLE 26: Yields and carbon recovery for batches on 1 % (w/v) glucose.

		VC	ACS_L641P
$Y_{X/S}$	$\text{Cmol Cmol}^{-1}$	$0.57 \pm 0.09$	$0.44 \pm 0.02$
$Y_{\text{CO}_2/S}$	$\text{Cmol Cmol}^{-1}$	$0.47 \pm 0.07$	$0.57 \pm 0.02$
$Y_{\text{O}_2/S}$	$\text{Omol Cmol}^{-1}$	$0.58 \pm 0.13$	$0.93 \pm 0.35$
$Y_{\text{CO}_2/X}$	$\text{Cmol Cmol}^{-1}$	$0.73 \pm 0.03$	$1.15 \pm 0.01$
C-recovery	%	104 $\pm$ 16	101 $\pm$ 4

yield (+20 %  $Y_{\text{CO}_2/S}$ ) (Table 26). In addition, an increased oxygen per substrate yield (+57 %  $Y_{\text{O}_2/S}$ ) indicates for ACS\_L641P that more substrate and oxygen was utilised to carbon dioxide towards biomass. Due to this loss of carbon, the biomass concentration at the end of the batch was 21 % lower for ACS\_L641P as for VC.

## Discussion

The comparison of ACS\_L641P and VC on 1 % (w/v) glucose revealed an increased specific carbon dioxide production rate and its associated effects of lower  $Y_{X/S}$  and increasing  $Y_{\text{O}_2/S}$ . Based on the assumptions made up in the mixed batch cultivations it could be interpreted that increased Acs activity caused by *acs\_L641P* overexpression in ACS\_L641P promotes simultaneous assimilation and dissimilation of acetate and acetyl-CoA through the Pta-AckA-Acs cycle (Enjalbert et al., 2017). In VC, Acs is apparently inactivated by the acetylation activity from Pat, which is under control of glucose-mediated CCR. Consequently recycling of acetyl-CoA is predominantly performed via the reversible Pta-AckA pathway which does not require one additional ATP such as Pta-AckA-Acs cycle does. Hence, ACS\_L641P cultivated under high glucose concentrations and without supplemented acetate would consume as well more energy compared to VC.

### 3.2. Strain characterization in batch cultivations

During aerobic cultivation on glucose, only small amounts of acetate (less than  $0.5 \text{ g l}^{-1}$ ) accumulated. This corresponds well with previous reports for *E. coli* W describing a highly oxidative metabolism (Arifin et al., 2014), distinguishing *E. coli* W from other strains such as BL21 and K12 (JM109) which accumulate higher amounts of extracellular acetate during glucose catabolism (Wolfe, 2005).

#### 3.2.3 Batch cultivations on acetate

##### ACS\_L641P

Further, the same two strains as in the previous experiment were cultivated twofold with 1 % (w/v) acetate as the sole carbon source. This attempt could prove how the expression of acetylation insensitive acetyl-CoA synthetase affects the acetate metabolism of *E. coli* W in absences of CCR inducing substrates. Time courses of cultivations are shown in Figure 18 and 19. Specific rates for MSU-phase and yields are listed in Table 27 and 28, respectively. The MSU-phase varied between both strains due to different lag phases and was defined from cultivation time 6 h and 22.5 h until acetate was depleted for ACS\_L641P and VC, respectively.

TABLE 27: Specific growth, uptake, production and titration rates for batches on 1 % (w/v) acetate, during MSU-phase.

		VC	ACS_L641P
$\mu$	$\text{h}^{-1}$	$0.19 \pm 0.03$	$0.18 \pm 0.04$
$q_{\text{ACE}}$	$\text{mmol g}^{-1} \text{h}^{-1}$	$12.42 \pm 2.13$	$12.36 \pm 1.96$
$q_{\text{CO}_2}$	$\text{mmol g}^{-1} \text{h}^{-1}$	$12.79 \pm 0.31$	$17.03 \pm 3.32$

TABLE 28: Yields and carbon recoveries for batches on 1 % (w/v) acetate.

		VC	ACS_L641P
$Y_{\text{X/S}}$	$\text{Cmol Cmol}^{-1}$	$0.34 \pm 0.01$	$0.26 \pm 0.02$
$Y_{\text{CO}_2/\text{S}}$	$\text{Cmol Cmol}^{-1}$	$0.77 \pm 0.02$	$0.71 \pm 0.03$
$Y_{\text{O}_2/\text{S}}$	$\text{Omol Cmol}^{-1}$	0.85 <sup>a</sup>	$1.12 \pm 0.07$
$Y_{\text{CO}_2/\text{X}}$	$\text{Cmol Cmol}^{-1}$	$2.26 \pm 0.04$	$2.66 \pm 0.14$
C-recovery	%	111 $\pm$ 3	97 $\pm$ 5

<sup>a</sup> calculation with only one value, due to  $\text{O}_2$  off-gas signal perturbations

The resulted specific growth rates and acetate uptake rates did not reveal significant differences between ACS\_L641P and the VC. Only the  $q_{\text{CO}_2}$  of ACS\_L641P was again

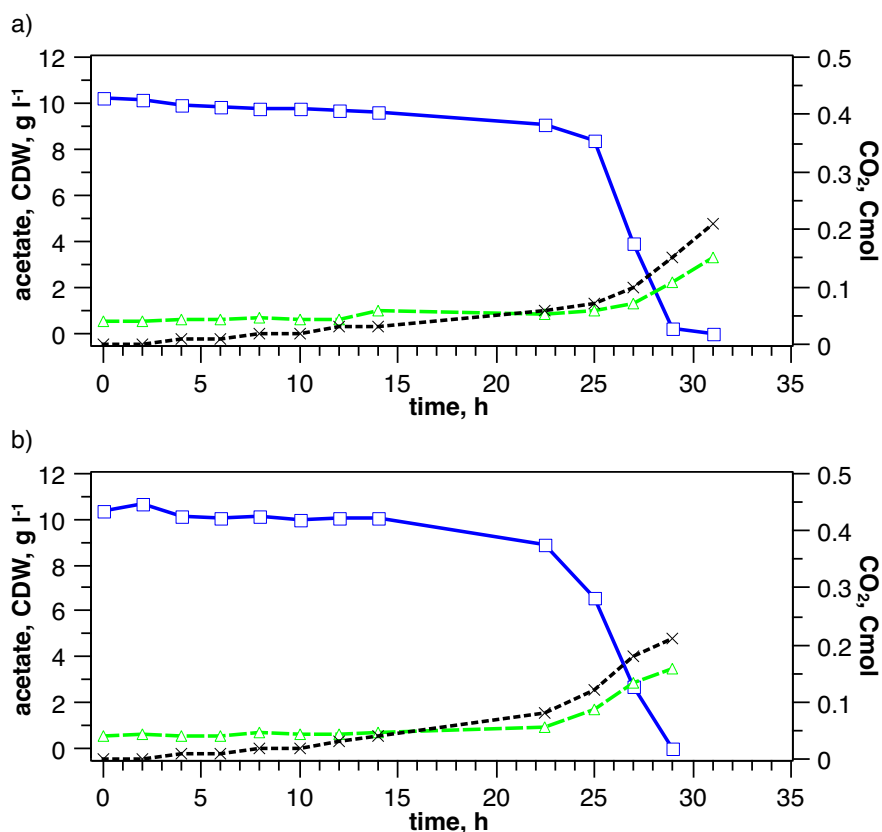


FIGURE 18: Batches on 1 % (w/w) acetate with VC in *E. coli* W. Concentration of acetate ( $\square$ —), CDW ( $\triangle$ —), cumulated  $\text{CO}_2$  ( $\times$ -----). a) VC (F09 C) b) VC (F09 D)

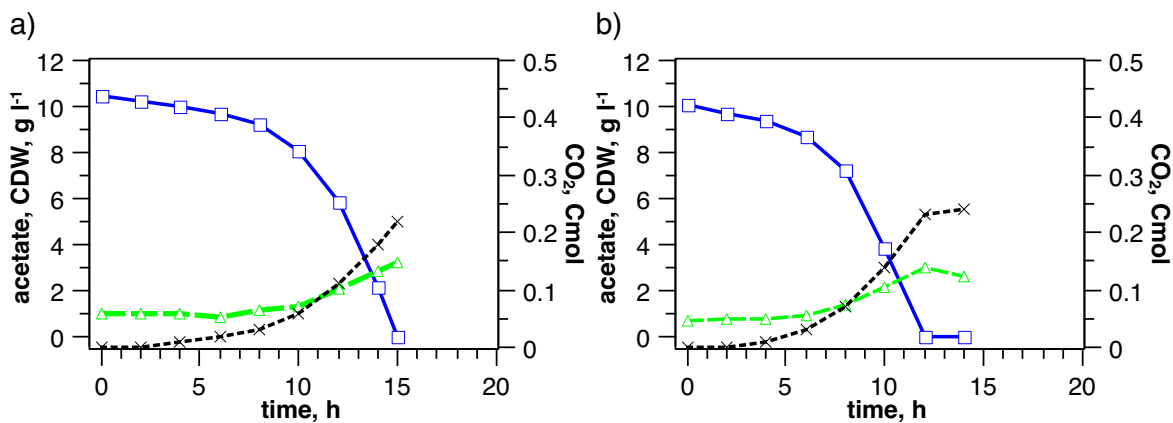


FIGURE 19: Batches on 1 % (w/v) acetate with aCS\_L641P in *E. coli* W. Concentration of acetate ( $\square$ —), CDW ( $\triangle$ —), cumulated  $\text{CO}_2$  ( $\times$ -----). a) ACS\_L641P (F09 A) b) ACS\_L641P (F09 B)

increased, in this case by +25 % compared to VC. The lag phase for VC was 3.8-times longer than for ACS\_L641P whereas duration of MSU-phase was identical.

The observed yields corresponded with the expected bias derived from the rates and the carbon recoveries prove that overall mass balancing seems to be correct.

## Discussion

Since enzymes of the Pta-AckA pathway have a much higher  $K_m$  value for acetate (7 to 10 mM, 0.413 to 0.590 g l<sup>-1</sup>) as Acs (200  $\mu$ M, 0.0118 g l<sup>-1</sup>), Pta-AckA enzymes presumably metabolise the majority of acetate present in this experiment (Wolfe, 2005).

In a previous study, Kumari, Tishel, et al. tested Acs- and Pta-AckA-deficient *E. coli* K-12 strains on minimal salts medium supplemented with a range of acetate concentrations. They found out that Acs-deficient and wild type strains grew well at higher concentrations ( $\geq 25$  mM,  $\geq 1.476$  g l<sup>-1</sup>) and poorly on lower concentrations ( $\leq 10$  mM). Pta-AckA-deficient strains conversely grew best at lower concentrations ( $\leq 10$  mM). Therefore it could be assumed that ACS\_L641P shows no further improvements in acetate uptake compared to VC due to the predominance of Pta-AckA in acetate conversion at higher concentrations ( $\geq 1.476$  g l<sup>-1</sup>). Indeed,  $q_{ACE}$  was not significantly different in the MSU-phase for both strains.

Whereas most surprisingly was the 3.7-fold longer lag phase of VC which indicates the inhibiting effects of acetate on the methionine biosynthesis and the increase in osmotic pressure of cells (1.5.1). ACS\_L641P is likely to be more efficient compared to VC due to overexpression of *acs\_L641P*.

The increased specific carbon dioxide production rate and the shift in  $Y_{X/S}$  and  $Y_{CO_2/S}$  compared to VC, furthermore proves the assumption of greater energy consumption due to an enhanced level of active Acs in ACS\_L641P.

### 3.2.4 Fed-batch cultivations on glucose-acetate

#### ACS\_L641P

Based on the findings of different batch cultivations, fed-batch cultivations were carried out to demonstrate that expression of acetylation insensitive acetyl-CoA synthetase in *E. coli* W also enables co-utilisation of increased glucose-acetate concentrations at high cell densities (until 25 g l<sup>-1</sup>).

The set up for the batch cultivation was practically the same as described in 3.2.1 with 1 % (w/v) glucose-acetate. For the subsequent fed-batch, the feed design was based on the calculated specific uptake rates for glucose and acetate. For each of both strains, a particular glucose feed was adjusted equivalent to 90 % of its maximum specific glucose uptake rate ( $q_{GLC, max}$ ) from the batch. The acetate feed, however, was set equivalent

to 75 % of maximum specific acetate uptake rate ( $q_{ACE, max}$ ) from the ACS\_L641P batch for both strains. A feeding solution containing 25 % (w/v) glucose and 10.127 % (w/v) acetate was therefore used.

With this specifications it was hypothesised that VC would accumulate acetate due to  $q_{ACE} > q_{ACE, max}$  and contrary ACS\_L641P would not accumulate acetate due to  $q_{ACE} < q_{ACE, max}$ . Furthermore, it would be interesting if ACS\_L641P produces equal higher amounts of carbon dioxide compared to VC in HCDC.

Cultivations were conducted twofold for each strain, shown in Figure 20, 21 and 22 for VC, ACS\_L641P and the comparison of mean values, respectively. The specific rates and yields are listed in Table 29 and 30, respectively.

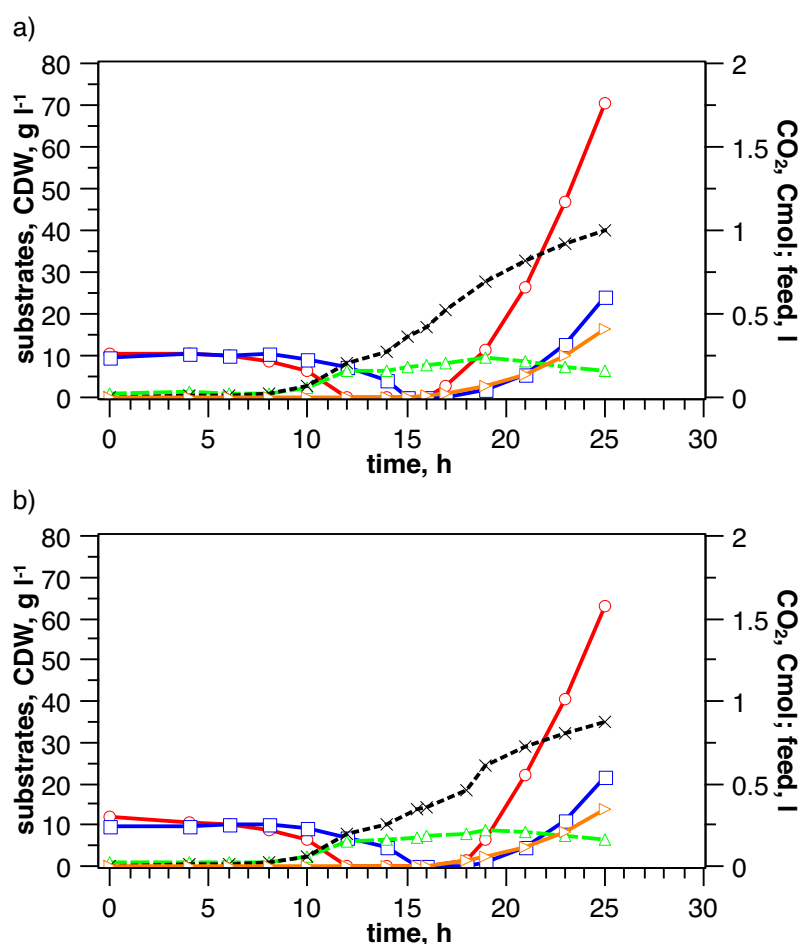


FIGURE 20: Fed-batches on 1 % (w/v) glucose-acetate (in batch) feed with submaximal uptake of glucose (90 %  $q_{GLC, max}$  VC) and supramaximal uptake of acetate (75 %  $q_{ACE, max}$  ACS\_L641P) with vector control in *E. coli* W. Concentration of glucose (○—), acetate (□—), CDW (△—), cumulated CO<sub>2</sub> (x-----), feed (△—). a) VC (F10 A) b) VC (F10 B)

### 3.2. Strain characterization in batch cultivations

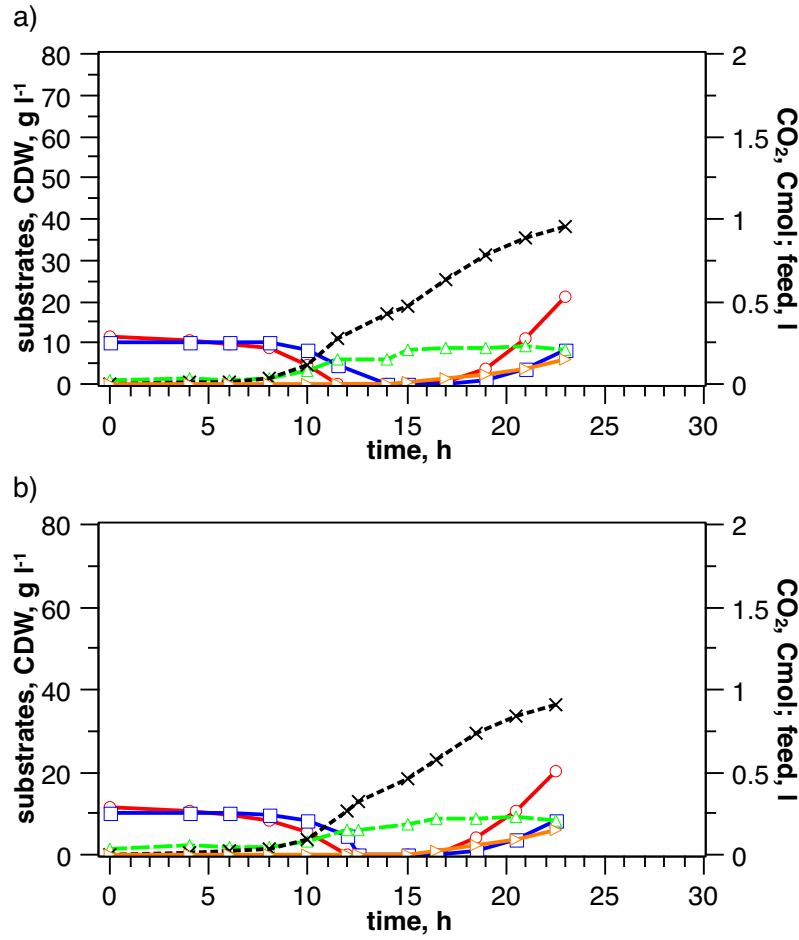


FIGURE 21: Fed-batches on 1 % (w/v) glucose-acetate (in batch) feed with submaximal uptake of glucose (90 %  $q_{\text{GLC}, \text{max}}$  ACS\_L641P) and submaximal uptake of acetate (75 %  $q_{\text{ACE}, \text{max}}$  ACS\_L641P) with *acs\_L641P* in *E. coli* W. Concentration of glucose ( $\circ$ —), acetate ( $\square$ —), CDW ( $\triangle$ —), cumulated  $\text{CO}_2$  ( $\times$ —), feed ( $\triangleright$ —). a) ACS\_L641P (F10 C) b) ACS\_L641P (F10 D)

TABLE 29: Specific growth, uptake, production and titration rates for fed-batches on 1 % (w/v) glucose-acetate (in batch) feed with submaximal uptake of glucose (90 %  $q_{\text{ACE}, \text{max}}$  VC/ACS\_L641P) and supra-/submaximal uptake of acetate (75 %  $q_{\text{ACE}, \text{max}}$  ACS\_L641P), during MSU-phase in batch and fed-batch.

		Batch		Fed-batch	
		VC	ACS_L641P	VC	ACS_L641P
$\mu$	$\text{h}^{-1}$	$0.22 \pm 0.03$	$0.15 \pm 0.05$	$0.06 \pm 0.01$	$0.05 \pm 0.01$
$q_{\text{GLC}}$	$\text{mmol g}^{-1} \text{h}^{-1}$	$3.28 \pm 0.20$	$2.90 \pm 0.71$	$1.35 \pm 0.32$	$1.09 \pm 0.27$
$q_{\text{ACE}}$	$\text{mmol g}^{-1} \text{h}^{-1}$	$2.00 \pm 0.39$	$3.33 \pm 0.24$	$2.92 \pm 0.05$	$1.94 \pm 0.88$
$q_{\text{CO}_2}$	$\text{mmol g}^{-1} \text{h}^{-1}$	$9.50 \pm 0.01$	$11.36 \pm 2.03$	$10.83 \pm 0.71$	$9.03 \pm 0.39$
$b_{\text{NH}_3}$	$\text{mmol g}^{-1} \text{h}^{-1}$	$7.63 \pm 1.44$	$3.07 \pm 0.72$	0	0

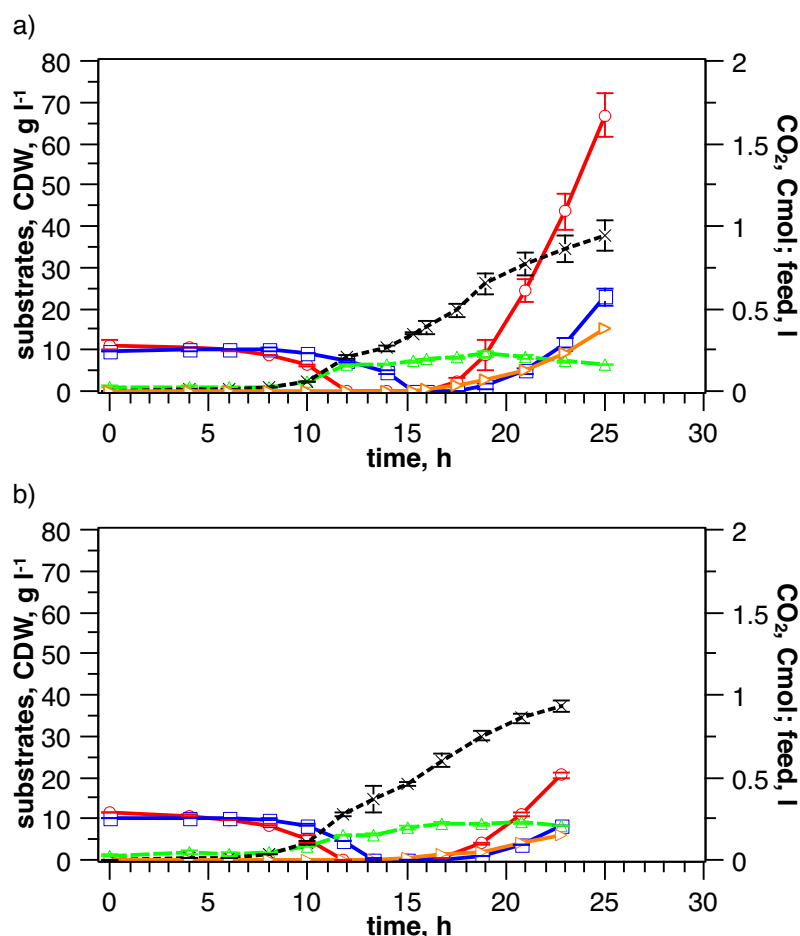


FIGURE 22: Fed-batches (mean) on 1 % (w/v) glucose-acetate (in batch) feed with submaximal uptake of glucose (90 %  $q_{GLC, max}$  VC/ACS\_L641P) and supra/submaximal uptake of acetate (75 %  $q_{ACE, max}$  ACS\_L641P) with vector control and *acs\_L641P* in *E. coli* W. Concentration of glucose ( $\circ$ —), acetate ( $\square$ —), CDW ( $\triangle$ —), cumulated  $CO_2$  ( $\times$ —), feed ( $\triangle$ —). a) VC (mean) b) ACS\_L641P (mean)

Compared to previous experiments in 3.2.1, the batch phases in this cultivations demonstrated slightly smaller distinctions between ACS\_L641P and VC. However, the trend was evident that ACS\_L641P co-utilised more acetate ( $q_{ACE}$  1.7-fold increased) than VC in the presence of glucose. As expected, batch phases of ACS\_L641P ended after 12 to 13 h while batch durations of VC lasted  $\sim 2.5$  h longer. Otherwise than expected,  $q_{CO_2}$  of ACS\_L641P was with  $11.36 \pm 2.03 \text{ mmol g}^{-1} \text{ h}^{-1}$   $\sim 30\%$  lower as in batches from previous cultivations ( $16.16 \pm 0.11 \text{ mmol g}^{-1} \text{ h}^{-1}$ ). A low specific base titration rate of ACS\_L641P confirmed once more that due to higher acetate consumption less ammonia per biomass was required to adjust the pH. The yields during batch phases were consistent with previous experiments (Table 30, 20).



### 3.2. Strain characterization in batch cultivations

TABLE 30: Yields and carbon recoveries for fed-batches on 1 % (w/v) glucose-acetate (in batch) feed with submaximal uptake of glucose (90 %  $q_{ACE, \max}$  VC/ACS\_L641P) and supra-/submaximal uptake of acetate (75 %  $q_{ACE, \max}$  ACS\_L641P).

			VC	ACS_L641P
Batch	$Y_{X/S}$	Cmol Cmol <sup>-1</sup>	$0.35 \pm 0.02$	$0.28 \pm 0.02$
	$Y_{CO_2/S}$	Cmol Cmol <sup>-1</sup>	$0.54 \pm 0.04$	$0.64 \pm 0.01$
	$Y_{O_2/S}$	Omol Cmol <sup>-1</sup>	$0.94 \pm 0.04$	$1.12 \pm 0.05$
	$Y_{CO_2/X}$	Cmol Cmol <sup>-1</sup>	$1.54 \pm 0.03$	$2.28 \pm 0.19$
	C-recovery	%	89 $\pm$ 6	92 $\pm$ 3
Fed-batch	$Y_{X/S}$	Cmol Cmol <sup>-1</sup>	$0.23 \pm 0.05$	$0.23 \pm 0.03$
	$Y_{CO_2/S}$	Cmol Cmol <sup>-1</sup>	$0.59 \pm 0.11$	$0.65 \pm 0.12$
	$Y_{O_2/S}$	Omol Cmol <sup>-1</sup>	$1.03 \pm 0.11$	$1.19 \pm 0.23$
	$Y_{CO_2/X}$	Cmol Cmol <sup>-1</sup>	$3.26 \pm 0.22$	$3.67 \pm 0.23$
	C-recovery	%	82 $\pm$ 16	88 $\pm$ 15

Feeding was started immediately after batch end (depletion of glucose and acetate). Therefore the feed rate for each cultivation was adjusted under consideration of particular cell densities, measured via OD<sub>600</sub>. All the specific rates and yields from the fed-batch were calculated from the end of batch until maximum biomass concentration was reached (Table 31).

TABLE 31: MSU-phase in fed-batch

Strain	Cultivation	$t_0$	$t_{end}$
VC	F11 A	15.0	19
	F11 B	15.3	19
ACS_L641P	F11 C	12.2	21
	F11 D	12.5	21

The specific growth rate during fed-batch was for both strains unexpectedly reduced, compared to prior batch phase (-67 % and -72 % for ACS\_L641P and VC, respectively). Equally,  $q_{GLC}$  was lower for both strains. Surprising was the fact that  $q_{ACE}$  of VC increased in the fed-batch 1.5-fold compared to the batch while for  $q_{ACE}$  of ACS\_L641P exactly the opposite was the case. Remarkable as well was, that during the entire fed-batch no ammonia for pH control was required.

The resulted yields for the fed-batch were characterised by increased variances.  $Y_{X/S}$ ,  $Y_{CO_2/S}$ , and  $Y_{O_2/S}$  were all in comparison with the yields during the batch. Whereas  $Y_{CO_2/X}$  for both strains were around double as high compared to the batch. Carbon recoveries were slightly underestimated. Unlike as intended, biomass concentrations in the fed-batch remained below the target of  $25 \text{ g l}^{-1}$  with maximum mean values of  $9.11 \pm 0.75 \text{ g l}^{-1}$  and  $9.02 \pm 0.07 \text{ g l}^{-1}$  for VC and ACS\_L641P, respectively.

## Discussion

Results from batch phase ensured that all specific rates and yields were in the same range as in the previous experiments. The subsequent fed-batch was growth restricted already from the beginning when feeding was started. Lee (1996) reports that feed-solutions need to be as simple as possible for *E.coli* fed-batch cultivations. The feed-solution used in this fed-batches contained only glucose, acetate,  $\text{MgSO}_4$ , trace metals, and kanamycin but no  $(\text{NH}_4)_2\text{HPO}_4$  such as defined in the initial batch media. Equally, as Riesenberger (1991) proposed for *E. coli* HCD fed-batch cultivations, ammonium hydroxide was separately added as the only nitrogen source since it also serves as base to control culture pH. However, as outlined in the previous cultivations, ammonia was only added in during glucose consumption due to catabolism related acidification. This suggests that the internal nitrogen level was almost depleted at the batch end with no chance to regenerate since acetate utilisation prevented a rising pH.

As a consequence, cells presumably starved under nitrogen limitation. About 1 h before the maximum biomass concentration was reached, substrates began to accumulate in the system (VC after 17.7 h, ACS\_L641P after 20 h).

## 3.3 Shake flask cultivations

### 3.3.1 Improved thermal tolerance by metE\_mut

The metE\_mut construct in *E. coli* W (METE\_mut) revealed in mixed batch fermentations (1 % (w/v) glucose-acetate) various results depending their acetate resistance. The improved growth rate of *E. coli* W, observed (F02 B) was supposable due to an stabilizing

### 3.3. Shake flask cultivations

effect of MetE\_mut which is in its unmodified form known as an aggregation-prone enzyme. However, this could not be proven, since two similar cultivations (F06 B and F06 C) appeared unaffected, compared to VC.

Since Mordukhova and J.-G. Pan (2013) tested metE\_mut already before in *E. coli* K-12 WE, demonstrating an increase in acetate and temperature resistance it was considered to grow METE\_mut on elevated temperatures. Therefore METE\_mut was cultivated in comparison to VC and to *E. coli* BL21 strains expressing the same constructs (metE\_mut = METE\_mut-BL21 or vector control = VC-BL21) on defined media supplemented with 1 % (w/v) glucose at reduced, optimal and elevated temperatures of 30, 37 and 44 °C, respectively.

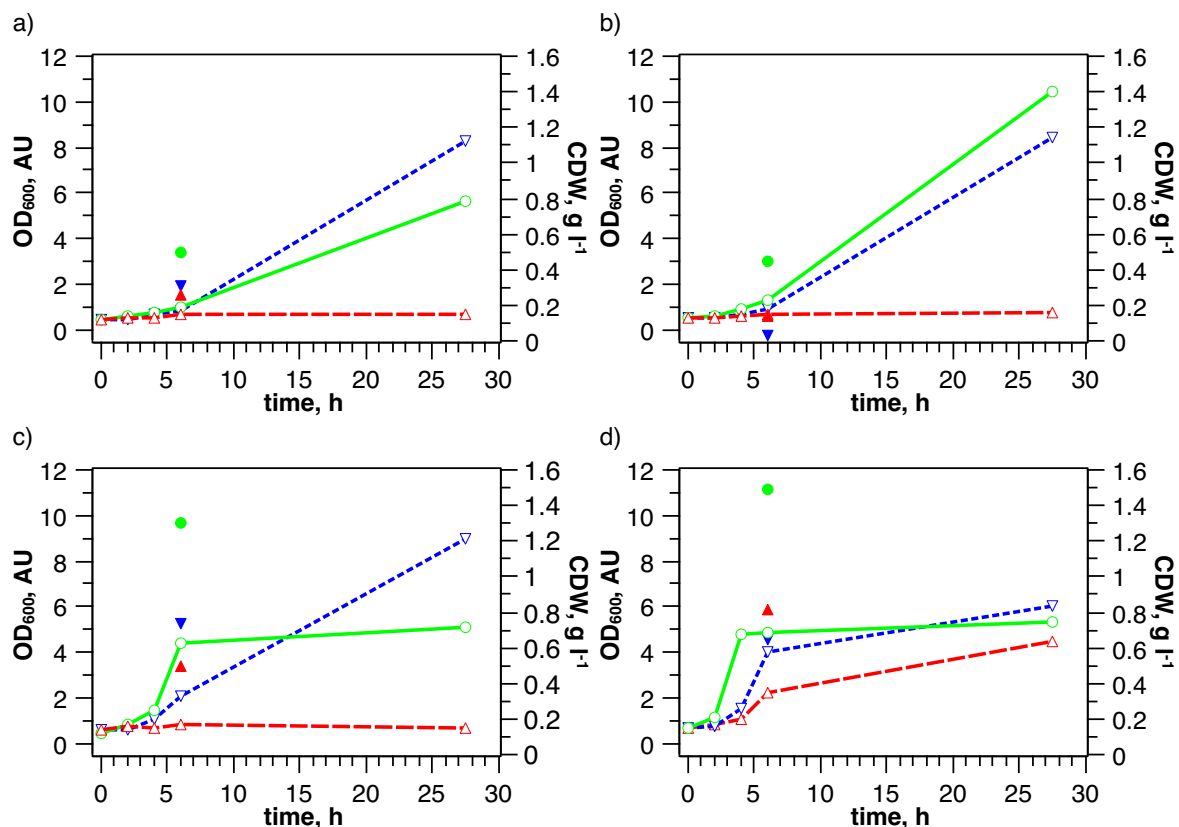


FIGURE 23: Comparative growth of engineered *E. coli* strains at various temperatures. OD values at 30 °C (▽---), 37 °C (○—) and 44 °C (△---). CDW values 6 h after inoculation at 30 °C(▼), 37 °C (●) and 44 °C (▲). a) VC-BL21 b) METE\_mut-BL21 c) VC d) METE\_mut

In Figure 23, all the cultivations below 44 °C indicates that *E. coli* W strains (c, d) grew much more rapidly compared to *E. coli* BL21 strains (a, b). Whereby the cell dry weight (6 h after inoculation) was slightly higher for METE\_mut (+15%) compared to VC at 37 °C. For cultivations at 44 °C, growth was only observed for METE\_mut.

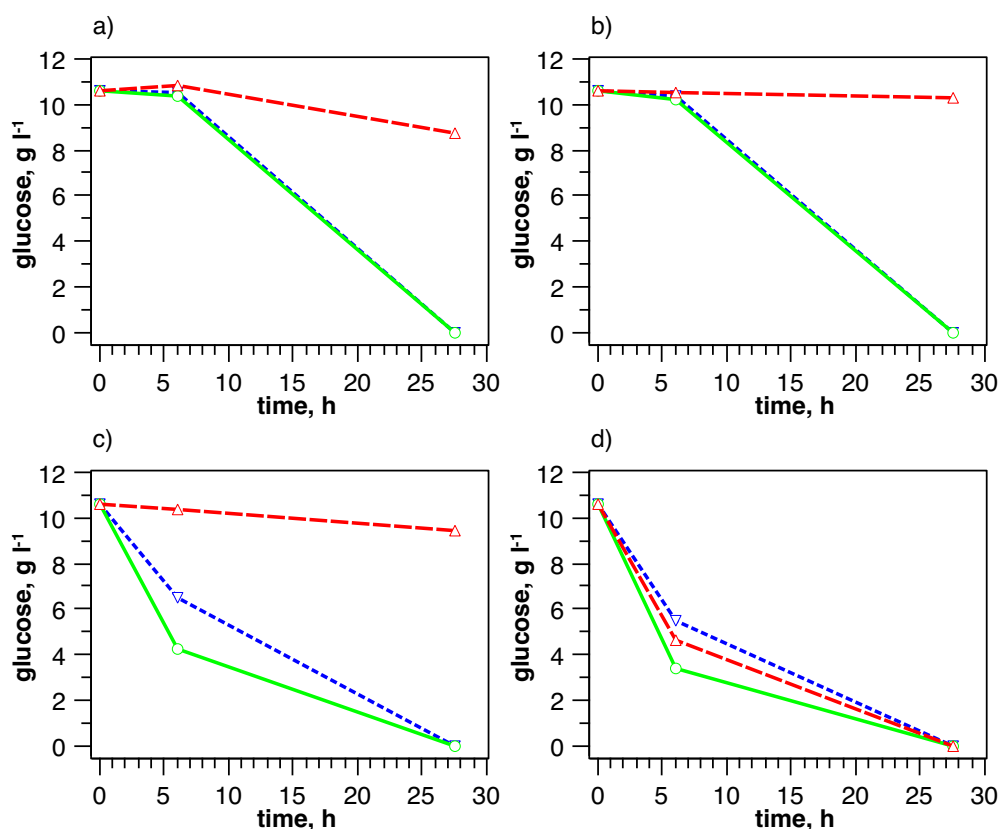


FIGURE 24: Comparative glucose uptake of engineered *E. coli* strains at various temperatures. Concentration of glucose at 30 °C ( $\nabla$ ---), 37 °C ( $\circ$ —) and 44 °C ( $\triangle$ ---). a) VC-BL21 b) METE\_mut-BL21 c) VC d) METE\_mut

The residual glucose concentrations over time in Figure 24 confirmed, that METE\_mut (d) was the only strain with an unaffected glucose uptake rate at elevated temperatures. For all *E. coli* BL21 strains (a, b), no glucose consumption was observable in the first 6 h of cultivation. This correlates with the extended lag phases indicated in Figure 23 a, b. After 27 h, glucose was used up among all the growing strains.

## Discussion

Mordukhova and J.-G. Pan (2013) stated that acetate-tolerant MetE mutants could as well stimulate the growth of its host strain at elevated temperatures (44 and 45 °C). Within this experiment, the thermostability of MetE\_mut in *E. coli* W was proven whereas for *E. coli* BL21 no additional thermal tolerance could be observed.

In Archer et al. (2011) it is described that *E. coli* W is a fast-growing strain which was further demonstrated by comparing VC and VC-BL21.

## 4 Conclusion and further perspectives

Within this work, eight different constructs have been generated via Golden MOCS cloning technique and successfully introduced into *E. coli* W. In the subsequent batch cultivations it turned out that *E. coli* W is a promising candidate for processes where low acetate secretion and efficient acetate uptake are crucial.

By analysing the strains for acetate co-utilisation in a mixed substrate batch system, it was shown, that the overexpression of acetylation-insensitive acetyl-CoA synthase significantly increased (2.7-fold) the specific acetate uptake rate in presence of glucose. This confirms that simultaneous utilisation of glucose and acetate is possible when post-translational control by CCR is circumvented. Furthermore, shorter batch durations during cultures using high concentrations of acetate were observed for the overexpression strain, presumably due to accelerated degradation of the toxic substrate. Still, a major drawback of this strain was that it emitted 2-fold more carbon dioxide during the co-utilisation phase which resulted in a 21 % lower end biomass.

For the second objective, the reduction of acetate initiated growth inhibition, a 1 to 3 h shorter process term could be noticed for a strain which overexpressed a modified aggregation-prone enzyme from the methionine biosynthesis. However, this phenomenon could not be confirmed due to divergent observations of strains possessing the same construct. Though, it is interesting that a related effect in protein stabilisation could be confirmed, by successfully cultivating this strain at elevated temperatures (44 °C). Another strain which comprised both, genes encoding for a stabilized metE enzyme (*metE\_mut*) and genes for improved acetate assimilation (*acs* and *cobB*) could significantly reduce process time and lag phase. As well, improvements in acetate co-utilisation could be observed, however, diauxic growth was still apparent.

The final attempt to achieve acetate co-utilisation in a high cell density fed-batch cultivation failed, likely due to nitrogen deprivation. Nonetheless, additional tests are required to set up a cultivation which reveals ideal growth conditions during acetate co-utilisation and to keep carbon dioxide emission low. For example, experiments on chemostat and

accelerostat cultivations could be adapted to define optimised dilution and growth rates and to analyse at carbon limiting conditions.

Additional tests on constructs which have not or insufficiently been cultivated so far are still crucial, to determine their potential. Moreover, to ensure efficient acetate utilisation without any further carbon loss, engineering the glyoxylate shunt seems to be inevitable. Evident approaches would include overexpression of glyoxylate shunt genes (*aceA*, *aceB*) as well as interfering into its regulation (deletion of *iclR*).

# Bibliography

- Adekunle, Kayode Feyisetan and Jude Awele Okolie (2015). "A review of biochemical process of anaerobic digestion". In: *Advances in Bioscience and Biotechnology* 6.03, p. 205.
- Ahn, S. et al. (2016). "Role of glyoxylate shunt in oxidative stress response". In: *Journal of Biological Chemistry* 291.22, pp. 11928–11938.
- Archer, C.T. et al. (2011). "The genome sequence of *E. coli* W (ATCC 9637): Comparative genome analysis and an improved genome-scale reconstruction of *E. coli*". In: *BMC Genomics* 12.
- Arifin, Yalun et al. (2014). "*Escherichia coli* W shows fast, highly oxidative sucrose metabolism and low acetate formation". In: *Applied microbiology and biotechnology* 98.21, pp. 9033–9044.
- Aristidou, Aristos A, Ka-Yiu San, and George N Bennett (1994). "Modification of central metabolic pathway in *Escherichia coli* to reduce acetate accumulation by heterologous expression of the *Bacillus subtilis* acetolactate synthase gene". In: *Biotechnology and bioengineering* 44.8, pp. 944–951.
- Arnold, Carrie N et al. (2001). "Global analysis of *Escherichia coli* gene expression during the acetate-induced acid tolerance response". In: *Journal of bacteriology* 183.7, pp. 2178–2186.
- Bauer, Andreas Peter, Wolfgang Ludwig, and Karl-Heinz Schleifer (2008). "A novel DNA microarray design for accurate and straightforward identification of *Escherichia coli* safety and laboratory strains". In: *Systematic and applied microbiology* 31.1, pp. 50–61.
- Castañó-Cerezo, Sara, Vicente Bernal, Jorge Blanco-Catalá, et al. (2011). "cAMP-CRP co-ordinates the expression of the protein acetylation pathway with central metabolism in *Escherichia coli*". In: *Molecular microbiology* 82.5, pp. 1110–1128.
- Castañó-Cerezo, Sara, Vicente Bernal, Teresa Röhrig, et al. (2015). "Regulation of acetate metabolism in *Escherichia coli* BL21 by protein N  $\epsilon$ -lysine acetylation". In: *Applied microbiology and biotechnology* 99.8, pp. 3533–3545.

- Chotani, Gopal et al. (2000). "The commercial production of chemicals using pathway engineering". In: *Biochimica et Biophysica Acta (BBA) - Protein Structure and Molecular Enzymology* 1543.2, pp. 434–455. ISSN: 0167-4838.
- Cornelis, Pierre (2000). "Expressing genes in different *Escherichia coli* compartments". In: *Current opinion in biotechnology* 11.5, pp. 450–454.
- De Anda, Ramón et al. (2006). "Replacement of the glucose phosphotransferase transport system by galactose permease reduces acetate accumulation and improves process performance of *Escherichia coli* for recombinant protein production without impairment of growth rate". In: *Metabolic engineering* 8.3, pp. 281–290.
- DeLisa, Matthew P et al. (1999). "Monitoring GFP-operon fusion protein expression during high cell density cultivation of *Escherichia coli* using an on-line optical sensor". In: *Biotechnology and bioengineering* 65.1, pp. 54–64.
- Deutscher, Josef (2008). "The mechanisms of carbon catabolite repression in bacteria". In: *Current opinion in microbiology* 11.2, pp. 87–93.
- Engler, C., R. Kandzia, and S. Marillonnet (2008). "A one pot, one step, precision cloning method with high throughput capability". In: *PLoS ONE* 3.11.
- Enjalbert, B. et al. (2017). "Acetate fluxes in *Escherichia coli* are determined by the thermodynamic control of the Pta-AckA pathway". In: *Scientific Reports* 7.
- Furdui, Cristina and Stephen W Ragsdale (2000). "The role of pyruvate ferredoxin oxidoreductase in pyruvate synthesis during autotrophic growth by the Wood-Ljungdahl pathway". In: *Journal of Biological Chemistry* 275.37, pp. 28494–28499.
- Gage, DANIEL J and FREDERICK C Neidhardt (1993). "Modulation of the heat shock response by one-carbon metabolism in *Escherichia coli*." In: *Journal of bacteriology* 175.7, pp. 1961–1970.
- Gimenez, Rosa et al. (2003). "The gene *yjcG*, cotranscribed with the gene *acs*, encodes an acetate permease in *Escherichia coli*". In: *Journal of bacteriology* 185.21, pp. 6448–6455.
- Görke, Boris and Jörg Stülke (2008). "Carbon catabolite repression in bacteria: many ways to make the most out of nutrients". In: *Nature Reviews Microbiology* 6.8, p. 613.
- Gschaedler, A, N Thi Le, and J Boudrant (1994). "Glucose and acetate influences on the behavior of the recombinant strain *Escherichia coli* HB 101 (GAPDH)". In: *Journal of industrial microbiology* 13.4, pp. 225–232.
- Han, Keehyun, Juan Hong, and Henry C Lim (1993). "Relieving effects of glycine and methionine from acetic acid inhibition in *Escherichia coli* fermentation". In: *Biotechnology and bioengineering* 41.3, pp. 316–324.
- Han, Keehyun, Henry C Lim, and Juan Hong (1992). "Acetic acid formation in *Escherichia coli* fermentation". In: *Biotechnology and bioengineering* 39.6, pp. 663–671.



- Hondorp, Elise R and Rowena G Matthews (2004). "Oxidative stress inactivates cobalamin-independent methionine synthase (MetE) in *Escherichia coli*". In: *PLoS biology* 2.11, e336.
- (2009). "Oxidation of cysteine 645 of cobalamin-independent methionine synthase causes a methionine limitation in *Escherichia coli*". In: *Journal of bacteriology* 191.10, pp. 3407–3410.
- Jönsson, Leif J and Carlos Martin (2016). "Pretreatment of lignocellulose: formation of inhibitory by-products and strategies for minimizing their effects". In: *Bioresource technology* 199, pp. 103–112.
- Katz, Chen et al. (2009). "Temperature-dependent proteolysis as a control element in *Escherichia coli* metabolism". In: *Research in microbiology* 160.9, pp. 684–686.
- Kleman, G.L. and W.R. Strohl (1994). "Acetate metabolism by *Escherichia coli* in high-cell-density fermentation". In: *Applied and Environmental Microbiology* 60.11, pp. 3952–3958.
- Kornberg, HL and e HA Krebs (1957). "Synthesis of cell constituents from C2-units by a modified tricarboxylic acid cycle". In: *Nature* 179.4568, p. 988.
- Korz, D.J. et al. (1995). "Simple fed-batch technique for high cell density cultivation of *Escherichia coli*". In: *Journal of Biotechnology* 39.1, pp. 59–65. ISSN: 0168-1656.
- Kumari, S., C.M. Beatty, et al. (2000). "Regulation of acetyl coenzyme A synthetase in *escherichia coli*". In: *Journal of Bacteriology* 182.15, pp. 4173–4179.
- Kumari, S., R. Tishel, et al. (1995). "Cloning, characterization, and functional expression of *acs*, the gene which encodes acetyl coenzyme A synthetase in *Escherichia coli*". In: *Journal of Bacteriology* 177.10, pp. 2878–2886.
- Lara, Alvaro R et al. (2008). "Utility of an *Escherichia coli* strain engineered in the substrate uptake system for improved culture performance at high glucose and cell concentrations: An alternative to fed-batch cultures". In: *Biotechnology and bioengineering* 99.4, pp. 893–901.
- Lee, Sang Yup (1996). "High cell-density culture of *Escherichia coli*". In: *Trends in biotechnology* 14.3, pp. 98–105.
- Leone, Serena et al. (2015). "Acetate: friend or foe? Efficient production of a sweet protein in *Escherichia coli* BL21 using acetate as a carbon source". In: *Microbial cell factories* 14.1, p. 106.
- Li, Yunjie et al. (2016). "Production of succinate from acetate by metabolically engineered *Escherichia coli*". In: *ACS synthetic biology* 5.11, pp. 1299–1307.
- Lim, Hyun Gyu et al. (2018). "Rediscovering Acetate Metabolism: Its Potential Sources and Utilization for Biobased Transformation into Value-Added Chemicals". In: *Journal of agricultural and food chemistry* 66.16, pp. 3998–4006.

- Lin, H. et al. (2006). "Acetyl-CoA synthetase overexpression in *Escherichia coli* demonstrates more efficient acetate assimilation and lower acetate accumulation: A potential tool in metabolic engineering". In: *Applied Microbiology and Biotechnology* 71.6, pp. 870–874.
- Liu, Min et al. (2017). "Improving the production of acetyl-CoA-derived chemicals in *Escherichia coli* BL21 (DE3) through *iclR* and *arcA* deletion". In: *BMC microbiology* 17.1, p. 10.
- Luli, Gregory W and WILLIAM R Strohl (1990). "Comparison of growth, acetate production, and acetate inhibition of *Escherichia coli* strains in batch and fed-batch fermentations." In: *Applied and environmental microbiology* 56.4, pp. 1004–1011.
- Lynch, Michael D, Tanya Warnecke, and Ryan T Gill (2007). "SCALES: multiscale analysis of library enrichment". In: *Nature Methods* 4.1, p. 87.
- Majewski, R.A. and M.M. Domach (1990). "Simple constrained optimization view of acetate overflow in *E. coli*". In: *Biotechnology and Bioengineering* 35.7, pp. 732–738.
- El-Mansi, EMT and WH Holms (1989). "Control of carbon flux to acetate excretion during growth of *Escherichia coli* in batch and continuous cultures". In: *Microbiology* 135.11, pp. 2875–2883.
- El-Mansi, Mansi et al. (2006). "Control of carbon flux through enzymes of central and intermediary metabolism during growth of *Escherichia coli* on acetate". In: *Current opinion in microbiology* 9.2, pp. 173–179.
- Mao, Chunlan et al. (2015). "Review on research achievements of biogas from anaerobic digestion". In: *Renewable and Sustainable Energy Reviews* 45, pp. 540–555.
- Marshall, Christopher W et al. (2012). "Electrosynthesis of commodity chemicals by an autotrophic microbial community". In: *Applied and environmental microbiology* 78.23, pp. 8412–8420.
- Mills, Tirzah Y, Nicholas R Sandoval, and Ryan T Gill (2009). "Cellulosic hydrolysate toxicity and tolerance mechanisms in *Escherichia coli*". In: *Biotechnology for biofuels* 2.1, p. 26.
- Mogk, Axel et al. (1999). "Identification of thermolabile *Escherichia coli* proteins: prevention and reversion of aggregation by DnaK and ClpB". In: *The EMBO journal* 18.24, pp. 6934–6949.
- Mordukhova, E.A. and J.-G. Pan (2013). "Evolved cobalamin-independent methionine synthase (MetE) improves the acetate and thermal tolerance of *Escherichia coli*". In: *Applied and Environmental Microbiology* 79.24, pp. 7905–7915.
- Nagata, Shinichi (2001). "Growth of *Escherichia coli* ATCC 9637 through the uptake of compatible solutes at high osmolarity". In: *Journal of bioscience and bioengineering* 92.4, pp. 324–329.

- Noh, Myung Hyun et al. (2018). "Production of itaconic acid from acetate by engineering acid-tolerant *Escherichia coli* W". In: *Biotechnology and bioengineering* 115.3, pp. 729–738.
- O'Beirne, D. and G. Hamer (2000). "The utilisation of glucose/acetate mixtures by *Escherichia coli* W3110 under aerobic growth conditions". In: *Bioprocess Engineering* 23.4, pp. 375–380.
- Oh, M.-K. et al. (2002). "Global expression profiling of acetate-grown *Escherichia coli* coli". In: *Journal of Biological Chemistry* 277.15, pp. 13175–13183.
- Pourmir, Azadeh and Tyler W Johannes (2012). "Directed evolution: selection of the host organism". In: *Computational and structural biotechnology journal* 2.3, e201209012.
- Rajaraman, Eashwar et al. (2016). "Transcriptional analysis and adaptive evolution of *Escherichia coli* strains growing on acetate". In: *Applied microbiology and biotechnology* 100.17, pp. 7777–7785.
- Repaske, David R and J Adler (1981). "Change in intracellular pH of *Escherichia coli* mediates the chemotactic response to certain attractants and repellents." In: *Journal of bacteriology* 145.3, pp. 1196–1208.
- Riesenberg, Dieter (1991). "High-cell-density cultivation of *Escherichia coli*". In: *Current opinion in biotechnology* 2.3, pp. 380–384.
- Roe, Andrew J, Debra McLaggan, et al. (1998). "Perturbation of anion balance during inhibition of growth of *Escherichia coli* by weak acids". In: *Journal of bacteriology* 180.4, pp. 767–772.
- Roe, Andrew J, Conor O Byrne, et al. (2002). "Inhibition of *Escherichia coli* growth by acetic acid: a problem with methionine biosynthesis and homocysteine toxicity". In: *Microbiology* 148.7, pp. 2215–2222.
- Ron, Eliora Z and Bernard D Davis (1971). "Growth rate of *Escherichia coli* at elevated temperatures: limitation by methionine". In: *Journal of bacteriology* 107.2, pp. 391–396.
- Rosano, Germán L and Eduardo A Ceccarelli (2014). "Recombinant protein expression in *Escherichia coli*: advances and challenges". In: *Frontiers in microbiology* 5, p. 172.
- Sandoval, Nicholas R et al. (2011). "Elucidating acetate tolerance in *E. coli* using a genome-wide approach". In: *Metabolic engineering* 13.2, pp. 214–224.
- Sarkari, Parveen et al. (2017). "An efficient tool for metabolic pathway construction and gene integration for *Aspergillus niger*". In: *Bioresource Technology*.
- Schuchmann, Kai and Volker Müller (2014). "Autotrophy at the thermodynamic limit of life: a model for energy conservation in acetogenic bacteria". In: *Nature Reviews Microbiology* 12.12, p. 809.

- Shiloach, J and S Bauer (1975). "High-yield growth of *E. coli* at different temperatures in a bench scale fermentor". In: *Biotechnology and Bioengineering* 17.2, pp. 227–239.
- Shin, Soan, Dong-Eun Chang, and Jae Gu Pan (2009). "Acetate consumption activity directly determines the level of acetate accumulation during *Escherichia coli* W3110 growth". In: *J Microbiol Biotechnol* 19.10, pp. 1127–1134.
- Smirnova, GV and ON Oktyabrskii (1988). "Effect of Activity of the Primary Proton Pumps on". In: *E. coli*, pp. 554–561.
- Starai, V.J., I. Celic, et al. (2002). "Sir2-dependent activation of acetyl-CoA synthetase by deacetylation of active lysine". In: *Science* 298.5602, pp. 2390–2392.
- Starai, V.J. and J.C. Escalante-Semerena (2004). "Identification of the protein acetyltransferase (Pat) enzyme that acetylates acetyl-CoA synthetase in *Salmonella enterica*". In: *Journal of Molecular Biology* 340.5, pp. 1005–1012.
- Starai, V.J., J.G. Gardner, and J.C. Escalante-Semerena (2005). "Residue Leu-641 of acetyl-CoA synthetase is critical for the acetylation of residue Lys-609 by the protein acetyltransferase enzyme of *Salmonella enterica*". In: *Journal of Biological Chemistry* 280.28, pp. 26200–26205.
- Straub, Melanie et al. (2014). "Selective enhancement of autotrophic acetate production with genetically modified *Acetobacterium woodii*". In: *Journal of biotechnology* 178, pp. 67–72.
- Terpe, Kay (2006). "Overview of bacterial expression systems for heterologous protein production: from molecular and biochemical fundamentals to commercial systems". In: *Applied Microbiology and Biotechnology* 72.2, p. 211. ISSN: 1432-0614.
- Valgepea, Kaspar et al. (2010). "Systems biology approach reveals that overflow metabolism of acetate in *Escherichia coli* is triggered by carbon catabolite repression of acetyl-CoA synthetase". In: *BMC Systems Biology* 4.1, p. 166. ISSN: 1752-0509.
- Vogl, Thomas et al. (2018). "Effect of plasmid design and type of integration event on recombinant protein expression in *Pichia pastoris*". In: *Applied and environmental microbiology*, AEM–02712.
- Waegeman, Hendrik et al. (2011). "Effect of *iclR* and *arcA* knockouts on biomass formation and metabolic fluxes in *Escherichia coli* K12 and its implications on understanding the metabolism of *Escherichia coli* BL21 (DE3)". In: *BMC Microbiology* 11.1, p. 70. ISSN: 1471-2180.
- Wang, Qingzhao et al. (2006). "Genome-scale in silico aided metabolic analysis and flux comparisons of *Escherichia coli* to improve succinate production". In: *Applied microbiology and biotechnology* 73.4, pp. 887–894.
- Weber, Ernst et al. (2011). "A modular cloning system for standardized assembly of multigene constructs". In: *PloS one* 6.2, e16765.

- Wendisch, Volker F et al. (2000). "Quantitative determination of metabolic fluxes during cointilization of two carbon sources: comparative analyses with *Corynebacterium glutamicum* during growth on acetate and/or glucose". In: *Journal of bacteriology* 182.11, pp. 3088–3096.
- Williams, Daniel C et al. (1982). "Cytoplasmic inclusion bodies in *Escherichia coli* producing biosynthetic human insulin proteins". In: *Science* 215.4533, pp. 687–689.
- Wolfe, A.J. (2005). "The acetate switch". In: *Microbiology and Molecular Biology Reviews* 69.1, pp. 12–50.
- Xiao, Yi et al. (2013). "Engineering *Escherichia coli* to convert acetic acid to free fatty acids". In: *Biochemical engineering journal* 76, pp. 60–69.
- Yanisch-Perron, Celeste, Jeffrey Vieira, and Joachim Messing (1985). "Improved M13 phage cloning vectors and host strains: nucleotide sequences of the M13mpl8 and pUC19 vectors". In: *Gene* 33.1, pp. 103–119.
- Zelcbuch, L. et al. (2016). "Pyruvate formate-lyase enables efficient growth of *Escherichia coli* on acetate and formate". In: *Biochemistry* 55.17, pp. 2423–2426.
- Zhuang, Kai, Goutham N Vemuri, and Radhakrishnan Mahadevan (2011). "Economics of membrane occupancy and respiration-fermentation". In: *Molecular systems biology* 7.1, p. 500.



## 5 Appendix

### 5.1 Elemental analysis raw data

TABLE A.1: Raw data: Main components of *E. coli* W

	Cell dry content, %					
	Carbon	Hydrogen	Nitrogen	Sulphur	Phosphate	Oxygen
1	45.96	6.38	12.51	0.611	2.18	26.99
2	46.15	6.54	12.54	0.622	2.18	26.92
3	46.07	6.52	12.66	0.618	2.23	26.85

TABLE A.2: Raw data: Minor components of *E. coli* W

	Cell dry content, %			
	Potassium	Sodium	Chloride	Ash content
1	1.74	0.849	0.891	9.75
2	1.70	0.859	0.779	9.6
3	1.75	0.845	1.041	9.77

## 5.2 Fermentation raw data

### 5.2.1 Batches

TABLE A.3: F02 B *E. coli* W metE\_mut glc-ace # 1

	time, h	CDW, g l <sup>-1</sup>	glucose, g l <sup>-1</sup>	acetate, g l <sup>-1</sup>	CO <sub>2</sub> , Cmol	O <sub>2</sub> , Omol	C-Rec, %
B0	0.01	0.75	9.88	10.23	0	0	
B1	1.62	0.77	9.88	9.94	0.01	0.01	99.80
B2	5.17	0.87	9.47	10.29	0.03	0.02	103.12
B3	6.40	1.39	8.61	10.08	0.04	0.03	98.36
B4	7.72	2.31	7.81	9.37	0.08	0.03	105.94
B5	9.13	5.98	5.77	7.47	0.18	0.06	121.16
B6	10.17	5.80	0	6.68	0.21	0.16	95.58
B7	11.53	6.40	0	4.34	0.24	0.64	93.48
B8	12.10	6.71	0	1.87	0.28	0.64	89.71
B9	12.75	7.19	0	0	0.32	0.64	90.64
B10	13.23	7.48	0	0	0.34	0.64	94.09

TABLE A.4: F02 D *E. coli* W acs\_metE\_mut\_cobB glc-ace # 1

	time, h	CDW, g l <sup>-1</sup>	glucose, g l <sup>-1</sup>	acetate, g l <sup>-1</sup>	CO <sub>2</sub> , Cmol	O <sub>2</sub> , Omol	C-Rec, %
D0	0.01	0.54	9.56	9.87	0	0	
D1	1.63	0.57	9.28	9.70	0	0.07	98.02
D2	3.87	0.75	8.58	9.85	0.01	0.22	97.06
D3	4.83	1.13	7.83	9.95	0.01	0.31	96.56
D4	6.38	2.77	4.93	9.16	0.02	0.44	89.77
D5	7.72	5.72	0	6.81	0.05	0.57	76.07
D6	8.45	5.89	0	6.91	0.08	0.68	82.25
D7	9.13	5.94	0	5.91	0.14	0.82	86.14
D8	10.17	6.76	0	3.56	0.19	0.98	87.94
D9	11.40	7.38	0	0	0.21	1.10	78.96
D10	12.73	6.90	0	0	0.28	1.31	85.74



## 5.2. Fermentation raw data

TABLE A.5: F05 A *E. coli* W vector control glc-ace # 1

	time, h	CDW, g l <sup>-1</sup>	glucose, g l <sup>-1</sup>	acetate, g l <sup>-1</sup>	CO <sub>2</sub> , Cmol	O <sub>2</sub> , Omol	C-Rec, %
A0	0.06	1.01	11.48	10.24	0	0	
A1	2	0.95	10.99	10.27	0	0.01	98.44
A2	4.01	1	10.87	10.50	0.01	0.03	99.59
A3	6	0.93	10.27	10.75	0.01	0.05	98.51
A4	8.02	0.88	10.17	10.74	0.01	0.06	98.13
A5	10.02	1.17	9.44	10.66	0.02	0.08	97.20
A6	12.02	1.91	7.76	10.32	0.05	0.14	96.04
A7	14.02	5.46	0	6.61	0.15	0.32	81.33
A8	16.02	5.72	0	5.57	0.23	0.47	89.30
A9	18	6.89	0	0	0.33	0.67	87.41

TABLE A.6: F05 C *E. coli* W acs\_L641P glc-ace # 2

	time, h	CDW, g l <sup>-1</sup>	glucose, g l <sup>-1</sup>	acetate, g l <sup>-1</sup>	CO <sub>2</sub> , Cmol	O <sub>2</sub> , Omol	C-Rec, %
C0	0.07	0.76	11.72	10.37	0	0	
C1	2	0.67	11.48	10.47	0	0.01	99.46
C2	4.03	1.01	11.19	10.58	0.01	0.02	100.97
C3	7.06	1.61	9.38	10.10	0.04	0.10	98.75
C4	8.04	1.80	8.68	9.64	0.07	0.16	97.90
C5	10.05	4.89	2.94	6.51	0.20	0.40	94.20
C6	12.02	6.12	0	1.90	0.40	0.75	95.01
C7	14.02	6.09	0	0	0.46	0.87	95.55
C8	24.08	4.38	0	0	0.47	0.86	89.84

TABLE A.7: F05 D *E. coli* W acs glc-ace # 1

	time, h	CDW, g l <sup>-1</sup>	glucose, g l <sup>-1</sup>	acetate, g l <sup>-1</sup>	CO <sub>2</sub> , Cmol	O <sub>2</sub> , Omol	C-Rec, %
D0	0.09	1.21	11.60	10.28	0	0	
D1	2.02	1.02	11.25	10.33	0.01	0.02	98.80
D2	4.04	1.05	11.42	11.02	0.01	0.03	103.11
D3	7.08	1.09	10.70	11	0.02	0.06	101.21
D4	8.07	1.23	10.30	11.04	0.02	0.07	101.97
D5	10.08	1.66	9.24	10.84	0.04	0.11	100.17
D6	12.05	3.14	4.50	9.57	0.09	0.21	90.13
D7	14.03	6.85	0	8.27	0.24	0.48	102.33
D8	16.08	5.95	0	4.20	0.29	0.60	90.23
D9	18	7.02	0	0	0.37	0.76	89.48
D10	24.10	6.12	0	0	0	0.79	40.20

TABLE A.8: F06 A *E. coli* W acs\_L641P glc-ace #3

	time, h	CDW, g l <sup>-1</sup>	glucose, g l <sup>-1</sup>	acetate, g l <sup>-1</sup>	CO <sub>2</sub> , Cmol	O <sub>2</sub> , Omol	C-Rec, %
A0	0.03	0.63	11.53	10.71	0	0	
A1	1.98	0.58	11.23	10.62	0	0.01	98.50
A2	4.02	1.15	10.91	10.66	0.01	0.02	100.96
A3	6.05	1.61	9.37	10.40	0.03	0.06	88.27
A4	8.02	3.26	5.74	8.78	0.10	0.20	87.18
A5	10.03	5.89	0	5.21	0.28	0.55	92.38
A6	12	5.65	0	4.35	0.30	0.61	90.61
A7	14.02	5.77	0	0	0.41	0.78	89.47
A8	16.05	5.81	0	0	0.42	0.79	91.45
A9	18.05	5.48	0	0	0.42	0.79	90.42

TABLE A.9: F06 B *E. coli* W metE\_mut glc-ace #2

	time, h	CDW, g l <sup>-1</sup>	glucose, g l <sup>-1</sup>	acetate, g l <sup>-1</sup>	CO <sub>2</sub> , Cmol	O <sub>2</sub> , Omol	C-Rec, %
B0	0.07	0.74	11.08	10.58	0	0	
B1	2.01	0.65	10.85	10.40	0	0.01	98.27
B2	4.04	0.79	10.35	10.84	0.01	0.02	99.55
B3	6.08	0.76	10.05	11.28	0.01	0.03	100.83
B4	8.03	0.89	9.43	10.91	0.02	0.03	98.15
B5	10.05	1.26	8.36	10.88	0.03	0.06	97.57
B6	12.02	3.21	4.64	9.81	0.08	0.16	95.40
B7	14.05	5.47	0	7.38	0.20	0.64	94.82
B8	16.08	7.24	0	0.67	0.30	0.64	92.64
B9	18.08	6.89	0	0	0.33	0.64	93.08

TABLE A.10: F06 C *E. coli* W metE\_mut glc-ace #3

	time, h	CDW, g l <sup>-1</sup>	glucose, g l <sup>-1</sup>	acetate, g l <sup>-1</sup>	CO <sub>2</sub> , Cmol	O <sub>2</sub> , Omol	C-Rec, %
C0	0.08	0.73	11.69	10.93	0	0	
C1	2.02	0.77	11.49	10.73	0	0.01	99.01
C2	4.05	0.89	11.03	10.40	0.01	0.02	96.87
C3	6.10	0.89	10.35	10.70	0.01	0.03	96.15
C4	8.05	1.07	9.82	10.84	0.02	0.05	96.50
C5	10.07	2.20	7.58	10.35	0.05	0.12	96.08
C6	12.05	6.40	0.42	7.91	0.17	0.33	93.88
C7	14.07	6.59	0	5.73	0.23	0.45	92.19
C8	16.10	6.94	0	2.95	0.28	0.57	89.96
C9	18.13	6.83	0	1.92	0.32	0.59	92.96

## 5.2. Fermentation raw data

TABLE A.11: F07 A *E. coli* W acs glc-ace #2

	time, h	CDW, g l <sup>-1</sup>	glucose, g l <sup>-1</sup>	acetate, g l <sup>-1</sup>	CO <sub>2</sub> , Cmol	O <sub>2</sub> , Omol	C-Rec, %
A0	0.05	0.69	11.45	11.02	0	0	
A1	2.08	0.75	11.03	11.05	0	0.01	99.31
A2	4	0.66	10.60	11.20	0.01	0.02	98.40
A3	6.13	0.86	9.95	11.31	0.02	0.04	98.09
A4	8.12	1.62	8.69	11.07	0.03	0.07	97.59
A5	10	2.52	8.74	11.75	0.08	0.16	110.35
A6	11.92	5.29	6.08	10.19	0.22	0.40	124.62
A7	14.02	6.23	0	5.20	0.27	0.50	94.44
A8	15.50	7.17	0	0	0.36	0.66	91.19
A9	16.12	7.18	0	0	0.37	0.69	92.64
A10	18.02	4.92	0	0	0.37	0.70	84.05

TABLE A.12: F07 B *E. coli* W acs glc-ace #3

	time, h	CDW, g l <sup>-1</sup>	glucose, g l <sup>-1</sup>	acetate, g l <sup>-1</sup>	CO <sub>2</sub> , Cmol	O <sub>2</sub> , Omol	C-Rec, %
B0	0.07	0.67	11.62	11.12	0	0	
B1	2.1	0.82	11.21	11.33	100.36	0	0.01
B2	4	0.74	10.83	11.35	99.04	0.01	0.01
B3	6.16	0.8	10.55	11.53	99.33	0.01	0.01
B4	8.15	0.8	10.18	11.66	98.78	0.01	0.01
B5	10.02	0.85	9.69	11.88	98.56	0.02	0.02
B6	11.97	1.37	5.95	10.38	83	0.03	0.02
B7	14.03	2.87	0.63	8.17	67.61	0.08	0.08
B8	15.53	5.58	0	7.99	88.14	0.17	0.26
B9	16.15	5.85	0	7.38	93.51	0.21	0.32
B10	18.05	7.57	0	6.31	100.69	0.24	0.37
B11	20.02	7.82	0	0	84.68	0.28	0.42
B12	21.23	6.93	0	0	88.09	0.33	0.52
B13	21.83	6.72	0	0	88.7	0.34	0.53

TABLE A.13: F07 D *E. coli* W vector control glc-ace #2

	<b>time, h</b>	<b>CDW, g l<sup>-1</sup></b>	<b>glucose, g l<sup>-1</sup></b>	<b>acetate, g l<sup>-1</sup></b>	<b>CO<sub>2</sub>, Cmol</b>	<b>O<sub>2</sub>, Omol</b>	<b>C-Rec, %</b>
D0	0.11	0.69	11.47	11.13	0	0	
D1	2.14	0.84	11.11	11.25	0.01	0.01	100.53
D2	4.03	0.81	10.73	11.30	0.01	0.01	99.84
D3	6.20	0.88	10.03	11.51	0.02	0.02	99.18
D4	8.18	1.31	8.85	11.22	0.03	0.04	97.13
D5	10.05	3.08	5.79	10.38	0.08	0.12	96.15
D6	11.23	6.40	0.22	8.78	0.17	0.27	94.32
D7	12	6.27	0	7.31	0.20	0.32	92.51
D8	14.05	7.38	0	2.55	0.28	0.44	89.64
D9	14.33	7.57	0	1.25	0.30	0.48	88.65
D10	14.95	7.23	0	0	0.33	0.53	87.39
D11	16.17	7.52	0	0	0.34	0.54	89.62

TABLE A.14: F08 C *E. coli* W acs\_L641P glc-ace #1

	<b>time, h</b>	<b>CDW, g l<sup>-1</sup></b>	<b>glucose, g l<sup>-1</sup></b>	<b>acetate, g l<sup>-1</sup></b>	<b>CO<sub>2</sub>, Cmol</b>	<b>O<sub>2</sub>, Omol</b>	<b>C-Rec, %</b>
C0	0.08	0.59	9.74	10.27	0	0	
C1	1.93	0.59	9.48	10.39	0	0.01	99.73
C2	4.12	0.63	8.99	10.48	0.01	0.04	98.92
C3	6.03	0.91	8.39	10.48	0.02	0.08	99.12
C4	8.22	1.66	6.94	9.78	0.06	0.19	99.52
C5	10.13	3.68	2.99	7.51	0.18	0.44	99.48
C6	11.08	5.12	0.02	5.17	0.28	0.63	97.88
C7	12.03	5.31	0.03	3.36	0.34	0.74	99.74
C8	13.27	5.88	0.03	0	0.40	0.87	100.66
C9	14.08	5.72	0	0	0.40	0.88	97.26

## 5.2. Fermentation raw data

TABLE A.15: F08 D *E. coli* W vector control glc-ace # 3

	time, h	CDW, g l <sup>-1</sup>	glucose, g l <sup>-1</sup>	acetate, g l <sup>-1</sup>	CO <sub>2</sub> , Cmol	O <sub>2</sub> , Omol	C-Rec, %
D0	0.08	0.53	10.11	10.18	0	0	
D1	1.95	0.67	9.70	10.43	0.01	0.01	101.02
D2	4.15	0.67	9.28	10.57	0.01	0.03	100.93
D3	6.07	0.75	8.91	10.67	0.02	0.05	100.79
D4	8.25	1.09	8.21	10.80	0.02	0.08	101.27
D5	10.15	1.63	6.73	10.38	0.05	0.14	99.42
D6	12.05	4.63	1.43	8.56	0.14	0.32	96.97
D7	12.68	5.67	0.02	7.73	0.20	0.42	100.16
D8	14.12	5.63	0.02	6.45	0.22	0.47	98.74
D9	15.52	7.08	0.02	1.34	0.30	0.62	96.28
D10	16.07	7.18	0.02	0	0.33	0.69	96.28
D11	16.62	7.07	0.01	0	0.34	0.70	97.10

TABLE A.16: F09 A *E. coli* W acs\_L641P ace # 1

	time, h	CDW, g l <sup>-1</sup>	glucose, g l <sup>-1</sup>	acetate, g l <sup>-1</sup>	CO <sub>2</sub> , Cmol	O <sub>2</sub> , Omol	C-Rec, %
A0	0.02	0.95	0	10.42	0	0	
A1	2.02	0.95	0	10.21	0	0	101
A2	4.02	0.99	0	10	0.01	0	102
A3	6.05	0.83	0	9.69	0.02	0	103
A4	8.02	1.10	0	9.22	0.03	0.01	104
A5	10	1.31	0	8.06	0.06	0.05	105
A6	12	2.03	0	5.86	0.11	0.14	106
A7	13.98	2.78	0	2.10	0.18	0.27	107
A8	14.92	3.21	0	0	0.22	0.35	108
A9	15.72	3.13	0	0	0.23	0.35	109
A10	18	0	0	0	0	0.35	110

TABLE A.17: F09 B *E. coli* W acs\_L641P ace # 2

	time, h	CDW, g l <sup>-1</sup>	glucose, g l <sup>-1</sup>	acetate, g l <sup>-1</sup>	CO <sub>2</sub> , Cmol	O <sub>2</sub> , Omol	C-Rec, %
B0	0.02	0.62	0	10.08	0	0	
B1	2.02	0.71	0	9.67	0	0	97.26
B2	4	0.76	0	9.40	0.01	0	98.09
B3	6.02	0.87	0	8.68	0.03	0.03	98.35
B4	8	1.32	0	7.20	0.07	0.10	100.39
B5	9.93	2.14	0	3.82	0.14	0.20	97.99
B6	11.82	2.97	0	0	0.23	0.38	98.86
B7	13.98	2.56	0	0	0.24	0.39	97.04

TABLE A.18: F09 C *E. coli* W vector control ace # 1

	time, h	CDW, g l <sup>-1</sup>	glucose, g l <sup>-1</sup>	acetate, g l <sup>-1</sup>	CO <sub>2</sub> , Cmol	O <sub>2</sub> , <sup>a</sup> Omol	C-Rec, %
C0	0.02	0.50	0	10.24	0	0	
C1	1.98	0.52	0	10.14	0	0	99.32
C2	3.98	0.56	0	9.92	0.01	0	99.49
C3	5.98	0.56	0	9.85	0.01	0	100.79
C4	7.97	0.63	0	9.77	0.02	0	102.66
C5	9.92	0.60	0	9.73	0.02	0	104.37
C6	11.90	0.59	0	9.71	0.03	0	105.40
C7	13.95	0.93	0	9.61	0.03	0	109.08
C8	22.55	0.81	0	9.09	0.06	0	111.79
C9	25	0.96	0	8.34	0.07	0	111.81
C10	27	1.28	0	3.89	0.10	0	87.25
C11	29.05	2.22	0	0.23	0.15	0	80.83
C12	30.93	3.29	0	0	0.21	0	105.89
C13	31.77	3.13	0	0	0.22	0	106.34

<sup>a</sup> O<sub>2</sub> offgas signal perturbations

## 5.2. Fermentation raw data

TABLE A.19: F09 D *E. coli* W vector control ace # 2

	time, h	CDW, g l <sup>-1</sup>	glucose, g l <sup>-1</sup>	acetate, g l <sup>-1</sup>	CO <sub>2</sub> , Cmol	O <sub>2</sub> , Omol	C-Rec, %
D0	0.02	0.48	0	10.38	0	0	
D1	1.97	0.61	0	10.69	0	0	104.07
D2	3.97	0.54	0	10.13	0.01	0	100.31
D3	5.97	0.50	0	10.07	0.01	0	101.07
D4	7.97	0.63	0	10.13	0.02	0	104.38
D5	9.88	0.61	0	9.99	0.02	0	104.52
D6	11.87	0.55	0	10.06	0.03	0.01	106.12
D7	13.93	0.70	0	10.04	0.04	0.01	108.98
D8	22.55	0.89	0	8.86	0.08	0.05	112.93
D9	25.02	1.71	0	6.60	0.12	0.10	114.13
D10	27.05	2.84	0	2.65	0.18	0.21	110.83
D11	27.98	3.74	0	0.29	0.21	0.24	111.12
D12	29.07	3.48	0	0	0.23	0.24	110.52

TABLE A.20: F10 A *E. coli* W acs\_L641P glc # 1

	time, h	CDW, g l <sup>-1</sup>	glucose, g l <sup>-1</sup>	acetate, g l <sup>-1</sup>	CO <sub>2</sub> , Cmol	O <sub>2</sub> , Omol	C-Rec, %
A0	0.04	0.44	10.69	0	0	0	
A1	2.10	0.59	8.98	0	0.03	0.07	92.47
A2	4.05	2.51	5.25	0.04	0.09	0.23	97.57
A3	4.95	4.67	0	0	0.18	0.41	97.94
A4	6.90	4.37	0	0	0.21	0.47	100.91

TABLE A.21: F10 B *E. coli* W acs\_L641P glc # 2

	time, h	CDW, g l <sup>-1</sup>	glucose, g l <sup>-1</sup>	acetate, g l <sup>-1</sup>	CO <sub>2</sub> , Cmol	O <sub>2</sub> , Omol	C-Rec, %
B0	0.02	0.48	11.14	0	0	0	
B1	2.07	0.73	8.33	0	0.02	0	83.37
B2	4.05	2.48	5.59	0.05	0.09	0.09	94.85
B3	4.98	4.55	0	0	0.18	0.25	91.51
B4	6.85	4.32	0	0	0.20	0.26	95.54

TABLE A.22: F10 C *E. coli* W vector control glc # 1

	time, h	CDW, g l <sup>-1</sup>	glucose, g l <sup>-1</sup>	acetate, g l <sup>-1</sup>	CO <sub>2</sub> , Cmol	O <sub>2</sub> , Omol	C-Rec, %
C0	0.05	0.62	9.81	0	0	0	
C1	2.18	0.78	10.33	0	0.02	0	112.04
C2	4.07	2.79	6.57	0	0.07	0.03	111.97
C3	5	5.94	0	0	0.15	0.15	108.13
C4	6.95	5.63	0	0	0.16	0.14	110.57

TABLE A.23: F10 D *E. coli* W vector control glc # 2

	time, h	CDW, g l <sup>-1</sup>	glucose, g l <sup>-1</sup>	acetate, g l <sup>-1</sup>	CO <sub>2</sub> , Cmol	O <sub>2</sub> , Omol	C-Rec, %
D0	0.02	0.49	11.88	0	0	0	
D1	2.06	0.62	10.47	0	0.02	0.03	93.70
D2	4	2.07	7.53	0.02	0.05	0.10	92.82
D3	5.17	5.73	0	0	0.14	0.26	88.23
D4	7.80	5.65	0	0	0.16	0.31	54.76



## 5.2.2 Fed-batches

TABLE A.24: F11 A *E. coli* W vector control glc-ace # 1

	time, h	CDW, g l <sup>-1</sup>	glucose, g l <sup>-1</sup>	acetate, g l <sup>-1</sup>	CO <sub>2</sub> , Cmol	O <sub>2</sub> , Omol	C-Rec, %	V Feed, ml
A0	0.03	1.12	10.47	9.75	0	0		0
A1	4.02	1.31	10.44	10.35	0.01	0.01	104.89	0
A2	6	1.01	9.78	10.13	0.01	0.02	100.23	0
A3	8.02	1.07	8.63	10.36	0.02	0.04	98.09	0
A4	10.05	2.36	6.21	9.13	0.07	0.12	94.30	0
A5	12.03	6.25	0	7.37	0.21	0.36	99.93	0
A6	14.03	6.44	0	4.28	0.27	0.47	95.99	0
A7	15.03	7.34	0	0	0.36	0.65	94.63	0
A8	15.93	7.79	0	0	0.42	0.74	93.51	10.38
A8.1	16.63		1.89	0	0.49	0.88	98	21.17
A9	17	8.20	2.74	0.18	0.52	0.95	101.06	27.47
A9.1	17.54		4.27	0.42	0.57	1.04	102.52	37.76
A9.2	18.05		5.64	0.71	0.62	1.12	102.71	48.54
A9.3	18.50		8.04	1.08	0.65	1.19	105.21	59.09
A10	19.02	9.64	11.45	1.66	0.69	1.27	112.15	72.50
A10.1	19.55		12.56	2	0.73	1.34	108.27	87.88
A10.2	20.08		18.96	3.33	0.76	1.41	115.84	105.08
A10.3	20.54		22.26	4.22	0.79	1.47	116.49	121.45
A11	21.02	8.49	26.39	5.49	0.82	1.52	116.06	140.11
A11.1	21.67		43.15	7.71	0.85	1.59	134.54	168.80
A11.2	22.10		36.53	8.83	0.87	1.64	118.71	190.16
A11.3	22.62		41.59	10.80	0.90	1.69	119.83	218.20
A12	23.07	7.18	46.62	12.54	0.92	1.74	107.97	245.14
A12.1	23.53		45.64	12.56	0.94	1.78	110.52	275.87
A12.2	24.02		57.02	18.04	0.96	1.82	120.97	310.98
A12.3	24.57		64.10	21.09	0.98	1.86	122.10	355.29
A13	25.10	6.38	70.45	24.12	1	1.90	121.64	403.42
A13.1	25.55		78.44	28	1.02	1.93	125.11	448.29
A13.2	26		84.44	30.14	1.03	1.96	124.73	497.38

TABLE A.25: F11 B *E. coli* W vector control glc-ace #2

	time, h	CDW, g l <sup>-1</sup>	glucose, g l <sup>-1</sup>	acetate, g l <sup>-1</sup>	CO <sub>2</sub> , Cmol	O <sub>2</sub> , Omol	C-Rec, %	V Feed, ml
B0	0.02	0.89	11.90	9.60	0	0		0
B1	4.02	0.88	10.62	9.81	0.01	0.02	96.45	0
B2	6.02	0.81	10.08	10.01	0.01	0.03	95.44	0
B3	8.03	1.02	8.83	9.89	0.02	0.05	92.22	0
B4	10.10	2.25	6.57	9.21	0.06	0.12	91.24	0
B5	12.05	6.19	0	7.02	0.20	0.36	92.08	0
B6	14	6.37	0	4.75	0.25	0.45	90.43	0
B7	15.33	7.03	0	0	0.34	0.63	86.73	0
B8	15.80	7.47	0	0	0.36	0.66	87.09	3.96
B8.1	16.62		1.07	0	0.43	0.80	89.68	15.05
B9	16.98	8.02	1.55	0.13	0.46	0.87	92.66	20.48
B9.1	17.57		2.53	0.15	0.51	0.97	92.80	30.15
B9.2	18.05		3.16	0.24	0.55	1.04	91.88	39.15
B9.3	18.52		6.60	0.88	0.58	1.11	98.87	48.75
B10	19	8.57	6.31	0.79	0.61	1.17	95.14	59.69
B10.1	19.53		8.79	1.52	0.64	1.24	96.82	73.13
B10.2	20.07		15.30	2.49	0.67	1.30	105.96	88.17
B10.3	20.48		17.97	3.26	0.69	1.35	107.08	101.10
B11	21	8.09	22.25	4.43	0.72	1.41	108.87	118.79
B11.1	21.67		27.49	5.98	0.75	1.47	110.71	144.53
B11.2	22.10		30.82	7.18	0.77	1.51	110.75	163.27
B11.3	22.60		31.94	8.12	0.79	1.56	106.26	187.05
B12	23.05	7.48	40.49	10.90	0.81	1.60	113.50	210.64
B12.1	23.50		44.73	13.63	0.82	1.63	115.10	236.53
B12.2	24		50.68	15.95	0.84	1.67	116.61	268.19
B12.3	24.55		56.82	18.58	0.86	1.71	117.47	306.94
B13	25.07	6.27	63.11	21.42	0.87	1.74	117.87	347.64
B13.1	25.53		69.21	24.68	0.89	1.77	119.26	388.24
B13.2	26		75.87	26.97	0.18	0.35	104.04	433.60

## 5.2. Fermentation raw data

TABLE A.26: F11 C *E. coli* W acs\_L641P glc-ace # 1

	time, h	CDW, g l <sup>-1</sup>	glucose, g l <sup>-1</sup>	acetate, g l <sup>-1</sup>	CO <sub>2</sub> , Cmol	O <sub>2</sub> , Omol	C-Rec, %	V Feed, ml
C0	0.04	0.83	11.53	9.95	0	0		0
C1	4.03	1.42	10.78	10.07	0.01	0.02	101.22	0
C2	6.03	1	9.81	10.31	0.01	0.03	97.18	0
C3	8.08	1.43	8.53	9.98	0.03	0.07	95.96	0
C4	10.06	3.20	4.38	8.35	0.11	0.21	90.44	0
C5	11.57	5.83	0	4.70	0.28	0.51	92.29	0
C5.1	12.17		0	0	0.33	0.59	79.58	0
C6	14.07	6.19	0	0.07	0.43	0.77	92.74	1.74
C6.1	14.78		0	0	0.45	0.81	93.80	3.58
C7	15.15	8.15	0	0	0.47	0.84	100.49	6.85
C7.1	15.67		0	0	0.50	0.89	98.83	11.77
C7.2	16.18		0	0	0.53	0.95	97.83	17.17
C7.3	16.68		0.51	0	0.58	1.03	99.28	22.80
C8	17.17	8.95	0.53	0.04	0.63	1.12	101.93	28.80
C8.1	17.68		2.08	0.24	0.67	1.21	105.56	35.63
C8.2	18.32		2.98	0.51	0.72	1.30	106.09	44.52
C8.3	18.65		3.67	0.79	0.75	1.35	106.86	49.59
C9	19.03	8.72	3.72	1.04	0.78	1.40	104.61	55.83
C9.1	19.75		6.25	1.59	0.82	1.49	106.22	68.61
C9.2	20.10		7.43	2.05	0.84	1.53	106.69	75.45
C9.3	20.62		8.82	2.66	0.86	1.58	106.02	86.29
C10	21.08	8.97	11.23	3.60	0.88	1.62	108.39	96.91
C10.1	21.67		12.72	4.28	0.91	1.67	106.15	111.38
C10.2	22.15		15.54	5.50	0.93	1.71	107.64	124.44
C10.3	22.57		17.40	6.59	0.94	1.74	107.71	136.54
C11	23.07	8.24	21.10	8.28	0.95	1.77	108.82	152.19
C11.1	23.55		23.30	9.82	0.97	1.80	108.47	168.53
C11.2	24.02		31.18	10.81	0.99	1.83	115.06	185.55

TABLE A.27: F11 D *E. coli* W acs\_L641P glc-ace # 2

	time, h	CDW, g l <sup>-1</sup>	glucose, g l <sup>-1</sup>	acetate, g l <sup>-1</sup>	CO <sub>2</sub> , Cmol	O <sub>2</sub> , Omol	C-Rec, %	V Feed, ml
D0	0.01	1.37	11.42	9.95	0	0		0
D1	4.07	2.29	10.51	10.09	0.01	0	101.91	0
D2	6.03	1.64	9.77	10.21	0.02	0	97.22	0
D3	8.08	1.93	8.47	9.75	0.04	0.04	94.43	0
D4	10.05	3.07	5.68	8.48	0.09	0.13	90.34	0
D5	12.10	6	0	4.77	0.27	0.45	88.51	0
D5.1	12.48		0	2.53	0.32	0.53	85.84	0
D6	13.88	6.01	0	0.20	0.42	0.72	89.28	1.75
D6.1	14.82		0	0	0.46	0.78	89.80	5
D7	15.08	7.36	0	0	0.47	0.81	95.19	7.56
D7.1	15.60		0	0	0.50	0.88	93.33	13.02
D7.2	16.12		0	0	0.53	0.92	91.45	19.03
D7.3	16.63		0.48	0	0.57	0.99	92.15	25.37
D8	17.08	8.75	0	0	0.62	1.07	94.86	31.44
D8.1	17.62		1.68	0.14	0.66	1.15	98.17	39.35
D8.2	18.17		2.68	0.53	0.70	1.23	99.30	47.89
D8.3	18.52		3.41	0.77	0.73	1.28	99.87	53.60
D9	19.07	8.51	4.22	1.09	0.76	1.34	98.37	63.31
D9.1	19.67		5.74	1.74	0.80	1.40	97.71	74.99
D9.2	20.07		7.05	2.16	0.82	1.44	99.18	83.56
D9.3	20.57		8.95	2.85	0.84	1.48	99.67	95.18
D10	21.03	9.08	10.62	3.61	0.86	1.52	100.79	106.95
D10.1	21.58		12.25	4.39	0.88	1.56	99.38	122.01
D10.2	22.08		15.22	5.90	0.90	1.59	101.33	136.91
D10.3	22.52		17.32	6.86	0.91	1.62	101.27	150.87
D11	23.02	8.14	20.16	8.37	0.92	1.64	100.53	168.21
D11.1	23.50		22.84	9.66	0.94	1.67	100.56	186.31
D11.2	23.95		24.74	10.78	0.95	1.69	99.28	204.50

## 5.3 Reprint permissions

Rightslink® by Copyright Clearance Center

11.06.18, 15:09



RightsLink®

Home

Account  
Info

Help



AMERICAN  
SOCIETY FOR  
MICROBIOLOGY

**Title:** The Acetate Switch  
**Author:** Alan J. Wolfe  
**Publication:** Microbiology and Molecular  
Biology Reviews  
**Publisher:** American Society for  
Microbiology  
**Date:** Mar 1, 2005

Logged in as:  
Lukas Flöckner  
Account #:  
3001288282

LOGOUT

Copyright © 2005, American Society for Microbiology

### Permissions Request

ASM authorizes an advanced degree candidate to republish the requested material in his/her doctoral thesis or dissertation. If your thesis, or dissertation, is to be published commercially, then you must reapply for permission.

BACK

CLOSE WINDOW

Copyright © 2018 Copyright Clearance Center, Inc. All Rights Reserved. [Privacy statement](#). [Terms and Conditions](#).  
Comments? We would like to hear from you. E-mail us at [customercare@copyright.com](mailto:customercare@copyright.com)

FIGURE A.1: Reprint permission of Figure 1 and 3

RightsLink Printable License		11.06.18, 16:49		RightsLink Printable License		11.06.18, 16:49	
<b>SPRINGER NATURE LICENSE TERMS AND CONDITIONS</b>				<b>Billing Type</b> Invoice			
Jun 11, 2018				<b>Billing Address</b> Mr. Lukas Flöckner Serverin-Schreiber-Gasse 29-33 1/1			
				Vienna, Austria 1180 Attn: Mr. Lukas Flöckner			
				<b>Total</b> 0.00 EUR			
				<b>Terms and Conditions</b>			
This Agreement between Mr. Lukas Flöckner ("You") and Springer Nature ("Springer Nature") consists of your license details and the terms and conditions provided by Springer Nature and Copyright Clearance Center.				<b>Springer Nature Terms and Conditions for RightsLink Permissions</b> <b>Springer Customer Service Centre GmbH (the Licensor)</b> hereby grants you a non-exclusive, world-wide licence to reproduce the material and for the purpose and requirements specified in the attached copy of your order form, and for no other use, subject to the conditions below:			
License Number 4351910533125				1. The Licensor warrants that it has, to the best of its knowledge, the rights to license reuse of this material. However, you should ensure that the material you are requesting is original to the Licensor and does not carry the copyright of another entity (as credited in the published version).			
License date May 18, 2018				If the credit line on any part of the material you have requested indicates that it was reprinted or adapted with permission from another source, then you should also seek permission from that source to reuse the material.			
Licensed Content Publisher Springer Nature				2. Where <b>print only</b> permission has been granted for a fee, separate permission must be obtained for any additional electronic re-use.			
Licensed Content Publication Nature Reviews Microbiology				3. Permission granted <b>free of charge</b> for material in print is also usually granted for any electronic version of that work, provided that the material is incidental to your work as a whole and that the electronic version is essentially equivalent to, or substitutes for, the print version.			
Licensed Content Title Carbon catabolite repression in bacteria: many ways to make the most out of nutrients				4. A licence for 'post on a website' is valid for 12 months from the licence date. This licence does not cover use of full text articles on websites.			
Licensed Content Author Boris Görke, Jörg Stülke				5. Where <b>'reuse in a dissertation/thesis'</b> has been selected the following terms apply: Print rights for up to 100 copies, electronic rights for use only on a personal website or institutional repository as defined by the Sherpa guideline ( <a href="http://www.sherpa.ac.uk/romeo/">www.sherpa.ac.uk/romeo/</a> ).			
Licensed Content Date Aug 1, 2008				6. Permission granted for books and journals is granted for the lifetime of the first edition and does not apply to second and subsequent editions (except where the first edition permission was granted free of charge or for signatories to the STM Permissions Guidelines ( <a href="http://www.stm-assoc.org/copyright-legal-affairs/permissions/permissions-guidelines/">http://www.stm-assoc.org/copyright-legal-affairs/permissions/permissions-guidelines/</a> ), and does not apply for editions in other languages unless additional translation rights have been granted separately in the licence.			
Licensed Content Volume 6				7. Rights for additional components such as custom editions and derivatives require additional permission and may be subject to an additional fee. Please apply to <a href="mailto:Journalpermissions@springernature.com">Journalpermissions@springernature.com</a> or <a href="mailto:bookpermissions@springernature.com">bookpermissions@springernature.com</a> for these rights.			
Licensed Content Issue 8				8. The Licensor's permission must be acknowledged next to the licensed material in print. In electronic form, this acknowledgement must be visible at the same time as the figures/tables/illustrations or abstract, and must be hyperlinked to the journal/book's homepage. Our required acknowledgement format is in the Appendix below.			
Type of Use Thesis/Dissertation				9. Use of the material for incidental promotional use, minor editing privileges (this does not			
Requestor type non-commercial (non-profit)							
Format print							
Portion figures/tables/illustrations							
Number of figures/tables/illustrations 1							
High-res required no							
Will you be translating? no							
Circulation/distribution <501							
Author of this Springer Nature content no							
Title Improved acetate co-utilisation by Escherichia coli W in high acetate-glucose fermentation							
Instructor name n/a							
Institution name n/a							
Expected presentation date Jun 2018							
Portions Box 1							
Requestor Location Mr. Lukas Flöckner Serverin-Schreiber-Gasse 29-33 1/1							
Vienna, Vienna 1180 Austria Attn: Mr. Lukas Flöckner							
<a href="https://x100.copyright.com/CustomerAdmin/PLF.jsp?ref=1e27442a-642a-4691-a435-768a06d88b2d">https://x100.copyright.com/CustomerAdmin/PLF.jsp?ref=1e27442a-642a-4691-a435-768a06d88b2d</a>				Seite 1 von 4			
RightsLink Printable License				RightsLink Printable License			
11.06.18, 16:49				11.06.18, 16:49			
include cropping, adapting, omitting material or any other changes that affect the meaning, intention or moral rights of the author) and copies for the disabled are permitted under this licence.							
10. Minor adaptations of single figures (changes of format, colour and style) do not require the Licensor's approval. However, the adaptation should be credited as shown in Appendix below.							
<b>Appendix — Acknowledgements:</b>							
<b>For Journal Content:</b> Reprinted by permission from [the Licensor]: [Journal Publisher (e.g. Nature/Springer/Palgrave)] [JOURNAL NAME] [REFERENCE CITATION (Article name, Author(s) Name), [COPYRIGHT] (year of publication)]							
<b>For Advance Online Publication papers:</b> Reprinted by permission from [the Licensor]: [Journal Publisher (e.g. Nature/Springer/Palgrave)] [JOURNAL NAME] [REFERENCE CITATION (Article name, Author(s) Name), [COPYRIGHT] (year of publication), advance online publication, day month year (doi: 10.1038/sj.JOURNAL ACRONYM)]							
<b>For Adaptations/Translations:</b> Adapted/Translated by permission from [the Licensor]: [Journal Publisher (e.g. Nature/Springer/Palgrave)] [JOURNAL NAME] [REFERENCE CITATION (Article name, Author(s) Name), [COPYRIGHT] (year of publication)]							
<b>Note: For any republication from the British Journal of Cancer, the following credit line style applies:</b> Reprinted/adapted/translated by permission from [the Licensor]: on behalf of Cancer Research UK: [Journal Publisher (e.g. Nature/Springer/Palgrave)] [JOURNAL NAME] [REFERENCE CITATION (Article name, Author(s) Name), [COPYRIGHT] (year of publication)]							
<b>For Advance Online Publication papers:</b> Reprinted by permission from The [the Licensor]: on behalf of Cancer Research UK: [Journal Publisher (e.g. Nature/Springer/Palgrave)] [JOURNAL NAME] [REFERENCE CITATION (Article name, Author(s) Name), [COPYRIGHT] (year of publication), advance online publication, day month year (doi: 10.1038/sj.JOURNAL ACRONYM)]							
<b>For Book content:</b> Reprinted/adapted by permission from [the Licensor]: [Book Publisher (e.g. Palgrave Macmillan, Springer etc)] [Book Title] by [Book author(s)] [COPYRIGHT] (year of publication)]							
<b>Other Conditions:</b> Version 1.0 Questions? <a href="mailto:customer@copyright.com">customer@copyright.com</a> or +1-855-239-3415 (toll free in the US) or +1-978-646-2777.							
<a href="https://x100.copyright.com/CustomerAdmin/PLF.jsp?ref=1e27442a-642a-4691-a435-768a06d88b2d">https://x100.copyright.com/CustomerAdmin/PLF.jsp?ref=1e27442a-642a-4691-a435-768a06d88b2d</a>				Seite 3 von 4			
RightsLink Printable License				RightsLink Printable License			
11.06.18, 16:49				11.06.18, 16:49			

FIGURE A.2: Reprint permission of Figure 2

## 5.3. Reprint permissions

Copyright Clearance Center

21.06.18, 10:54

Copyright Clearance Center

21.06.18, 10:54

Back to view orders

Copy order

Confirmation Number: 11723237  
Order Date: 06/11/2018

Print this page  
Print terms & conditions  
Print citation information  
(What's this?)

Customer Information

Customer: Lukas Flöckner  
Account Number: 3001280282  
Organization: Lukas Flöckner  
Email: l.floekner@igmu.at  
Phone: +43 6641041024

Search order details by:

Sort order details by:

This is not an invoice

Order Details

Journal of biological chemistry

Billing Status: N/A

Order detail ID: 71242848  
ISSN: 1083-351X  
Publication Type: e-Journal  
Volume:  
Issue:  
Start page:  
Publisher: AMERICAN SOCIETY FOR BIOCHEMISTRY AND MOLECULAR BI  
Author/Editor: AMERICAN SOCIETY FOR BIOCHEMISTRY & MOLECULAR BIOL.

Permission Status: ☒ Granted  
Permission type: Republish or display content  
Type of use: Thesis/Dissertation  
Order License Id: 4365981039056  
Hide details  
Requestor type: Academic institution  
Format: Print, Electronic  
Number of charts/tables/figures: 1  
The requesting person/organization: lukas floekner  
Title or numeric reference of the portion(s): FIG.2. Model of posttranslational control of Acs by the SDPADS.  
Title of the article or chapter the portion is from: Residue Leu-641 of Acetyl-CoA Synthetase is Critical for the Acetylation of Residue Lys-609 by the Protein Acetyltransferase Enzyme of Salmonella enterica\*  
Editor of portion(s): N/A  
Author of portion(s): N/A  
Volume of serial or

monograph

N/A

Page range of portion

280:26202

Publication date of portion

17.05.2005

Rights for

Main product

Duration of use

Life of current edition

Creation of copies for the disabled

yes

With minor editing privileges

no

For distribution to

Worldwide

In the following language(s)

Original language of publication

With incidental promotional use

no

Lifetime unit quantity of new product

Up to 499

Title

Improved acetate co-utilisation by Escherichia coli W in high acetate-glucose fermentation

Instructor name

n/a

Institution name

n/a

Expected presentation date

Jun 2018

Note: This item was invoiced separately through our RightsLink service. [More info](#)

\$ 0.00

Microbiology

Billing Status: N/A

Order detail ID: 71184969  
ISSN: 1350-0872  
Publication Type: Journal  
Volume:  
Issue:  
Start page:  
Publisher: Microbiology Society  
Author/Editor: SOCIETY FOR GENERAL MICROBIOLOGY

Permission Status: ☒ Granted  
Permission type: Republish or display content  
Type of use: Republish in a thesis/dissertation  
Job Ticket: 501461686  
Order License Id: 4371810444016  
View details

Note: This item was invoiced through CCC's RightsLink service. [More info](#)

\$ 0.00

https://www.copyright.com/orderView.do

Saite 1 von 2

https://www.copyright.com/orderView.do

Saite 2 von 2

FIGURE A.3: Reprint permission of Figure 4

Rightslink® by Copyright Clearance Center

18.06.18, 10:09

Rightslink® by Copyright Clearance Center

18.06.18, 10:09

Copyright Clearance Center

RightsLink®

Account info Help

Logged in as:  
Lukas Flöckner  
Account #: 3001280282  
Logout

Order Completed

Thank you for your order.

This Agreement between Lukas Flöckner ("You") and Microbiology Society ("Microbiology Society") consists of your order details and the terms and conditions provided by Microbiology Society and Copyright Clearance Center.

License number

Reference confirmation email for license number

License date

Jun, 18 2018

Licensed content publisher

Microbiology Society

Licensed content title

Microbiology

Licensed content date

Jan 1, 1994

Type of use

Thesis/Dissertation

Requestor type

Not-for-profit entity

Format

Print, Electronic

Portion

chart/graph/table/figure

Number of charts/tables/figures

1

The requesting person/organization

Lukas Flöckner

Title or numeric reference of the portion(s)

Fig. 1. A schematic of the methionine biosynthetic pathway of E. coli.

Title of the article or chapter the portion is from

Inhibition of Escherichia coli growth by acetic acid: a problem with methionine biosynthesis and homocysteine toxicity

Editor of portion(s)

N/A

Author of portion(s)

Andrew J. Roe

Volume of serial or monograph

148

Page range of portion

2216

Publication date of portion

22 March 2002

Rights for

Main product

Duration of use

Current edition and up to 10 years

Creation of copies for the disabled

yes

With minor editing privileges

no

For distribution to

Other territories and/or countries

In the following language(s)

Original language of publication

With incidental promotional use

no

Lifetime unit quantity of new product

Up to 499

Title

Improved acetate co-utilisation by Escherichia coli W in high acetate-glucose fermentation

Instructor name

n/a

Institution name

n/a

Expected presentation date

Jun 2018

Requestor Location

Mr. Lukas Flöckner  
Serven-Schreiber-Gasse 29-33 1/1  
Vienna, Vienna 1180  
Austria  
Attn: Mr. Lukas Flöckner

Billing Type

Invoice

Billing address

Mr. Lukas Flöckner  
Serven-Schreiber-Gasse 29-33 1/1  
Vienna, Austria 1180  
Attn: Mr. Lukas Flöckner

Total (may include CCC user fee)

0.00 USD

Total

0.00 USD

CLOSE WINDOW

Copyright © 2018 Copyright Clearance Center, Inc. All Rights Reserved. [Privacy statement](#). [Terms and Conditions](#).  
Comments? We would like to hear from you. E-mail us at [customerservice@copyright.com](mailto:customerservice@copyright.com)

https://v100.copyright.com/AppDispatchServlet

Saite 1 von 2

https://v100.copyright.com/AppDispatchServlet

Saite 2 von 2



FIGURE A.4: Reprint permission of Figure 5

Rightlink® by Copyright Clearance Center

21.06.18, 10:12

Rightlink® by Copyright Clearance Center


21.06.18, 10:12



Account Info

Help

Logout



**Title:** An efficient tool for metabolic pathway construction and gene integration for *Aspergillus niger*

**Author:** Parveen Sarkar,Hans Mann,Marzena L. Blumhoff,Diethard Mattanovich,Michael Sauer,Matthias G. Steiger

**Publication:** Bioscience Technology

**Publisher:** Elsevier

**Date:** December 2017

Copyright © 2017, Elsevier

Logged in as:  
Lukas Flöckner  
Account #: 3001298352

Logout

**Austria**  
Attn: Mr. Lukas Flöckner  
GB-494 6272 12  
Invoice  
Mr. Lukas Flöckner  
Serverin-Schreiber-Gasse 29-33 1/1  
Vienna, Austria 1180  
Attn: Mr. Lukas Flöckner  
0.00 EUR

CLOSE WINDOW

Copyright © 2018 Copyright Clearance Center, Inc. All Rights Reserved. [Privacy statement](#), [Terms and Conditions](#).  
Comments? We would like to hear from you. E-mail us at [customerservice@copyright.com](mailto:customerservice@copyright.com)

**Order Completed**  
Thank you for your order.

This Agreement between Lukas Flöckner ("You") and Elsevier ("Elsevier") consists of your order details and the terms and conditions provided by Elsevier and Copyright Clearance Center.

License number	Reference confirmation email for license number
License date	Jun, 21 2018
Licensed Content	Elsevier
Publisher	
Licensed Content	Bioscience Technology
Publication	
Licensed Content Title	An efficient tool for metabolic pathway construction and gene integration for <i>Aspergillus niger</i>
Licensed Content Author	Parveen Sarkar,Hans Mann,Marzena L. Blumhoff,Diethard Mattanovich,Michael Sauer,Matthias G. Steiger
Licensed Content Date	December 2017
Licensed Content Volume	245
Licensed Content Issue	n/a
Licensed Content Pages	7
Type of Use	reuse in a thesis/dissertation
Portion	figures/tables/illustrations
Number of figures/tables/illustrations	1
Format	both print and electronic
Are you the author of this Elsevier article?	No
Will you be translating?	No
Original figure numbers	Fig. 1
Title of your thesis/dissertation	Improved acetate co-utilisation by <i>Escherichia coli</i> W in high acetate-glucose fermentation
Expected completion date	Jun 2018
Estimated size (number of pages)	74
Requestor Location	Mr. Lukas Flöckner Serverin-Schreiber-Gasse 29-33 1/1 Vienna, Vienna 1180

<https://x100.copyright.com/AppDispatchServlet>

Selle 1 von 2

<https://x100.copyright.com/AppDispatchServlet>

Selle 2 von 2

FIGURE A.5: Reprint permission of Figure 6